ISSN 1000-9620

海洋通报

Marine Science Bulletin

LIBRARY
Science Center
NOAA Fisheries

NATIONAL MARINE DATD AND
INFORMATION SERVICE OF CHINA

2017
Volume 19
Number 2

MARINE SCIENCE BULLETIN

Vol. 19 No. 2 Oct. 2017

CONTENTS

Bacterial diversity in the sea surface microlayer of the Northern Yellow Sea of China
……MING Hong-xia et al. (01)

Input characteristics and risk analysis of ballast water from offshore entry ships in China
……DU Huan et al. (20)

Community characteristics of macrobenthos community in Changli Gold Coast National Nature Reserve of Hebei in China…… KOU Cun-hui et al. (38)

Inversion and verification of chlorophyll *a* concentration in the Bohai Bay
…… ZHENG Xiao-shen et al. (51)

Comparison of inversion of Chlorophyll concentration in the Bohai Bays based on GOCI data……ZHANG Xue et al. (62)

Classification system and structure analysis of marine cultural landscapes of China
…… LI Jia-lin et al. (75)

Ocean ecological compensation mechanism in Liaoning Area from the angle of ecological civilization — based on analysis of Dalian's cooperative governance
…… CAI Jing et al. (88)

Bacterial diversity in the sea surface microlayer of the Northern Yellow Sea of China

MING Hong-xia[1], FAN Jing-feng[1*], WANG Xiao-hui[1,2], LI Hong-bo[1], ZAN Shuai-jun[1, 2]

1. *National Marine Environmental Monitoring Center, Dalian* 116023, *Liaoning province, China;*

2. *Dalian Ocean University, Dalian* 116023, *Liaoning province, China*

Abstract: The surface microlayer (SML) is a thin biogenic film found between the marine environment and troposphere that comprises a unique marine ecosystem with its own physicochemical and microbiological compositions. In this study, we compared the bacterial cell abundance and community structure of the SML and subsurface waters (0.50 m depth) using traditional culture and flow cytometry methods. Overall, 53 strains were screened and sequenced. In addition, DNA was extracted from the SML and corresponding subsurface water and used for bacterial community analysis by denaturing gradient gel electrophoresis (DGGE). The results revealed that the SML had a distinct microbial community structure from the corresponding subsurface water. This is the first compresensively detailed molecular biological analysis of the bacterioneuston in the Yellow Sea of China.

Keywords: surface microlayer; bacterial diversity; denaturing gradient gel electrophoresis

NOAA CENTRAL LIBRARY
OCT 22 2018
WITHDRAWN
National Oceanic &
Atmospheric Administration
US Dept of Commerce

1 Introduction

The sea surface microlayer, which is part of the air–sea interface between the atmosphere and aquatic environments, is loosely defined as the upper 1 mm of the ocean (Liss and Duce, 2005). It is now well recognized that the sea surface microlayer is physicochemically very different from the underlying subsurface water with respect to its physical, chemical, and biological processes (Zhang et al., 1998; Zhang et al., 2003; Liss and Duce, 2005). Indeed, this layer comprises a distinct ecosystem that is often referred to as the neuston (Naumann, 1917).

The enrichment factor (EF) is used to express the enrichment effect, which is defined as the concentration of a specific constituent in the microlayer divided by its concentration in subsurface water directly below the microlayer (Hardy et al., 1997). Many studies have quantified the EFs of a diverse range of microlayer components such as nitrate, phosphate,

Received on April. 5, 2017

*Corresponding author: jffan@nmemc.org.cn

dissolved organic carbon, chlorophyll *a*, transparent exopolymer particles, biogenic gases, dimethylsulfoxide (DMSO) and dimethylsulfoniopropionate (DMSP) in different aquatic systems (Carlson, 1983; Agogue et al., 2004; Joux et al., 2006; Obernosterer et al., 2007; Reinthaler et al., 2008; Wurl and Holmes, 2008; Baastrup-Spohr L. and Staehr P. A., 2009; Cunliffe et al., 2009b; Wurl et al., 2009; Hörtnagl et al., 2010). Nevertheless, reports of the EF of total bacteria in the SML vary greatly among studies (Agogue et al., 2004; Marumo et al. 1971; Harvey and Young 1980).

Relatively few studies have used molecular biological techniques to investigate the microbial communities of sea surface microlayers, and those that have had variable results (Agogue et al., 2005; Franklin et al., 2005). Agogue et al. (2005) found no consistent difference between the bacterioneuston community structure and the bacterioplankton community structure at two sites. In contrast, analysis of surface microlayer samples collected from the coast of the North Sea in the United Kingdom showed a distinct bacterioneuston community (Franklin et al., 2005). More recently, Cunliffe et al. (2009a) found that bacterioneuston denaturing gradient gel electrophoresis (DGGE) profiles from two sampling sites on opposite sides of an island were more similar to each other than the cognate bacterioplankton DGGE profiles, while Archaea 16S rRNA gene DGGE profiles from the same samples did not show the same pattern. Another recent study employed a mesocosm to compare microbial diversity in the bacterioneuston with that of cognate bacterioplankton during an artificially induced phytoplankton bloom (Cunliffe et al., 2009b). Throughout the experiment, a distinct bacterioneuston community that was conserved between the replicated mesocosms, was formed (Cunliffe et al., 2009b).

The objective of the present study was to evaluate whether the top layer of the ocean is inhabited by a distinct bacterioneuston community. We used the DGGE to profile the 16S rRNA genes of bacteria present in the surface microlayer samples obtained using glass plates (GP) sampling devices.

2 Material and methods

2.1 Sample sites and sampling

Samples were collected during calm conditions (wind speed <5 m/s) from eight stations in the Northern Yellow Sea in China: B1, B3, B5, C3, A3, T1, BY5 and SY3. A3 was located on the coast, while B1, B3 and B5 were located in the central Northern Yellow Sea. Additionally, BY5 was in the Yellow Sea Strait and SY3 was located in the center of the South Yellow Sea. Samples were collected during four field surveys (June 2010, August 2010, March 2011 and July 2011).

The surface microlayer (SML) was sampled using glass plate samplers. The GP had dimensions of 400 × 300 × 4 mm, with an effective sampling area of about 1 800 cm^2 (including both sides of the plate). Samples were collected by vertically inserting the GP into the water column and withdrawing it in the same way with a sampling velocity of about 10 cm/s. The surface microlayer samples were then removed from the glass plate using a wiper and collected in sterilized glass bottles. This process resulted in a sampling depth of 20 to 100 μm (Harvey, 1965; Harvey and Burzell, 1972). Before sampling, the glass plate and wiper blade were washed in ethanol (75%v/v). Overall, 200 ml of water were collected into sterile bottles before being filtered through a membrane filter (Sterivex-GS, 0.22 μm filter unit, Millipore, Billerica, MA, USA), after which the filters were stored at –20 °C. Samples from underlying waters (UW) were collected for direct comparison with each surface microlayer sample by submerging a sterile bottle and opening it at a depth of 0.5 m. A total of 200 ml of subsurface water was filtered and stored as described above.

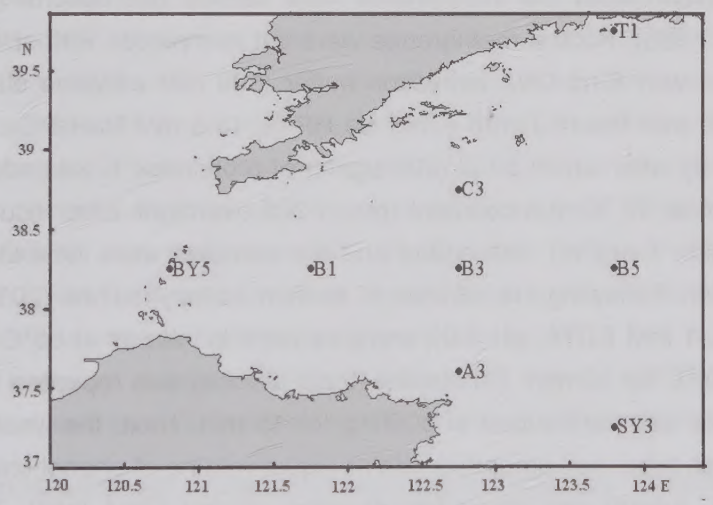

Fig. 1 Sampling stations in the Northern Yellow Sea

2.2 Enumeration and isolation of cultivable heterotrophic bacteria by traditional culture methods

Samples for cultivable heterotrophic bacteria were processed within 1 h of sampling. Serial dilutions (1:10, 1:100 and 1:100) were prepared using filter-sterilized seawater, after which 100 μl of each dilution was plated on three replicate plates of Marine Agar 2216. Colony forming units were counted after incubation at 25 °C in the dark for 1 to 2 weeks. Colonies were selected, picked and purified according to differences in color and shape. We assigned a triple code for each strain, for example B3/SML/02 indicates strain number 2 isolated from Site B3 using a glass plate.

2.3 Enumeration of total bacteria by flow cytometry

Samples (6 ml) for flow cytometry analyses of total bacteria and photosynthetic eukaryotes were fixed with formaldehyde (2% final concentration). The samples were then left at room temperature for 10 to 15 min, frozen and stored at -80 °C until the analysis. Bacteria were stained with a nucleic acid dye (Genefinder™; final concentration 0.01% [v/v]) and stored for at least 15 min at room temperature in the dark before counting was conducted. The samples were run through a flow cytometer (FACScan, Becton Dickinson) equipped with a 488 nm, 15 mW Argon laser. Stained bacteria were discriminated and counted according to their right angle light scatter, and the green fluorescence was then measured at 530/30 nm (Marie et al., 1997; Marie et al., 2000).

2.4 DNA extraction

DNA extraction from the membranes was carried out according to established methods (Zhou, 1996). Pooled membranes were cut into pieces with scissors in the tube and then shaken with 5 ml DNA extraction buffer (100 mM ethylene diamine tetraacetic acid (EDTA), 100 mM Tris-HCl, 186.4 mM Na_2HPO_4, 13.6 mM NaH_2PO_4, 1.5 M NaCl, 1% (w/v) CTAB, pH 8), after which 50 µl (200 µg/ml) of proteinase K was added to each tube before incubation at 37 °C at a constant rpm of 225 overnight. After incubation, lysozyme (final concentration 1 mg/ml) was added and the samples were incubated for 30 min at 37°C and 225 rpm. Following the addition of sodium dodecyl sulfate (20% [w/v]) and 1 ml TE (10 mM Tris, 1 mM EDTA, pH 8.0), samples were incubated at 65°C for 30 min, then incubated at −80 °C for 30 min. This freeze–thaw process was repeated three times, after which the sample was centrifuged at 8000×*g* for 15 min. Next, the lysate was removed, placed into a fresh tube, and amended with an equal volume of phenol:chloro-form:isoamyl alcohol (25:24:1, [v/v/v]) and chloro-form-isoamyl alcohol (24:1 [v/v]). The sample was subsequently centrifuged at 15,000×*g* for 15 min, after which the supernatant was placed into a fresh tube and mixed with an equal volume of chloroform-isoamyl alcohol (24:1 [v/v]). Following centrifugation (15,000×*g*, 15 min), DNA was precipitated with 0.6 volumes of isopropanol and recovered by centrifugation for 10 min at 12,000×*g* and 4 °C. The recovered DNA was then washed with ice-cold ethanol (70%, v/v, 4°C), air dried and diluted in 100 µl of sterile TE Buffer (10 mM Tris, 1 mM EDTA, pH 8.0). Finally, the DNA samples were stored at -20 °C until use. PCR products were purified using a PCR Purification Kit (Takara, Japan) according to the manufacturer's instructions.

2.5 PCR and DGGE

Following DNA extraction, PCR amplification of 16S rRNA was performed using the

27f (5′-AGAGTT TGATCCTGGCTCAG-3′) and 1492R (5′-GGTTACCTTGTTACGACTT-3′) (Lane, 1991) primers, which correspond to *Escherichia coli* positions 8 - 27 and 1 492 - 1 510, respectively. For all PCR analyses, a total volume of 50 ml, containing 2.5 μM dNTP (deoxynucleoside triphosphate), 4 pmol of each primer, 1.25 U Taq DNA polymerase (TaKaRa, Japan), 5.0 μL 10×PCR buffer (TaKaRa, Japan) and 30 ng DNA, was used. The PCR program consisted of initial denaturation at 94 °C for 5 min followed by 30 cycles of 94 °C for 30 s, annealing at 52 °C for 30 s, extension at 72 °C for 1 min and final elongation at 72 °C for 10 min. PCR products were verified by agarose gel electrophoresis and stored at −20 °C.

For DGGE with bacterial 16S rRNA genes, a nested PCR approach was employed by first conducting the reaction using primers 27F and 1492R, followed by PCR with primers 338F (5′-CGCCCGCCGCGCGCGGCGGGCGGGGCGGGGGCACGGGGGGACTCCTAC GGGAGGCAGCAG-3′) and 518R (5′-ATT ACC GCG GCTGCT GG-3′) (Muyzer et al., 1993). Primer 338F has a GC-clamp at the 5′-end. For PCR, a total volume of 50 μl that contained 5.0 μM dNTP, 6 pmol of each primer, 1.25 U Taq DNA polymerase (TaKaRa, Japan), 5.0 μl 10 × PCR buffer (TaKaRa, Japan) and 30 ng DNA was used. The PCR program consisted of initial denaturation at 95 °C for 5 min, followed by 30 cycles of 95°C for 1 min, annealing at 53°C for 1 min, elongation at 72 °C for 2 min and a final elongation step at 72 °C for 10 min. A negative control was used for each set of reactions to ensure no contamination. DGGE was conducted with the Dcode™ Universal Mutation Detection System (BioRad, USA). Gels were prepared using 8% (w/v) acrylamide/bisacrylamide with a 30% to 60% linear denaturant gradients. The gel was run in 1× TAE buffer at 60°C for a total of 1000 Vh (constant voltage 200 V, 5 h). Gels were stained with Genefinder™ before the image was captured on a UV trans-illuminator (Kodak GL2000, USA).

DGGE bands were then excised as described previously (Schwieger and Tebbe, 1998), washed in sterile molecular-grade water, crushed in 20 μl of molecular-grade water and incubated at 4 °C for 10 h. The eluted DNA was employed for reamplification and another round of electrophoresis again in a DGGE gel using the same PCR primers and conditions as before. The PCR products with the appropriate forward PCR primer without the GC clamp were purified using a PCR purification kit (Takara, Japan), then ligated into pMD®19-T Vector (Takara, Japan) before being transformed into *Escherichia* coli DH5. Positive colonies were selected at random and their inserts were amplified and screened to determine their migration positions by agarose gel electrophoresis. Subsequently, clones with migrating inserts were sequenced (Sangon, Shanghai, China).

2.6 Phylogenetic analyses and community analysis

The sequences of the DGGE bands determined in this study were investigated for homology and closest relatives in GenBank using the BLASTN search tool (http: //www.ncbi. nlm.nih.gov). To construct a cladogram, the sequences determined in this study were aligned with Clustal X1.8 (Thompson, J. R. et al., 1997). A neighbor-joining tree was created using Kimura two-parameter, and cluster stability was assessed by bootstrap analyses based on 1000 replicates using the MEGA program (version 3.1) (Kumar, S. et al., 2004).

The DGGE image was analyzed using the Kodak MI Analysis software (Kodak G L, 2000). Principal component analysis (PCA) was employed to estimate the extent of the correlation between the bacterial community (i.e. DGGE bands) using the software program Canoco (version 4.15). Bacterial 16S rRNA gene DGGE profiles were compared using NTsys 2.10 by constructing an UPGMA dendrogram from the calculated similarity coefficients using an SM coefficient. The relative data of the DNA bands from the bacterial communities were analyzed to detect grouping patterns. The Shannon-Weaver index of general diversity, *H'*, was calculated according to the relative intensity of each band with the following equation: $H=-\sum(ni/N)ln(ni/N)$, where *ni* is the intensity of gel band fluorescence and *N* is total intensity of all bands in that lane.

3 Results

3.1 Total counts, percentage culturability and enrichment factors (EF)

The total average bacterial counts for SML and subsurface waters in the Northern Yellow Sea ranged from 1.43×10^6 to 2.26×10^6 cells ml^{-1} and 0.74×10^6 to 1.38×10^6 cells/ml, respectively (Tab.1). Higher cell concentrations were found in C3, while slightly higher, but not significant, levels were observed in the SML samples relative to the subsurface water samples. Colonies grown on marine agar showed higher percent culturability vs. total counts in SML than in subsurface waters (Tab. 1). Additionally, the average culturability was 7.86% to 33.57% in SML, while it was 0.13% to 1.03% in subsurface waters. The culturable bacteria for SML and subsurface water were 2.85×10^5 and 3.45×10^3, respectively (data not shown). Therefore, the percentage culturable bacteria were higher in SML than those in subsurface waters.

EF was calculated as the ratio of biological parameters in the SML to those in subsurface waters. An EF > 1.0 indicates enrichment in the SML, while an EF < 1.0

indicates depletion. In the present study, the EF values of samples collected from different sites differed significantly. The variation in EF of culturable bacteria (13.81 - 165.65) was higher than that of total bacteria (1.08 - 2.95) in this study.

Tab. 1 Bacterial counts, culturability (percentage vs. total cells count) and EF in the sea surface microlayer (SML) and subsurface water (sub) from eight sites

Sites		A3	B1	B3	B5	BY5	C3	SY3	T1
Total countsa (10^6 cells/ml)	SML	1.84±1.17	1.93±0.92	1.53±1.10	1.43±1.11	1.59±1.87	2.26±1.24	1.76±0.96	1.76±0.90
	sub	1.26±1.04	1.01±0.62	1.02±0.59	0.79±0.40	1.38±1.53	1.08±0.52	0.74±0.40	1.28±0.38
Average culturability (%) mean	SML	33.57	11.68	18.40	7.86	1.14	8.89	12.76	10.07
	sub	0.59	0.50	0.33	0.13	0.40	0.30	1.03	0.32
EF mean	Total bacteria	2.10	2.91	1.56	1.65	1.08	2.48	2.95	1.43
	Cultural bacteria	165.65	81.62	81.82	91.35	13.81	90.10	25.53	43.38

EF: enrichment factors; a: Mean ± SD.

3.2 Phylogenetic diversity of culturable heterotrophic bacterial strains

Overall, 53 isolates from eight sites and both layers were isolated for 16S rDNA sequencing and phylogenetic analysis (Fig. 2). We did not detect differences in bacterial species. All strains could be clustered into four phylogenetic bacterial groups (Fig. 2): proteobacteria (94.34%), firmicutes (1.89%), bacteroidetes (1.89%) and actinobacteria (1.89%). Gammaproteobacteria was the predominant group cultured in all samples. The similarities of the 16S rRNA gene sequences from each culture with previously reported species are presented in Tab. 2. Sequence homologies to known sequences in the NCBI database ranged from 97% to 100%. Fifty isolates belonging to Proteobacteria fell into the Alpha and Gamma subdivisions. Additionally, 43 isolates were affiliated with nine genera: *Alteromonas* (5), *Marinobacter* (4), *Idiomarina* (1), *Pseudoalteromonas* (19), *Cobetia* (2), *Halomonas* (3), *Acinetobacter* (1), *Psychrobacter* (6) and *Vibrio* (2), while seven isolates were affiliated with three genera: *Paracoccus* (4), *Maricaulis* (1) and *Erythrobacter* (2). The remaining three isolates belonged to *Bacillus*, *Frigoribacterium* and *Mesonia*.

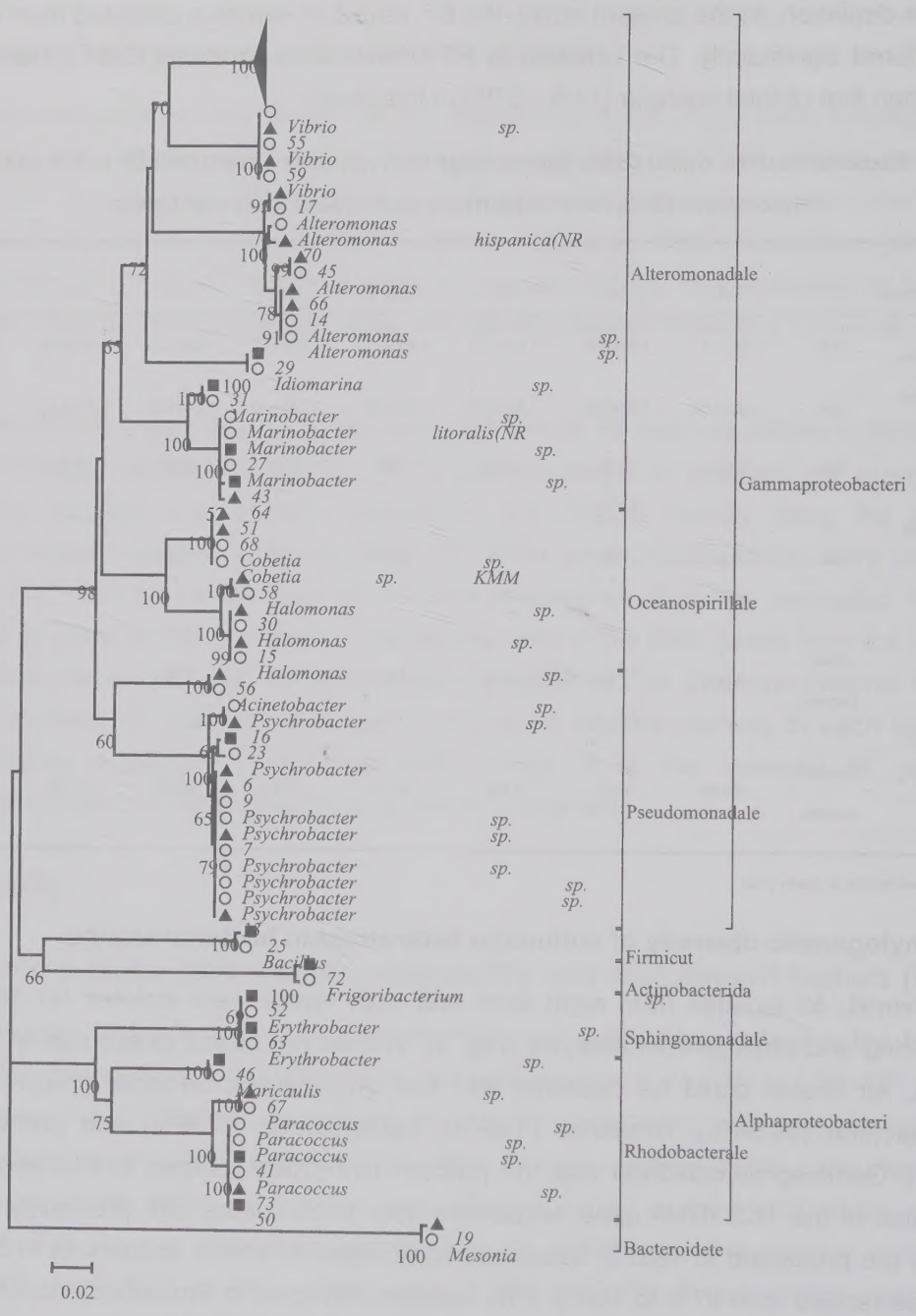

Fig. 2 Phylogenetic analysis of the cultured bacterial groups inhabiting the Northern Yellow Sea stations. A tree was constructed using the Neighbor-Joining method. Sequences from this study are in boldface type. Bootstrap values > 55% (of 100 iterations) are shown. The scale bar represents one substitution for every ten nucleotides.

Tab. 2 Sequence similarity of the 16S rRNA gene of isolated strains to the closest matching relative in the data bank

Code	Closest Sequence Accession	Closest species	Homology / %
T1/Sub/23	FJ161358	*Psychrobacter celer*	98
BY5/Sub/25	HQ143564	*Bacillus cereus*	99
B5/Sub/45	AB238950	*Alteromonas macleodii*	98
BY5/Sub/29	DQ985070	*Idiomarina sp.* JL1018	98
BY5/Sub/35	AB106189	*Pseudoalteromonas sp.* FRA000006	98
BY5/Sub/41	AB526330	*Paracoccus sp.* JAM-AL07	98
B5/Sub/43	NR_028841	*Marinobacter litoralis*	98
BY5/Sub/46	AJ301666	*Maricaulis sp.* MCS31	99
BY5/Sub/50	FJ457301	*Paracoccus sp.* S4495	99
BY5/Sub/52	FM992798	*Erythrobacter sp.* M71_N109	99
B3/Sub/66	FM992724	*Alteromonas sp.* M71_D56	99
BY5/Sub/72	DQ166179	*Frigoribacterium sp.* TSBY-18	99
BY5/Sub/4	FR750947	*Pseudoalteromonas tetraodonis*	98
BY5/Sub/31	JN684908	*Marinobacter sp.* MnI7-9	99
B1/Sub/63	AB429067	*Erythrobacter sp.* OC4	99
BY5/Sub/27	DQ328954	*Marinobacter sp.* BWDY-54	99
A3/Sub/22	FJ665500	*Pseudoalteromonas sp.* LJ1	99
BY5/SML/44	GU120031	*Pseudoalteromonas sp.* ArcB8453012	99
SY3/SML/55	JF700503	*Vibrio alginolyticus*	98
SY3/SML/56	EU037279	*Acinetobacter sp.* G3DM-29	98
B5/SML/51	FJ210806	*Cobetia sp.* QDHT-10	99
B5/SML/59	EF187013	*Vibrio sp.* Y4tang	100
B3/SML/73	GU338411	*Paracoccus sp.* DB11	99
BY5/SML/2	HQ658897	*Pseudoalteromonas tetraodonis*	99
B5/SML/3	JN578478	*Pseudoalteromonas sp.* H7	99
BY5/SML/5	EU268239	marine bacterium 8ORI3	99
BY5/SML/6	HM584266	*Psychrobacter sp.* CJ-G-PYD3	100
B5/SML/8	AY028199	marine bacterium Tw-4	97
B5/SML/18	GQ885144	*Pseudoalteromonas issachenkonii*	99
BY5/SML/61	AB526340	*Pseudoalteromonas sp.* JAM-GA17	99
B1/SML/12	AB563179	*Pseudoalteromonas tetraodonis*	99
B5/SML/7	JF706641	*Psychrobacter sp.* ST4	100
BY5/SML/16	AY553082	*Psychrobacter sp.* GSP50	99
A3/SML/17	AB015135	*Alteromonas sp.*	99
BY5/SML/26	HM627538	*Pseudoalteromonas sp.* HJ24	99
SY3/SML/30	FJ889578	*Halomonas sp.* K1B-11	99
B5/SML/14	GQ200198	*Alteromonas sp.* DQHS-18	99
T1/SML/58	FJ746582	*Halomonas sp.* H146B85	98
SY3/SML/28	FJ170035	*Pseudoalteromonas sp.* CF14-5	98
BY5/SML/42	FJ497705	*Pseudoalteromonas sp.* VS-4	98
B5/SML/64	FJ903190	*Marinobacter sp.* H3(2009)	99

T1/SML/67	GQ199613	*Paracoccus sp.* BSw21443	98
T1/SML/68	AB646236	*Cobetia sp.* KMM 1561	99
A3/SML/1	DQ412067	*Pseudoalteromonas sp.* LOB-15	99
SY3/SML/10	AF280818	*Pseudoalteromonas sp.* DC1	98
SY3/SML/11	DQ412067	*Pseudoalteromonas sp.* LOB-15	99
B3/SML/13	HM593102	*Psychrobacter sp.* Z1	99
BY5/SML/15	AB526344	*Halomonas sp.* JAM-GA21	100
SY3/SML/9	HM584288	*Psychrobacter sp.* CJ-G-R2A6	99
BY5/SML/20	FR839670	*Pseudoalteromonas sp.* NW 4327	99
A3/SML/19	AF536384	*Mesonia algae*	98
T1/SML/70	NR_043274	*Alteromonas hispanica*	99
SY3/SML/24	FJ461453	*Pseudoalteromonas sp.* SCSWD13	98

3.3 Bacterial community structures and diversity

To identify the specific dominant species in the bacterial community based on the DGGE patterns, 32 specific bands were excised from the gel, reamplified and sequenced (Fig. 3). Tab. 3 and Fig. 4 show the relationship of sequences from the excised DGGE bands and the closest sequences in GenBank. Bands with the same number in the DGGE patterns showed similar sequences. Phylogenetic analysis revealed that all sequences were affiliated with five different subtaxa, Actinobacteria, Bacteroidetes, Cyanobacteria, Proteobacteria and Verrucomicrobia (Fig. 4). Bacteroidetes, Proteobacteria, Cyanobacteria and other groups contained eight bands, 20 bands, two bands and one band, respectively.

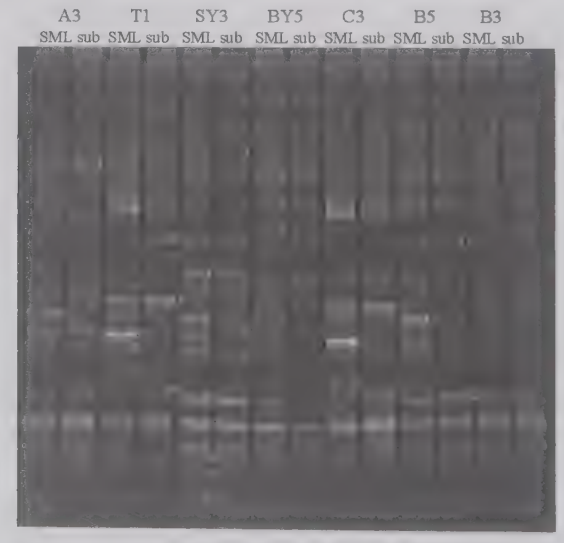

Fig. 3 Denaturing gradient gel electrophoresis (DGGE) profiles of bacterial 16S rRNA gene PCR amplicons showing microbial community structure in the surface microlayer (SML) and subsurface (sub) of seven sites (A3, T1, SY3, BY5, C3, B5 and B3) in the Northern Yellow Sea. The numbered DGGE bands are those that were excised and sequenced (Tab. 1)

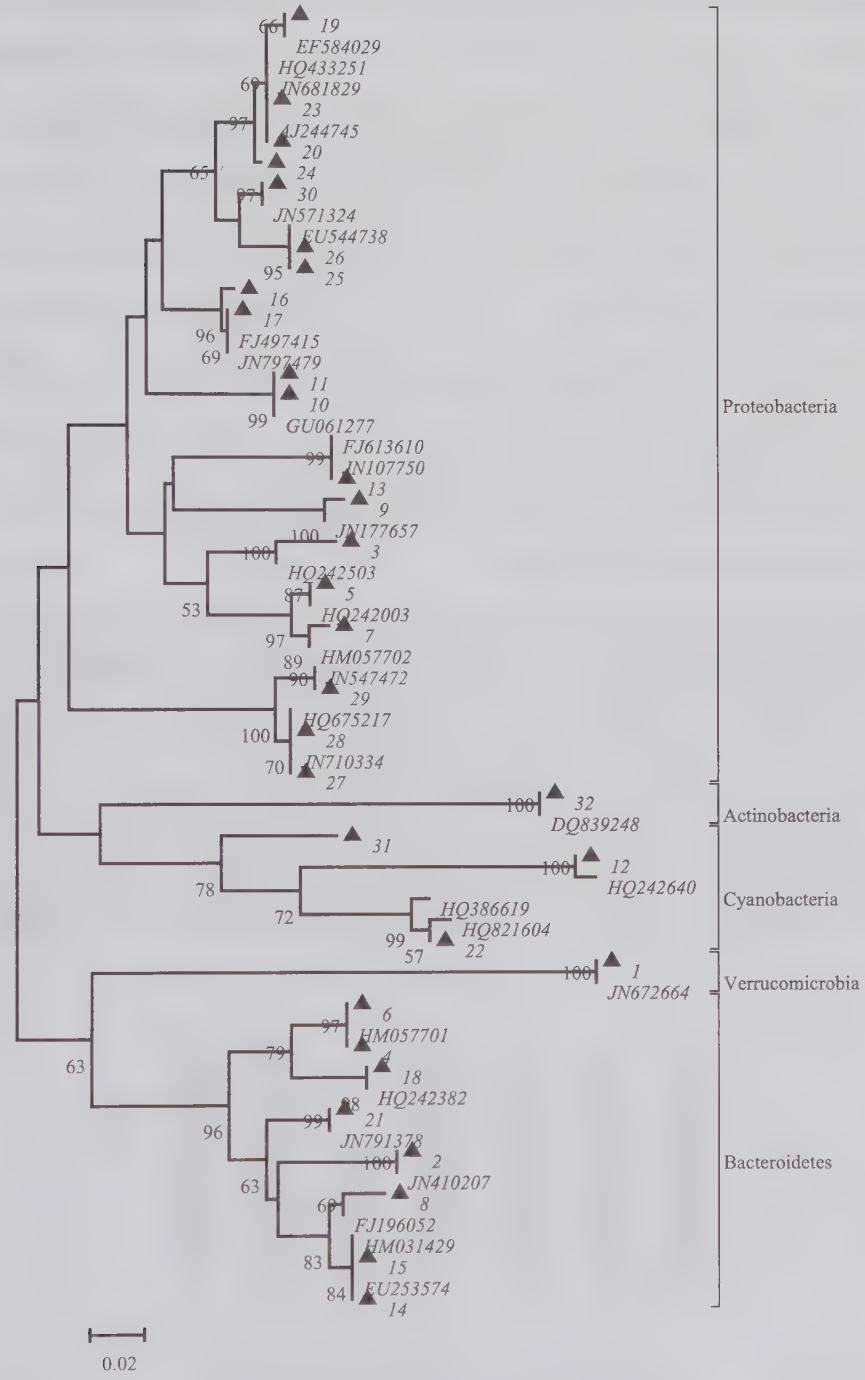

Fig. 4 Phylogenetic analysis of bacterial 16S rRNA gene sequences obtained from the surface microlayer and subsurface waters of seven sites and sequences available from public nucleotide databases. The tree was derived using the Neighbor-Joining method and the scale bar represents one substitution for every ten nucleotides.

Proteobacteria were found in this study and the members of this division were environmentally widespread and ecologically important. In addition, Proteobacteria is a recently recognized bacterial division with several cultivated representatives. In this study, two monophyletic subdivisions were identified based on the available sequences (Fig. 4 and Tab. 3). Four sequences fell into the Alphaproteobactera, while 16 bands clustered with Gammaproteobactera based on the phylogenetic analysis. Sequences 19, 20, 23 and 24 showed > 99% similarity to *Pseudoalteromonas*, while sequences 13 and 30 showed 100% similarity to *Psychrobacter* (JN107750) and *Enterobacteriaceae* (JN571324), respectively. The sequence of band 31 exhibited 91% sequence similarity with *Psychrobacter* (FJ613610), whereas it clustered with Cyanobacteria. Therefore, it may be a branch of the cyanobacteria. Bands 16 and 17 showed 100% homology with *Alteromonas*, clustering within the subphylum of Gammaproteobactera (Fig. 3 and Fig. 4), while the other bands were not defined in Gammaproteobactera. However, bands 3, 5, 27, 28 and 29 were related to the SAR cluster.

The phylogenetic relationships of the 32 sequenced bands are shown in Fig. 4. The sequence corresponding to band 21 exhibited 100% sequence similarity with *Gramella* (JN791378), which is a member of the Flavobacteriaceae family. Band 8 showed about 99% homology to *Polaribacter* (FJ196052), while bands 14 and 15 were about 100% homologous with *Tenacibaculum*. In addition, the taxonomic status of the sequences of bands 4, 6 and 18 need to be determined. Moreover, the sequence of band 18 was 100% homologous with that of an uncultured Bacteroidetes/Chlorobi group bacterium clustered with Flavobacteriaceae. Hence, it was more appropriately classified as Bacteroides.

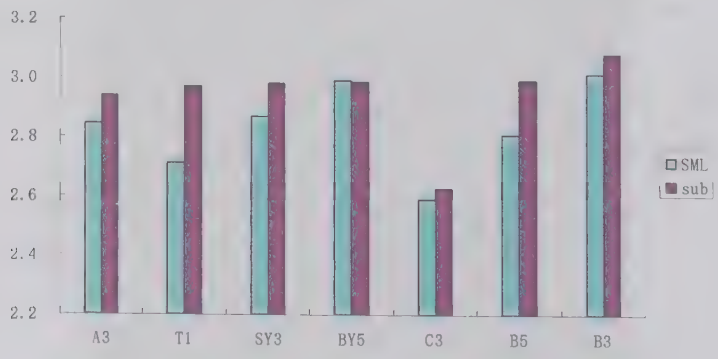

Fig. 5 Shannon diversity index (H) values

In this study, the Shannon diversity index revealed differences between the relative diversities estimated by DGGE. The Shannon indexes of bacterial diversity, H, are presented in Tab. 1. The indexes varied between 2.587 and 3.076, and the values showed a higher diversity of bacterial populations in subsurface waters than the sea surface

microlayer. In addition, the evenness values observed were 0.920 and 0.955 in the SML and subsurface waters, respectively.

Tab. 3 Phylogenetic affiliations of bacterial 16S rRNA gene sequences obtained from DGGE (Fig. 3)

No.	Locus	Source	similarity	Title
1	JN672664	uncultured Verrucomicrobia bacterium	99	East China sea
2	FQ032809	uncultured Flavobacteria bacterium	100	Direct Submission
3	HQ24250	uncultured SAR11 cluster alpha proteobacterium	100	the North East Pacific
4	HM05770	uncultured Flavobacteriia bacterium	100	Yellow Sea water
5	HQ24200	uncultured SAR86 cluster bacterium	100	the North East Pacific
6	HM05770	uncultured Flavobacteriia bacterium	100	in Yellow Sea water
7	HM05770	uncultured gamma proteobacterium	99	in Yellow Sea water
8	FJ196052	*Polaribacter* sp. NF3-11	99	Antarctic Sea water
9	JN177657	uncultured gamma proteobacterium	99	in the Arctic Ocean
10	GU06127	uncultured gamma proteobacterium	99	from the Yellow Sea
11	GU06127	uncultured gamma proteobacterium	99	from the Yellow Sea
12	HQ24264	uncultured cyanobacterium	100	the North East Pacific
13	JN107750	Psychrobacter nivimaris	100	?
14	HM03142	uncultured Flavobacteriaceae bacterium	100	marine fishes
15	EU253574	*Tenacibaculum* sp. MED341	100	in the NW Mediterranean Sea
16	FJ497415	uncultured gamma proteobacterium	99	Vailulu'u Seamount
17	JN797479	*Alteromonas* sp. AP3	100	?
18	HQ24238	uncultured Bacteroidetes/Chlorobi group bacterium	100	the North East Pacific
19	EF584029	*Pseudoalteromonas* sp. CCS2	100	from Sydney Harbour, Australia
20	HQ43325	Pseudoalteromonas sp. CBMAI 1223	100	Brazilian coast
21	JN791378	*Gramella* sp. MM24	100	marine sediment from Ximen Island
22	HQ82160	uncultured bacterium	100	Coastal Bacterioplankton
23	JN681829	*Pseudoalteromonas* arctica	100	Danish coastal waters
24	AJ244745	*Pseudoalteromonas* sp. V4.ME.31	99	Westlichen Mittelmeer
25	EU544738	uncultured gamma proteobacterium	100	in the Laptev Sea
26	EU544738	uncultured gamma proteobacterium	100	in the Laptev Sea
27	JN710334	uncultured Pelagibacter sp.	99	in tropical Atlantic Ocean
28	HQ67521	alpha *proteobacterium* SCGC AAA298-C11	100	in the dark ocean
29	JN547472	uncultured SAR11 cluster alpha proteobacterium	100	in the Red Sea
30	JN571324	*Enterobacteriaceae* bacterium DJC-1-1	100	in Tibetan Plateau lakes
31	FJ613610	*Psychrobacter* celer	91	he southwest Pacific
32	DQ83924	uncultured actinobacterium	99	Bacteria associated with copepods

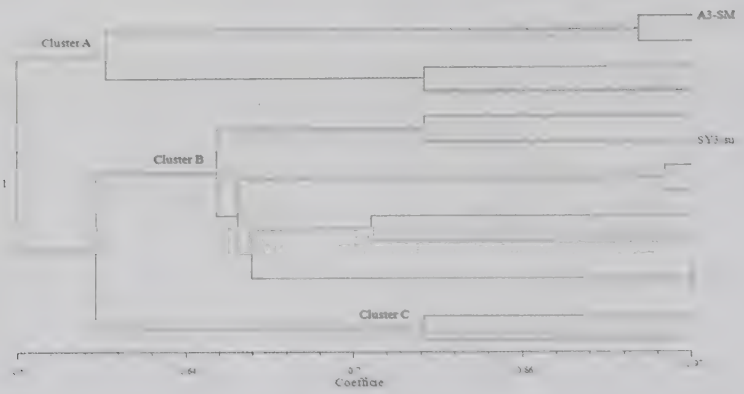

Fig. 6 Dendrograms showing the similarity of DGGE profiles of 16S rRNA gene PCR amplicons of bacteria from samples collected from the sea microlayer surface (SML) and subsurface water (sub) at seven sites in the Northern Yellow Sea

DNA extracted from the surface microlayer and subsurface water samples from seven sites was used as a template for PCR with primers targeting bacterial 16S rRNA genes. This was followed by DGGE of the PCR amplicons to compare the total patterns of bacterial communities present. Bacterial community structures, banding patterns of bacterial 16S rRNA gene PCR amplicons from DGGE and subsequent pattern cluster analysis indicated that the bacterial communities in the surface microlayer and subsurface waters had different distributions (Fig. 3 and Fig. 6). There was a high degree of similarity between samples from the same site (Fig. 6). Bacterial community structures in samples collected from the SML were more similar (>76% similarity) to their cognate subsurface (0.5 m) samples than to the bacterial community structures of SML at all sites. Bacterial communities in the SML and subsurface water samples differed greatly between the sites (Fig. 3 and Fig. 4). UPGMA dendrograms revealed two distinct clusters of the DGGE profile. One cluster was composed of samples collected from A3 and T1, indicating that the bacterial community structure of the coastal sites was different from that of the other sites.

Principal component analysis showed a clear distinction between samples, reflecting the diversity of the bacterial communities. The presence/absence of bands of the PCA plot for the bacterial communities resolved the 14 samples into three distinct clusters and indicated the similarity of bacterial communities among sites (Fig. 7). These groups corresponded to clusters A, B and C in the cluster analysis. The first component accounted for 24.0% of the variance, while the second component accounted for 15.9%, which explained 39.9% of the total variance in the plot (Fig. 7). The PCA plot revealed that samples 1 - 4 (A3 and T1 sites) and 9 - 10 (C3 site) were contained within two well-resolved groups, while there was an overlap of the remaining sites.

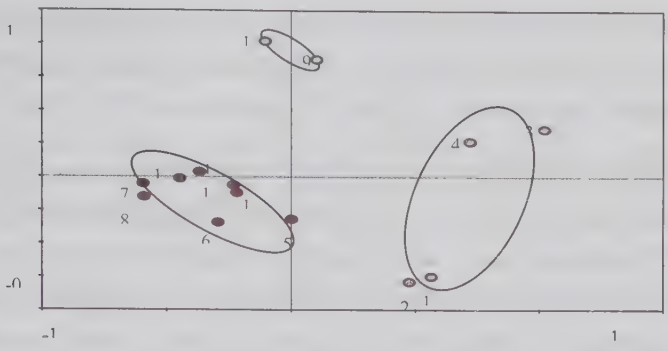

Fig. 7 Principal component analysis plot of DGGE profiles of SML and subsurface water samples from the seven sites. The first two components explained 24.0% and 15.9% of the total variance, respectively.

4 Discussion

The percentages of bacterial culturability reported in this study greatly varied from 0.13% to 33.57% of the total cell counts, but the mean values were consistently higher for the surface microlayer. This is easily explained by the accumulation of organic matter at this interface. In addition, other reports have shown that biochemical and bacterial activities increase in the surface microlayer when compared to underlying waters (Carlucci, A.F. et al., 1985; Mudryk, Z. et al., 1991). This would explain why bacterial species isolated from the surface microlayer represent a higher fraction of total bacteria than in underlying waters.

Reports of the abundance of total bacteria in the SML vary greatly among studies. While some studies have reported EF values from 102 to 103 (Marumo, et al., 1971; Harvey and Young, 1980a, 1980b; Carlucci, et al., 1991), Agogué found only a slight, but significant enrichment of total bacterial counts in the SML when samples were collected with the GP and the mesh screens (MS) (Hélène Agoguéet, et al., 2004). In the present study, the EF of cultured bacteria was higher than that of total bacteria. The enrichment of CFU in the SML could be explained by (1) the higher concentrations of dissolved and colloidal organic compounds in the SML providing energy and nutrients, (2) the protective agents against stress factors such as radiation (Liss and Duce, 2005), and (3) the preferential attachment of living cells with polarized membranes to bubbles and particles (Agogué, et al., 2004). The lower values reported in this study could have been due to the fact that particle-attached bacteria could not be counted by flow cytometry and may represent a significant part of the total bacteria present in the SML (Harvey and Young, 1980). Furthermore, the depth at which samples of subsurface water are collected should

be carefully defined because variations in the depth at which subsurface water are collected may result in different EF. Obviously, comparison of the data obtained in different layers is closely related to the different types of organisms.

There have been problems reported with analysis of the bacterial community structure using DGGE. Muyzer et al. stated that DGGE only detected dominant bacterial groups. Specifically, only one band would appear when nucleotide sequences from two different microorganisms had the same GC contents. In such cases, microbial diversity would be underestimated. Additionally, 32 bands in the DGGE pattern were further selected, cloned and sequenced. Based on similarity matching, all sequences formed five major clusters, Actinobacteria, Bacteroidetes, Cyanobacteria, Proteobacteria and Verrucomicrobia. Bands that showed the same electrophoretic mobility were excised (bands 10 and 11, 14 and 15, 16 and 17, 19 and 20, 23 and 24, 26 and 27, 28 and 29). We found that the sequences of 10 and 11 were equivalent, as were those of 14 and 15, and 25 and 26. Moreover, only one base pair differed between band 16 and 17. BLAST analyses revealed that the sequences of band 19 and 20 belonged to the same genus, although there were some differences between them. Interestingly, the same results were observed for bands 23 and 24. The results of this study indicated that there was some bias in the use of DGGE to detect microbial diversity. Overall, it is best to sequence the bands on the same level and attempt to excise all bands from different samples to reflect the microbial diversity of the environment more accurately. The sequence of band 3 exhibited 91% sequence similarity with uncultured SAR11 cluster alpha proteobacterium, whereas it grouped with Gammaproteobactera. Furthermore, bands 27, 28 and 29 fell in the SAR11 cluster. Based on these findings, the results of phylogenetic tree analysis should be combined with those of the BLAST analyses to define the species classification and explain the evolutionary development of bacteria more comprehensively.

The SAR11 cluster of alpha proteobacterium was found in both the surface microlayer and subsurface waters, suggesting that surface microlayer species are the same as subsurface water species. Overall, the DGGE profile indicated that, in most cases, the same bacterial populations dominated the surface microlayer and subsurface waters. This can be explained by the finding that most bacteria in the surface microlayer are planktonic cells that accumulate from a passive flotation process, although these cells may grow in the surface microlayer (Helene Agogue, et al., 2005). The predominant bacterial populations were proteobacterium (*Pseudoalteromonas*, band 19 and 20) and bacteroidetes (14 b and 15) for SML and the corresponding subsurface waters at sites T1 and C3. Additionally, the fact that similar DGGE profiles were found suggests that some neustonic species do not occur in subsurface waters. It has been suggested that specific

neustonic bacterial species are rare rather than abundant. Additionally, they are likely well-adapted to handle high concentrations of detrimental factors (such as intense solar radiation, high concentrations of heavy metals and organic pollutants, temperature fluctuations and salinity changes) that are present in the surface microlayer.

The results of this study confirm that the SML has a distinct microbial community structure from the corresponding subsurface water and for the first time describes a detailed molecular biological analysis of the bacterioneuston in the Yellow Sea in China. Furthermore, future studies should be aimed at investigating the factors influencing bacterioneuston activity and gaining detailed insights into its structure and function. For this purpose, it is essential to characterize the effects of different physicochemical parameters at the molecular level using not only 16S rRNA technology, but also molecular ecology techniques.

Acknowledgements

This work was supported by the Natural Science Foundation of China (No. 41406129), the National Key Research Program (Grant 2016YFA0601400), and the State Oceanic Administration of China(Grant GASI-03-01-02-05).

References

[1] Agogué H, Casamayor E O, Joux F, et al. Comparison of samplers for the biological characterization of the sea surface microlayer [J]. Limnol. Oceanogr. Meth., 2004, 2: 213 - 225.

[2] Agogué H, Casamayor E O, Bourrain M, et al. A survey on bacteria inhabiting the sea surface microlayer of coastal ecosystems [J]. FEMS. Microbiol. Ecol., 2005, 54:269 - 280.

[3] Baastrup-Spohr L, Staehr P A. Surface microlayers on temperate lowland lakes [J]. Hydrobiologia, 2009, 625: 43 - 59.

[4] Carlson D J. A field evaluation of plate and screen microlayer sampling techniques [J]. Mar. Chem., 1982, 11:189 - 208.

[5] Carlucci A F, Craven D B, Henrichs S M. Surface-film microheterotrophs: amino acid metabolism and solar radiation effects on their activities [J]. Mar. Biol., 1985, 85: 13 - 22.

[6] Carlucci A F, D B Craven, D M Wolgast. Microbial populations in surface films and subsurface waters: amino acid metabolism and growth [J]. Mar. Biol., 1991, 108: 329 - 339.

[7] Cunliffe M, M Salter, P J Mann, et al. Dissolved organic carbon and bacterial populations in the gelatinous surface microlayer of a Norwegian fjord mesocosm [J]. FEMS Microbiol. Lett., 2009, 299: 248 - 254.

[8] Franklin M P, McDonald I R, Bourne D G, et al. Bacterial diversity in the bacterioneuston (sea

surface microlayer): the bacterioneuston through the looking glass [J]. Environ. Microbiol., 2005, 7: 723 - 736.

[9] Fromin N, Hamelin J, Tarnawski S, et al. Statistical analysis of denaturing gel electrophoresis (DGE) fingerprinting patterns. Environmental Microbiology, 2002, 4: 634 - 643.

[10] Harvey G W. Microlayer collection from the sea surface: a new method and initial results [J]. Limnol. Oceanogr., 1996, 11: 608 - 614.

[11] Harvey G W, Burzell L A. A simple microlayer method for small samples [J]. Limnol Oceanogr., 1972, 11: 156 - 157.

[12] Marie D, Partensky F, Jacquet S, et al. Enumeration and cell cycle analysis of natural populations of marine picoplankton by flow cytometry using the nucleic acid stain SYBR Green I [J]. Appl. Environ. Microbiol., 1997, 63: 188 - 193.

[13] Harvey R W, L Y Young. Enrichment and association of bacteria and particulates in salt march surface waters [J]. Appl. Environ. Microbiol., 1980a, 39: 894 - 899.

[14] Hardy J T. Biological effects of chemicals in the seasurface microlayer. In: Liss PS, Duce RA (eds) The sea surface and global change [M]. Cambridge: Cambridge University Press, 1997, p339 - 370.

[15] Hörtnagl P, M T Pérez, R Sommaruga. Living at the border: a community and single-cell assessment of lake bacterioneuston activity [M]. Limnol. Oceanogr., 2010, 55: 1 134 - 1 144.

[16] Joux F, H Agogue, I Obernosterer, et al. Microbial community structure in the sea surface microlayer at two contrasting coastal sites in the northwestern Mediterranean Sea [J]. Aquat. Microb. Ecol., 2006, 42:91 - 104.

[17] Kumar S, Tamura K, Nei M. Integrated software for molecular evolutionary genetics analysis and sequence alignment. Briefings in bioinformatics, 2004, 5(2):150 - 163.

[18] Lane D J. 16S/23S rRNA sequencing. In Nucleic Acid Techniques in Bacterial Systematics [M]. UK: John Wiley and Sons. 1991, p115 - 175.

[19] Liss P S, R A Duce. The sea surface and global change [M]. Cambridge University Press, 2015.

[20] Marumo R, N Taga, T Nakai. Neustonic bacteria and phytoplankton in surface microlayers of the Equatorial waters [J]. Bull. Plank. Soc. Japan, 1971, 18: 36 - 41.

[21] Marie D, Simon N, Guillou L, et al. Flow cytometry analysis of marine picoplankton. In: DeMaggio S.(ed) Living color: protocols in flow cytometry and cell sorting. Springer Verlag, Berlin. 2000, p421 - 454.

[22] Michael C, Andrew S W, Lindsay N, et al. Comparison of Bacterioneuston and Bacterioplankton Dynamics during a Phytoplankton Bloom in a Fjord Mesocosm [J]. Applied and environment microbiology, 2009, 75(22): 7 173 - 7 181.

[23] Mudryk Z, Korzeniewski K, Falkowska L. Bacteriological investigation of the surface microlayer of the Gulf of Gdansk [J]. Oceanologia, 1991, 30: 93 - 103.

[24] Muyzer G, de Waal E C, Uitterlinden A G. Profiling of complex microbial populations by denaturing gradient gel electrophoresis analysis of polymerase chain reactionamplified genes coding for 16S

rRNA [J]. Appl. Environ. Microbiol., 1993, 59: 695 - 700.

[25] Nauman E. Beiträge zur Kenntnis der Teichnannoplanktons. II. Über das Neuston des Süsswassers [J]. Biol. Zentralbl., 1917, 37(2): 98 - 106.

[26] Obernosterer I P, Catala R, Lami J, et al. Biochemical characteristics and bacterial community structure of the sea surface microlayer in the South Pacific Ocean [J]. Biogeosciences, 2008, 5: 693 - 705.

[27] Reinthaler T, Sintes E, Herndl G J. Dissolved organic matter and bacterial production and respiration in the sea-surface microlayer of the open Atlantic and the western Mediterranean Sea [J]. Limnol. Oceanogr., 2008, 53: 122 - 136.

[28] Thompson J R, Gibson T J, Plewniak F, et al. The ClustalX windows interface: flexible strategies for multiple sequence alignment aided by quality analysis tools [J]. J. Nucleic Acids Research, 1997, 24: 4 876 - 4 882.

[29] Wur O, Holmes M. The gelatinous nature of the sea-surface microlayer [J]. Mar. Chem., 2008, 110: 89 - 97.

[30] Wurl O, Miller L, Röttgers R, et al. The distribution and fate of surface-active substances in the sea-surface microlayer and water column. Mar. Chem., 2009, 115: 1 - 9.

[31] Zhang Z B, Lui L S, Wu Z J, et al.. Physiochemical studies of the sea surface microlayer-I. Thickness of the sea surface microlayer and its experimental determination [J]. J. Colloid and Interface Sci., 1998, 204: 294 - 299.

[32] Zhang Z, Liu L, Liu C, et al. Studies on the sea surface microlayer. II. The layer of sudden change of physical and chemical properties [J]. J. Colloid and Interface Sci., 2003, 264: 148 - 159.

中国北黄海微表层海水中细菌多样性

明红霞[1,2]，樊景凤[1,2*]，王小慧[1,2,3]，李洪波[1,2]，咎帅君[1,2,3]

（1. 国家海洋环境监测中心，辽宁 大连 116023；2. 国家海洋局近岸海域生态环境重点实验室 辽宁 大连 116023；3. 大连海洋大学，辽宁 大连 116023）

摘 要：微表层是海洋环境与大气对流层之间的一层生物膜，具有独特的海洋生态系统和物理化学、微生物组成。本研究采用传统的培养和流式细胞计数方法，比较了微表层和次表层（0.50 米深）的细菌丰度，并对筛选的 53 株菌进行了测序，分析了可培养细菌的群落结构。此外，直接从微表层和相应次表层海水中提取 DNA，通过变性梯度凝胶电泳（DGGE）方法分析了总细菌的群落结构。结果表明，海洋微表层存在一个特殊的生态群，其微生物群落结构明显不同于其相应次水层。本研究采用生态学分子技术全面阐述了中国北黄海微表层海水中的漂浮细菌群落结构。

关键词：微表层，细菌多样性，变性梯度凝胶电泳

Input characteristics and risk analysis of ballast water from offshore entry ships in China

DU Huan[2], ZHANG Xiao-fang[2], ZHANG Zhi-tao[1, 2], LIU Kai-ying[1], LI Ri-hong[2]

1. Environmental Engineering Institute, Dalian Maritime University, Dalian 116026, *Liaoning province, China;*

2. Marine Engineering College, Dalian Maritime University, Dalian 116026, *Liaoning province, China*

Abstract: Large quantities of ballast water discharge from ocean going ships in sea ports of China is one of the important factorswhich cause the spread of aquatic nonindigenous harmful species isolated geographically by waters, the deteriorating environment of the near-shore water area and the frequent outbreaks of red tides. In this paper, the total amount of the ballast water input estimation model for entry ships in Chinese ports was established. The information of foreign trade shipping and the import and export goods released publicly by the State Department of Transportation and the State General Administration of Customs were investigated. And then, the input features and its ecological environment risk of ballast water in China's offshore entry ships from 2007 to 2012 were analyzed based on the established total input amounts of ballast water from entry ships to Chinese sea ports together with the ballast water input ratio of the five major port-groups in China. The results show that: the total ballast water input amounts from entry ships of the five major port-groups in China are extremely imbalanced. The most developed Yangtze River Delta in economy has the biggest total ballast water input amounts, 103.61 million tons in 2012. The second is the Circum-Bohai Sea Region (73.66 million tons) and the third is the Pearl River Delta (67.24 million tons). The total ballast water input amounts of the northwest and the southwest coastal areas are less, only 16.57 and 5.71 million tons respectively. The large quantity of entry ships' ballast water discharge has been an enormous threat to ecological environment of our country's sea areas, especially to economically developed regions.

Keywords: ballast water; input of ballast water; marine environment and ecology; risk analysis

China has a coastline more than 18 000 kilometers long, and the scale of its ports

Received on Sep. 22, 2016

Corresponding author: dlmuduhuan@126.com

ranks first in the world (Ministry of Transport of China, 2013). Today, in China, there are thirty-nine foreign trade ports, 1 886 deep-water berths of over 10 000 ton class, and twenty-nine large ports of 108 ton class. Eight out of the world's top ten ports are located in China. Among them, the Ningbo-Zhoushan port boasts a cargo throughput of 744.01 million tons, becoming the largest one in the world. As one of the world's top ten marine transport countries, China owns enormous fleets, and the size of which ranks the third in the world, accounting for about 10.5% of the global fleets.

Considering safe navigation, cargo loading and other needs, ocean transport vessels will inevitably have to inject or discharge ballast water in coastal waters. The amount of ballast water in a ship with 100 000 tons of cargo carriers can be up to 50 to 60 thousand tons. According to the estimate of several researchers, there is about 3.5 to 12 billion tons of ballast water transferred and emitted across the world each year (Oemcke DJ, et al., 2003; Endresen O, et al., 2004; Pimentel D, et al., 2005; Chen C, 2013). Just within the Galveston Bay of the United States, from 2005 to 2010, approximately 120 million tons of ballast water was discharged through 45,000 ships (Jamie L S, et al., 2012).

An ocean transport vessel not only discharges ballast water from one sea area into another, but also emits a large number of aquatic organisms and pollutants into the latter area. In a ballast tank, there are 110 million planktons, 100 billion bacteria, 1 000 billion viruses per cubic meter of ballast water (Ruiz G M, et al., 2000; Mackenzie, et al., 1999; Fred C D, 2005). Ballast water is one of the main reasons that lead to the destruction of marine biodiversity on a global scale (Global Ballast Water Management Programme, 2003). The International Maritime Organization (IMO) has confirmed that around the world, there are 500 kinds of marine organisms spreading through ballast water (Carlton JT, 1994), through which sixteen kinds of exotic red tide algae have intruded into Chinese waters through ballast water of ships (Liang Y B, et al., 2001).

While the invasion of exotic marine organisms has brought shocking disasters to different sea areas around the world (Oemcke D J, et al., 2003; Ruiz G M, et al., 2000; Carlton J T, 2008), China is also facing a serious threat of invasion of exotic marine organisms. In recent years, China has a growingly severe problem of offshore red tide, and one important reason of which is the hazards caused by the exotic red tide organisms with strong viability. China's survey over the ballast water organisms within the ports of southeast coast of China found that 309 kinds of exotic marine organisms, among which there were 60 kinds of red tide organisms, which were detected in the ballast water of seventeen foreign ships (Yang Q L, 2011). Temporal and Spatial Distribution of Chinese offshore red tide (Luo H et al., 2013; Xu H L et al., 2014) shows that the occurrence frequency and geographical distribution of offshore red tide is closely related to the

situation of economic development. High frequent occurrence of red tide in waters of China in recent years is precisely the negative result of rapid economic development, and the estuaries of Pearl River and Yangtze River, where the red tide has a high incidence, are also the country's most economically developed regions. Clearly, the ballast water emitted by the ships that bear more than 90% of global seaborne cargo is an important factor causing deterioration of both offshore marine ecology and environment.

Scientists of the United States predict that (Deborah A R, et al., 2013), even if the ballast water discharged by all the ships within the sea area is up to the IMO standards, there will still be about one kind of new biological invading the research area every 10 to100 years. The larger the port scale and the higher cargo throughput, the greater the total amount of ballast water discharge in port waters will get, and correspondingly, the more the exotic marine organisms invading will be. Unfortunately, however, by now few researchers are concerned with the research, from the regional dimension, on the impact of total amount of ballast water discharge upon the prevention against the invasion of exotic marine organisms (Newton NP, et al., 2014; Farrah TC, et al., 2013), and the total discharge of ballast water and its distribution characteristics of five major ports in China have not yet been appropriately calculated and recounted.

China has lately raised maritime shipping to the level of a national strategy (State Council, 2014), thus it will become mainstream to ship China goods with China vessels. Therefore, the size of the its ports and capacity of maritime shipping will continue to increase, along with which the amount of ballast water exchange of trade ships within the waters of the China's ports will certainly continue to grow. The diversity of both the climate of China's coastal waters and ecological environment, and the hospitability of these sea areas toward most marine life, are undoubtedly exacerbating the spread of exotic invasive marine species and threatening the marine biodiversity and the marine environmental security of this country's port waters. Therefore, it is rather necessary to analyze the input characteristics and risk of the ballast water of entry ships within coastal waters of China.

1 Data and methodology

1.1 The typical vessels' ratio of ballast water loading to cargo loading

Based on the requirement of the types of cargo and specialized transportation, the main maritime vessels currently working can be divide into four categories: oil tankers (including liquid chemical tankers), which are mainly employed for the transport of crude oil, refined oil or liquid chemicals; bulk carriers, which are mainly used to transport coal, ore, grain and other dry bulk cargo; general cargo ships, which are primarily for the transport of

steel machinery goods and large-scale structural components (including wheeled machinery and cars), etc.; container ships, which are mainly for the transport of other unclassified goods.

Due to the different ways of loading, different vessels have different ratios of ballast tank capacity to deadweight (DWT), resulting in different ratios of ballast water loading to cargo loading. At present, a tanker's ballast water loading is generally 20% to 55% of the deadweight of the ship; a bulk carrier's loading ballast water is generally 30% to 60% of the deadweight; a cargo ship's ballast water loading is 30% to 40% of the deadweight; a container ship's ballast water loading is generally 20% to 40% of its deadweight.

Tab. 1 Data statistics of ballast tank capacity and dead weight for bulk carrier(Unit：tons)

NO.	Ballast tank capacity	DWT	NO.	Ballast tank capacity	DWT	NO.	Ballast tank capacity	DWT	NO.	Ballast tank capacity	DWT
1	250000	75000	19	175882	58558	37	73192	22647	55	170039	53535
2	250000	112500	20	31807	9525	38	27140	9005	56	(55624)	(31002)
3	150000	45000	21	31744	9525	39	24021	8123	57	74293	24491
4	150000	67500	22	180335	57491	40	54393	26994	58	73659	20934
5	150000	45000	23	74293	26291	41	46195	14191	59	177805	53531
6	150000	67500	24	75570	21657	42	27383	8780	60	177987	53531
7	70000	31500	25	180246	57491	43	24159	7813	61	82153	22061
8	70000	21000	26	76773	24663	44	93297	27314	62	181417	61444
9	70000	25200	27	27172	9006	45	45215	21179	63	75200	21090
10	(70000)	(39900)	28	47760	16384	46	73242	22646	64	28499	9685
11	(35000)	(19950)	29	180388	57491	47	73251	22547	65	93103	43260
12	35000	11550	30	52424	15792	48	93252	27314	66	92500	28772
13	35000	10500	31	45259	15196	49	93204	27879	67	47000	16307
14	35000	17150	32	(27338)	(16820)	50	56050	16004	68	168800	56775
15	56876	15596	33	75474	21681	51	73725	20934	69	206254	75098
16	15965	5544	34	71399	34233	52	71290	34554	70	56975	16742
17	(56104)	(32010)	35	52385	15787	53	(58081)	(31204)			
18	179869	62840	36	175868	53169	54	(77549)	(41744)			
Average ratio value							33.9%				

Through consulting literatures and researching on real ships, we obtained the data, as shown in Tab. 1 - 4, of deadweight and ballast water tank capacity of 70 bulk carriers, 38 container ships, 52 tankers and 18 general cargo ships (at the request of the owners, names of the vessels have been replaced with serial numbers). After removing those

individual data (in parentheses) with large deviation from the data group, average of the rest of the data was calculated according to the following formula (expressed in percentage):

Tab. 2 Data statistics of ballast tank capacity and dead weight for container vessel (Unit: tons)

NO.	Ballast tank capacity	DWT	NO.	Ballast tank capacity	DWT	NO.	Ballast tank capacity	DWT	NO.	Ballast tank capacity	DWT
1	40000	12000	11	12597	4408	21	64537	18578	31	11700	3998
2	40000	15200	12	5958	1747	22	50137	11930	32	8200	3383
3	40000	11200	13	12829	4389	23	52223	11903	33	28400	9738
4	40000	16000	14	12569	4408	24	102396	24282	34	19500	6355
5	15000	4500	15	5962	1747	25	101661	25352	35	42000	12198
6	15000	4500	16	12568	4408	26	13760	5199	36	3595	969
7	63515	18125	17	12597	4408	27	8015	3333	37	(7150)	(3321)
8	61441	22868	18	80246	21078	28	13760	4797	38	108350	28495
9	39383	11340	19	65066	19108	29	33800	9430			
10	63523	18125	20	63157	22392	30	(11000)	(5389)			
Average ratio value							29.5%				

$$\text{Average ratio of a vessel type}(\%) = \frac{\text{Sum of ballast water loading of all surveyed vessels}}{\text{Sum of cargo loading capacity of all surveyed vessels}} \times 100$$

Tab. 3 Data statistics of ballast tank capacity and dead weight for oil tanker (Unit: tons)

NO.	Ballast tank capacity	DWT	NO.	Ballast tank capacity	DWT	NO.	Ballast tank capacity	DWT	NO.	Ballast tank capacity	DWT
1	100 000	40 000	14	38 615	17 903	27	14 411	6 804	40	100 063	38 781
2	100 000	45 000	15	(95 663)	(56 018)	28	281 050	107 862	41	46 953	20 610
3	40 000	12 000	16	111 561	56 018	29	88 259	25 614	42	43 929	20 742
4	40 000	15 200	17	8 882	3 364	30	16 500	8 303	43	49 999	22 032
5	40 000	17 200	18	105 381	38 133	31	5 300	2 563	44	12 922	5 150
6	10 025	3 472	19	297 863	101 266	32	16 500	7 175	45	17 725	5 996
7	(4 772)	(1 031)	20	110 000	45 924	33	12 600	5 515	46	47 823	21 681
8	13 100	3 877	21	105 544	39 472	34	7 000	3 075	47	(4 858)	(986)
9	320 000	102 300	22	297 115	102 058	35	7 800	1 999	48	284 497	108 300
10	50 376	22 032	23	7 016	2 449	36	13 500	6 868	49	302 493	99 350
11	115 273	39 766	24	48 764	20 529	37	8 500	4 126	50	75 618	29 697
12	115 577	39 766	25	66 094	29 428	38	73 000	26 240	51	46 043	20 212
13	291 613	105 088	26	30 038	16 050	39	116 000	40 948	52	38 615	18 350
Average ratio value							37.6%				

With sufficient data as basis, the average ratio of a vessel type can represent, under normal conditions and within a wide region, the ratio of the total ballast water loading to deadweight of this type of vessel. And the results were: the tankers 37.6%, the bulk carrier 33.9%, the general cargo ships 34.9%, and the container ships 29.5%.

1.2 Estimation method of entry ships' ballast water input at five major port groups of China

It is quite difficult to measure the ballast water discharge amount of each entry ship.

Therefore, statistics and computing of entry ships' ballast water input are more difficult to achieve.

Tab. 4 Data statistics of ballast tank capacity and dead weight for genera! cargo vessel (Unit: tons)

NO.	Ballast tank capacity	DWT	NO.	Ballast tank capacity	DWT	NO.	Ballast tank capacity	DWT	NO.	Ballast tank capacity	DWT
1	8 000	3 040	6	2 150	673	11	(28 148)	(18 933)	16	3 759	1 018
2	17 000	5 950	7	(7 003)	(3 805)	12	32 509	12 344	17	5 323.8	1 446
3	23 800	8 622	8	4 980	1 674	13	29 600	8 371	18	4 400	1 333
4	14 763	5 538	9	2 200	857	14	(6 679)	(1 250)			
5	(6 117)	(826)	10	32 485	12 344	15	5 105	1 674			
Average ratio value							34.9%				

Normally, ballast water discharge mainly occurs during the process of cargo loading. And the more a cargo ship is loaded, the more its ballast water is discharged.

Thus, the entry ships' ballast water inputs at the five major port groups in China, the total amount of foreign trade cargo in China, and the total amount of export goods by ships in the corresponding ports must be positively correlated. Within a certain port, the larger the amount of foreign trade goods loaded on ships or total amount of export goods by ships, the greater the total amount of ballast water discharged by entry ships entering a port's waters.

Fig. 1 shows the estimation model of entry ships' ballast water input at the five major port groups in China, which was based on the correlation between the total amount of cargo loading and total amount of ballast water discharge. In this model, foreign trade, shipping and merchandise exports authoritative information was used, which was released by the Ministry of Transport and the State General Administration of Customs and included the amount of typical foreign trade goods at ports of China, foreign trade cargo throughput at ports of China, the amount foreign trade cargo loading at the ports above designated size. Among them, the amount of typical foreign trade goods at ports of China was counted through the export amount (cargo loading) of the categories, which were crude oil, coal, ore, and grain.

First, after the amount of throughput and cargo loading of foreign trade goods in ports above designated size was obtained, and the ratio of them was calculated.

Second, through the import and export goods information released by the General Administration of Customs, the total amount of China's annual export by sea transport and the ratio of steel machinery export amount to the total amount of annual exports were counted, and then with annual amount of China's import and export goods, the ratio of

export goods amount to total amount of import and export goods was calculated.

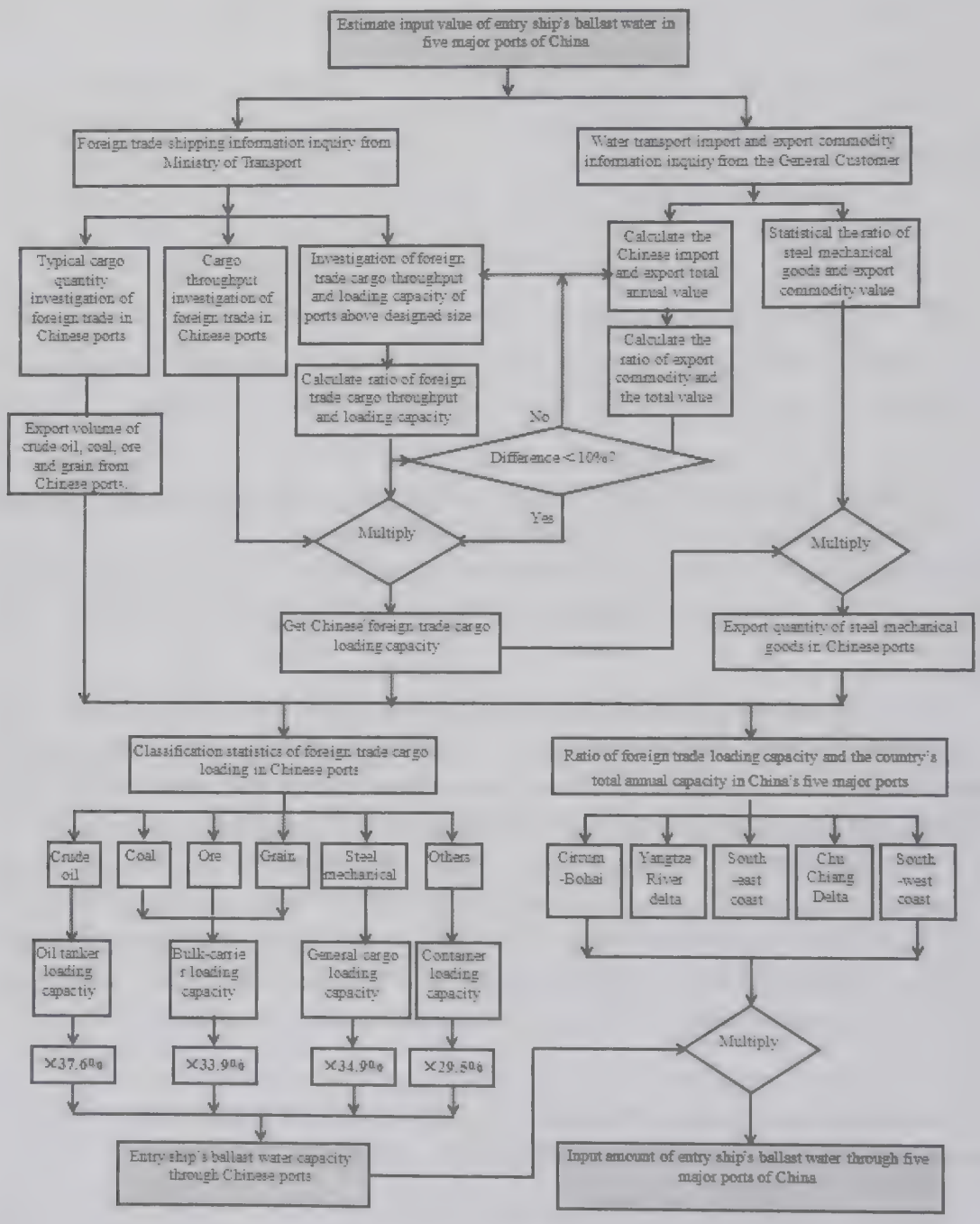
Estimate input value of entry ship's ballast water in five major ports of China
Foreign trade shipping information inquiry from Ministry of Transport
Water transport import and export commodity information inquiry from the General Customer
Typical cargo quantity investigation of foreign trade in Chinese ports
Cargo throughput investigation of foreign trade in Chinese ports
Investigation of foreign trade cargo throughput and loading capacity of ports above designed size
Calculate the Chinese import and export total annual value
Statistical the ratio of steel mechanical goods and export commodity value
Calculate the ratio of export commodity and the total value
Calculate ratio of foreign trade cargo throughput and loading capacity
Export volume of crude oil, coal, ore and grain from Chinese ports.
No
Difference < 10%?
Yes
Multiply
Multiply
Get Chinese foreign trade cargo loading capacity
Export quantity of steel mechanical goods in Chinese ports
Classification statistics of foreign trade cargo loading in Chinese ports
Ratio of foreign trade loading capacity and the country's total annual capacity in China's five major ports
Crude oil
Coal
Ore
Grain
Steel mechanical
Others
Circum -Bohai
Yangtze River delta
South -east coast
Chu Chiang Delta
South -west coast
Oil tanker loading capactiy
Bulk-carrie r loading capacity
General cargo loading capacity
Container loading capacity
×37.6%
×33.9%
×34.9%
×29.5%
Multiply
Entry ship's ballast water capacity through Chinese ports
Input amount of entry ship's ballast water through five major ports of China

Fig.1 The estimation model of entry ships' ballast water input at five major port groups in China

Third, the ratio of cargo loading to foreign trade port throughput was compared with the ratio of export goods amount to total amount of import and export goods. If the

difference was greater than 10%, re-verification of the survey data was necessary, and the data should be corrected after the problem was identified. If the difference was less than 10%, after multiplying the foreign trade throughputs with the ratio of port cargo loading amount to foreign trade throughput respectively, the foreign trade cargo loading in China's ports would be obtained.

Fourth, with the amount of typical foreign trade goods (crude oil, coal, ore, grain), the cargo loading of foreign trade goods, the amount of steel machinery goods exports in China's ports, the cargo loadings of crude oil, coal, ore, grain, steel machinery goods and other types of foreign trade goods were counted respectively. Among them, the export amount of steel machinery goods was obtained by multiplying the cargo loading of foreign trade goods in China's ports with the ratio of steel machinery goods to the total amount of export.

Fifth, the cargo loadings of all kinds of goods were classified into vessel types and multiplied with the ratio of the corresponding type. Among them, crude oil goods were listed under tankers, whose ballast water ratio was 37.6%; coal, ore, and grain classified into bulk carriers, whose ballast water ratio was 33.9%; steel machinery goods were classified into cargo ships, whose ballast water ship ratio was 34.9%; the rest of the goods were all classified into container ships, the ship ballast water ratio of which was 29.5%. After adding the ballast water amounts of four vessel types, the total input of entry ships' ballast water in sea areas of China's ports was obtained.

Sixth, through the cargo loading of foreign trade goods in China's ports over designated size and the cargo loading of foreign trade goods in China's ports, a sub-regional statistical calculation of the annual ratio of foreign trade cargo loading within China's five major port groups (Bohai Rim, Yangtze River Delta, the southeast coast, the Pearl River Delta and the southwest coast) to the national total foreign trade cargo loading was accomplished; finally, by multiplying the total input of entry ships' ballast water entering China ports' waters with the annual ratio of foreign trade cargo loading within China's five major port groups, the amount of input of entry ships' ballast water within China's five major port groups was obtained.

1.3 Annual ratio of foreign trade cargo loading in China's five major port groups to national total amount

On the whole, China's five major port groups are similar both in types of ports and proportion of cargo types. Therefore, the ratio can be calculated through the ratio of foreign trade cargo loading in ports above designated size within each area to the total amount of national ports above designated size.

With the import and export data of China ports released on website of Chinaports, sub-regional statistical results of China's foreign trade port cargo from 2007 to 2012 were achieved and shown in Tab. 5. Among them, there were a total of twelve statistical ports above designated size in Bohai Rim, six in Yangtze River Delta region, four in the southeast coastal region, eleven in Pearl River Delta region, and five in southwest coast region included in counting of the cargo loading. Among them, the data from 2007 to 2010 of Xiamen port were those of the previous Xiamen port before its merge with Zhangzhou port, while because of the geographic location of Hong Kong and Macao, their data were included in Pearl River Delta region. Total foreign trade throughput of these ports accounted for more than 90% of the national foreign trade ports' throughput. Also, because marine transport vessels entering and coming out of the inland rivers need to exchange ballast water at the estuaries, the inland ports' foreign trade cargo loading via the Yangtze River estuary was included in the statistics of Yangtze River Delta region and that via the Pearl River estuary included in the data of Pearl River Delta region.

Tab. 5 Annual statistics of foreign trade cargo loading capacity of regional ports in China (Unit: 10 thousands Ton)

Annual	Circum-Bohai	Yantze river delta	South-east coast	Chu Chiang Delta	South-west coast	Total
2007	26 780	23 227	3 536	18 257	1 567	73 367
2008	24 652	25 016	4 059	19 422	1 350	74 499
2009	17 817	21 057	4 154	17 835	1 103	61 966
2010	21 077	26 276	4 261	20 791	1 408	73 813
2011	22 671	31 197	4 699	21 886	1 571	82 024
2012	23 563	33 144	5 302	21 510	1 826	85 345

With data in Tab. 5, the annual ratios from 2007 to 2012 of foreign trade cargo loading in China's five major port groups to national total amount have been shown in Tab. 6. The amount of input of entry ships' ballast water within China's five major port groups could be calculated through these annual ratios.

Tab. 6 Ratio of foreign trade cargo loading capacity and total loading capacity (%)

Annual	Circum-Bohai	Yangtze river delta	South-east coast	Chu Chiang Delta	South-west coast
2007	36.50	31.66	4.82	24.88	2.14
2008	33.09	33.58	5.45	26.07	1.81
2009	28.75	33.98	6.70	28.78	1.78
2010	28.55	35.60	5.77	28.17	1.91
2011	27.64	38.03	5.73	26.68	1.92
2012	27.61	38.84	6.21	25.20	2.14

The amount of port groups' ballast water input equals the total amount of entry ships' ballast water input multiplied by the annual ratio of foreign trade cargo loading in port groups to national total amount of foreign trade cargo loading.

2 Results and analysis

2.1 Foreign trade cargo loading in major ports of China

With the data released on website of Chinaports from 2007 to 2012, the ratios of foreign trade cargo loading to throughput of China's fifty-six major ports were calculated as follows: 38.63% (2007), 36.32% (2008), 26.78% (2009), 27.74% (2010), 27.74% (2011) and 26.45% (2012). These included all the ports above designated size in China, whose cargo throughput accounted for more than 90% of the national aggregate. The ratio, which has been calculated above, of foreign trade cargo loading to foreign trade cargo throughput, could be representing the situation across the country. The difference between the previously calculated ratio and the computation results of the customs authority website (haiguan.info) was quite small, between 1.28 to 5.48%, and showed a decreasing trend in the past five years.

The annual statistics, based on the ratio of foreign trade cargo loading to throughput of China's fifty-six major ports, of national foreign trade port cargo loading from 2007 to 2012 has been shown in Tab. 7. Among them, data of foreign trade throughput were obtained from China Shipping Development Report released by the Ministry of Transport, and the amount of foreign trade cargo loading was calculated through the following formula:

Foreign trade cargo loading equals foreign trade cargo throughput multiplied by the ratio of foreign trade port cargo loading to foreign trade cargo throughput

Tab. 7 Annual statistic of foreign trade cargo loading capacity in Chinese ports (Unit: 10 thousands Ton)

Annual	Ratio of loading capacity	Cargo throughput	Loading capacity
2007	38.63%	184921	71435
2008	36.32%	198578	72124
2009	26.78%	217976	58374
2010	27.74%	250068	69369
2011	27.74%	278585	77279
2012	26.45%	305630	80839

Referring to China Shipping Development Report with statistics, the amounts of import and export of crude oil, coal, ore and grain through ports of China have been obtained. And according to the following formula the export amounts of steel and machinery and other unclassified goods could be calculated:

Steel mechanical export amount is foreign trade cargo loading multiplied by the ratio

of steel machinery export amount to the total amount of import and export in China.

Other goods = foreign trade - crude oil - coal - ore - grain - cargo loading of steel machinery

Among them, the ratio of steel machinery export amount to the total amount of import and export was calculated in accordance with of the data released by the State Customs Service: 15.7% (2007), 14.7% (2008), 10.0% (2009), 13.4% (2010), 19.9% (2011) and 23.6% (2012).

Data associated with the types of China's export goods and main ship types have been summarized in Tab. 8, wherein the data in italics were statistical supplement based on data released by the State General Administration of Customs in 2012.

Tab. 8 Data statistics of the types of China's export goods and main ship types (Unit: 10 thousands Ton)

Cargo type	Crude oil	Coal	Ore	Grain	Steel mechanical	Others	Hongkong	Macao
Vessel type	Oil tanker	Bulk carrier	Bulk carrier	Bulk carrier	General cargo	Container	Container	Container
2007	337	6763	156	868	12516	50795	5232	-
2008	349	6011	111	201	12202	53250	5867	36
2009	309	2281	51	139	6664	48930	4770	13
2010	296	2196	73	114	10451	56239	5867	13
2011	369	1963	69	142	16532	58204	6397	14
2012	473	1164	*114*	104	19078	59906	5824	14

Considering the fact that Hong Kong and Macao's particular geographical position, in Pearl River Delta region, the foreign trade cargo loading of the Hong Kong and Macao were also included in that of China ports' sea areas. Because container transport was the main transportation method in Hong Kong and Macao, their cargo loadings were classified into the category of other goods (that is, in the category of container transport).

2.2 The total input of entry ships' ballast water in China ports' sea area

On the basis of the basic data calculated in accordance with Tab. 8, through the estimation model, which has been provided by Fig. 1, the amount of the five major port entry ships' ballast water input in China, and the amount of entry ships' ballast water input in the sea area of China's ports in 2007 - 2012 have been calculated and shown in Tab. 9.

It can be seen that from 2007 to 2012, the total amount of ballast water input from global sea areas into China's ports increased from 237 million tons to 267 million tons; while during the 5 years the amount of ballast water discharged into China sea did not increase greatly, only 12.83%, and even due to the global economic downturn in 2008

when the amount reduced by 20.26% in 2009, the total input of ballast water was still enormous, which was equivalent to thirteen to nineteen times of the water capacity of West Lake in Hangzhou (14.29 million m^3).

2.3 The input characteristics of entry ships' ballast water in sea areas of the five major port groups in China

The state of ballast water input in the China's five major port groups, which was based on the amount of input that was obtained through the estimation model, has been shown in Fig. 2.

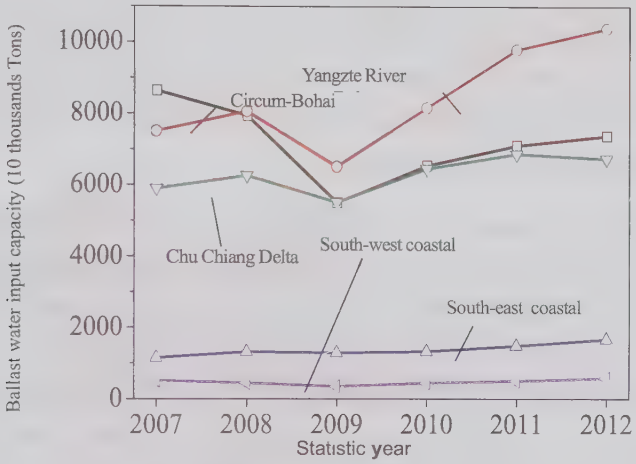

Fig. 2 Ship's ballast water input conditions of top five port areas in China

It can be seen that from 2007 to 2012, the most foreign ballast water entered Yangtze River Delta, Bohai Rim and Pearl River Delta region. Among them, the amount of foreign ballast water that entered Yangtze River Delta region accounted for 31.7% - 39.0% of the national input, which had been the first place across China from 2008. In 2012, this area received ballast water of 103.68 million tons, equivalent to seven times of the West Lake water volume, and was the most severely affected area globally, which was directly related to the activity level of economy in this region. Ballast water input in Bohai Rim region accounted for 27.6% - 36.5% of the national input, which was in the second place after 2009. In 2012, the total input into Bohai Rim region was 73.71 million tons, which was the equivalent of nearly five times the West Lake water. The foreign ballast water input in Pearl River Delta region was slightly less than that in Bohai Rim region, accounting for 24.7% to 28.8% of the national input, which was in the third place after 2009. In 2012 the total input reached 67.29 million tons, equivalent to more than four and a half times the West Lake water. The least foreign ballast water was input into the southeast and southwest coastal regions. The ballast water input in southeast coastal regions only accounted for 4.8% to

6.7%, whose annual total was merely 16.59 million tons in 2012, while the southwest only 1.8% to 2.1%, and the annual total of which was only 5.71 million tons. The input in southwest coastal regions was so small that it was less than one-twelfth of total input in Pearl River Delta region.

3 Risk analysis of entry ships' ballast water input

The results of research based on the estimation model for ballast water input of entry ships entering China's port sea areas has indicated an enormous amount. From 2007 to 2012, the amount of ballast water transferred from global seas to China's sea areas was over 1.421 billion tons. And only in 2012 alone, it reached nearly 267 million tons, far more than the 80 million tons discharged in the sea areas of United States and 120 million tons into the sea of Australia. Ballast water from global seas was poking a huge potential threat to the ecological environment of China's port areas.

In order to meet the requirements of International Convention for the Control and Management of Ships' Ballast Water and Sediments, which was enacted by the International Maritime Organization (IMO), many countries are involved in research and development of ballast water treatment technologies and devices. Up to now, 42 ballast water management systems have passed the IMO type approval, which can be used for more than ten kinds of technical methods, such as filtering (including cyclones, flocculation), deoxygenation, cavitation, ultrasound, ultraviolet radiation, electrolysis, ozone, chlorine (including the chlorine dioxide, sodium hypochlorite, calcium hypochlorite), adding chemical reagent and advanced oxidation etc. However, due to the great difference of water quality and marine organism state between different global sea areas, none of the ballast water treatment technologies and devices can be applied to most of the sea areas and ships. Meanwhile, because of the ambiguity of environmental and biological baseline of China's port waters, the lack of effective rapid ballast water and monitoring technology and methods, as well as the imperfection of system for ballast water management and control, it is difficult to ensure that all foreign trade ships' ballast water reach the IMO emission standards, and thus, quite high risk of exotic marine species invasion exits.

The input characteristics of ship ballast water in China can be expressed as: the more active economic development of an area, the greater the total input of foreign ballast water entering it, and the greater the input intensity of foreign trade ships' ballast water. Figure 3 shows the input intensity of foreign trade ships' ballast water across China and in the five major port groups in 2012, which characterizes the amount of ballast water exchanged per unit length of a production dock. It reflects the risk degree of impact that the

foreign trade ships' ballast water exchange in those port groups was poking on the ecological environment.

Input intensity of ballast water = input amount of ballast water / length of a production dock(t/m). It can be seen that, among the five major regional port groups, the input intensity of trade ship ballast water at Yangtze River Delta region was the greatest, which was 519 t/m, higher than the national level by 30.1% (the national foreign trade ship ballast water input intensity was 399 t/m). The input intensities within Pearl River Delta and Bohai Rim regions were also higher, 398 t/m and 393 t/m, respectively, both very close to the national level, which were in the second and third place of the country. The input intensity in southeast coastal region ranked No. 4, which was 317 t/m, lower than the national level by 20.6%, while the input intensity in the southwest coastal region was the smallest of all, 116 t/m, lower than the national level by 71.9%.

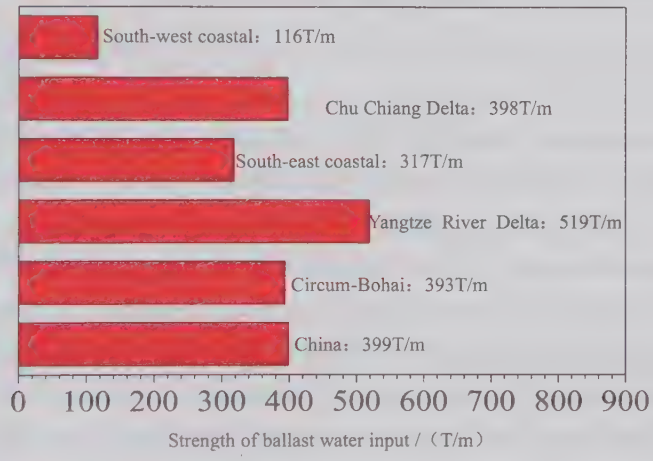
South-west coastal: 116T/m
Chu Chiang Delta: 398T/m
South-east coastal: 317T/m
Yangtze River Delta: 519T/m
Circum-Bohai: 393T/m
China: 399T/m
0 100 200 300 400 500 600 700 800 900
Strength of ballast water input / (T/m)

Fig. 3 Strength of ballast water input (Ton/m)

Among China's seas, the coastline length of Bohai Rim is about 5 923 kilometers, Yangtze River Delta region about 3 461 kilometers, southeast coastal areas about 3 024 kilometers, Pearl River Delta about 4 314 kilometers, southwest coastal area about 3 159 kilometers. When it comes to the input, unit length of the coastline, of foreign trade ship ballast water in the five major port groups in 2012, it was 12 400 t/km in Bohai Rim, 30 000 t/km in Yangtze River Delta region, 5 500 t/km in southeast coastal region, 15 600 t/km in Pearl River Delta region, and 1 800 t/km in southwest coastal region.

Therefore, in China's five major port groups, the regional characteristics of entry ships' ballast water exchange were very obvious, among which Yangtze River Delta region, Bohai Rim and Pearl River Delta region were the main regions of entry ships' ballast water discharge, whose discharge amounts in 2012 reached 103.68 million tons, 73.71 million

tons and 67.29 million tons, respectively. The ballast water input in these three regions nearly accounted for 91.65% of the national total of input. Among them, the ballast water in Yangtze River Delta region had the greatest total input, and its input intensity is also the highest, whose input per unit length of coastline was 1.9 to 16.7 times that of other regions, causing the highest risk of exotic marine organism invasion if other environmental factors remained in the same situation. Pearl River Delta region and Bohai Rim also had quite large total input of ballast water. While the latter had a slightly larger number, the former had higher input intensity and greater input per unit length of coastline. Therefore, the Pearl River Delta region had a slightly higher risk of exotic marine organism invasion through ballast water than Bohai Rim region. The total input in the southeast coastal region was modest, but with high intensity, the risk of exotic marine organism invasion remained high. The total input amount, input intensity and input per unit length of coastline in the southwest coastal region were all at a low level, and the risk of exotic marine organism invasion through ballast water in this region was relatively low.

The risk that entry ships' ballast water is discharged without effective control lies in the fact that a lot of harmful aquatic animals, plants and pathogens can be transferred from one port to another across the world, and once under appropriate environmental conditions they can cause the ecological imbalance and epidemics upon offshore aquaculture within the sea areas into which ballast water is input. According to the statistics data in some of the public reports on exotic marine organisms entering China seas through ballast water, by then over 97 species in 9 phyla of them had been identified. Among them, there were 84 species of aquatic plants in 7 phyla and 13 species of aquatic animals within 2 phyla, while algae were the major species carried by ballast water. The exotic marine organisms borne in ballast water had spread all over the port water in Bohai Sea, Yellow Sea, East China Sea and South China Sea etc. Although the majority of these exotic marine organisms were of unknown origins, the identified species of them indicated that they came from almost all the sea areas of countries China had shipping trade with. More than 24 harmful species had been identified, which were primarily the red tide organisms.

In general, the more the species of exotic marine organisms entering a certain sea area through ballast water, the higher the biological density, the greater the amount of ballast water discharge, and the higher the risk that this sea area would be invaded. Amongst China's five major port groups, Yangtze River Delta region, Bohai Rim and Pearl River Delta region were not only the most important regions of entry ships' ballast water discharge, the most economically developed regions of China, but also regions most seriously threatened by exotic marine organisms. It should also be noted that despite a modest total input of ballast water in the southeast and southwest coastal region, since the

impact of pollution upon marine environment was smaller than in other regions, exotic marine organisms invading these regions were relatively more likely to survive. Therefore, the risk of being invaded by exotic marine organisms borne in ballast water should not be ignored.

4 Conclusions and Suggestions

Development of China's ocean shipping economy and trade has caused a huge input of entry ships' ballast water from global waters into China's ports. The amount of input in 2012 was nearly 267 million tons, nearly 91.65% of which was emitted to Yangtze River Delta, Bohai Rim and Pearl River Delta regions which are the most economically developed in China. The emission amounts were 103.68 million tons in the Yangtze River Delta region, 73.71 million tons in Bohai Rim, and 67.29 million tons in Pearl River Delta region. The most economically developed regions, Yangtze River Delta, Bohai Rim and Pearl River Delta regions have been experiencing the highest risk of being invaded by exotic marine organisms.

To prevent and control the damage that the foreign trade ships' ballast water causes to China seas, to maintain the ecological environment security of coastal waters, and to avoid the impact of the green trade barriers in developed countries on China's ocean shipping industry, China's marine, maritime, inspection and quarantine departments and relevant enterprises are suggested to take actions soon to establish information platform of ocean vessel ballast water management, to track the progression that IMO's International Convention for the Control and Management of Ships' Ballast Water and Sediments comes into effect, to track the introduction of ballast water discharge regulations in developed countries; to actively participate IMO's sampling, standard-testing of ballast water; to encourage and guide the transport enterprises to install suitable ballast water treatment equipment; to establish a monitoring mechanism for prevention against and control on ship's ballast water pollution in coastal waters as soon as possible; to establish the system of mandatory reporting on ballast water discharge ; to unify the sampling, testing and monitoring methods of ocean vessel ballast water, and establish binding and nationally applicable laws, regulations and management systems; to encourage research institutions and relevant enterprises to actively develop ship-borne mobile technology and devices that suitable to be used in the ports for prevention against and control on ballast-water-borne exotic marine organisms' invasion risk, and develop emergency contingency plans for ballast water pollution in advance.

The main error sources for results of calculation based on the estimation model of

entry ships' ballast water input in China's five major port groups are including the conversion ratio of container transport cargo weight, the ratio of vessel types, the statistical errors, annual climatic factors, and the statistical data errors etc., among which the ratio of vessel types is most influenced and will continue to be improved and amended with the increase of data about vessel types.

Acknowledgements

Thanks for Wang G S from China Shipping Industry (Shanghai) and Shi X B from Minsheng Financial Leasing (Beijing) who have provided the help for the investigation of many vessel's data.

References

[1] Chinese Ministry of Transport. Reports of Chinese shipping development [M]. Beijing: China Communication Press, 2013. 2012.

[2] Oemcke D J, Vanleeuwen J. Chemical and physical characterization of ballast water. Part 2: Determining the efficiency of ballast exchange [J]. Journal of Marine Environment and Engineering, 2003, 7(1): 65 - 76.

[3] Endresen O, Behrens H L, Brynestad S, et al. Challenges in global ballast water management [J]. Marine Pollution Bulletin, 2004, 48: 615 - 623.

[4] Pimentel D, Zuniga R., Morrison D. Update on the environmental and economic costs associated with alien - invasive species in the United States [J]. Ecological Economics, 2005, 52, 273 - 288.

[5] Chen C. Management and control of ship's ballast water [J]. China Water Transport, 2013, 10: 30 - 31.

[6] Jamie L S, Rachel W, Robin B, et al. Ecosystem under pressure: Ballast water discharge into Galveston Bay, Texas (USA) from 2005 to 2010 [J]. Marine Pollution Bulletin, 2012, 64: 779 - 789.

[7] Ruiz G M, Rawlings T K, Dobbs F C, et al. Global Spread of Microorganisms by Ships [J]. Nature, 2000, 408 (6808): 49 - 50.

[8] Mackenzie, Debora. Alien invader s[J]. New Scientist, 1999, 162 (ISS.2183): 18 - 19.

[9] Fred C D. Ridding ships' ballast water of microorganisms [J]. Environmental Science & Technology, 2005, (3): 259 - 264.

[10] Global Ballast Water Management Programme [EB/OL], 2003. http://globallast.imo.org.

[11] Carlton J T. Biological invasions and biodiversity in the sea: The ecological and human impacts of nonindigenous marine and estuarine organisms. Keynote address in Nonindigenous Estuarine and Marine Organisms (NEMO) [C], Proceedings of the Conference and Workshop. 1994.

[12] Liang Y B, Wang B. Alien marine species and their impacts in China [J]. Biodiversity Sci., 2001,

9(4): 458 - 465.

[13] Carlton J T. The zebra mussel Dreissenapolymorpha found in North America in 1986 and 1987 [J]. Journal of Great Lakes Research, 2008, 34: 770 - 773.

[14] Yang Q L, Cai L H, Gao Y H, et al. Plankton found in ballast waters of foreign ships harboring in ports of Southeast China [J]. Marine Science, 2011, 35(1): 22 - 28.

[15] Luo H, Ma M H, Liang B, et al. Basic characteristics and mitigation countermeasures of red tides in China Seas [J]. Marine Science Bulletin, 2013, 32(5): 595 - 600.

[16] Xu H L, Gu D X, Zhang W L, et al. Analysis of the red tide features based on time series in the China Sea [J]. Marine Science Bulletin, 2014, 33(4): 469 - 474.

[17] Deborah A R, Henry L I, Melanie F, et al. Per capita invasion probabilities: an empirical model to predict rates of invasion via ballast water [J]. Ecological Applications, 2013. 23 (2): 321 - 330.

[18] Newton N P, Rui C B, Rafael D F, et al. Ballast water: A threat to the Amazon Basin [J]. Marine Pollution Bulletin, 2014,84: 330 - 338.

[19] Farrah T C, Sarah A B, Chris J W, et al. Relative risk assessment for ballast-mediated invasions at Canadian Arctic ports [J]. Biological Invasions, 2013, 15: 295 - 308.

[20] Chinas State Council. Several opinions about promote the healthy development of maritime industry[M], 2014, 32.

中国近海入境船舶压舱水输入特征与风险分析

杜 还[2]，张小芳[2]，张芝涛[1,2]，刘开颖[1]，李日红[2]

（1. 大连海事大学 环境工程研究所，辽宁 大连 116026；2. 大连海事大学 轮机工程学院，辽宁 大连 116026）

摘 要：远洋船舶压舱水在我国港口海域的大量排放是造成地理性隔离水体间外来海洋有害生物传播和近岸海域环境日益恶化、赤潮灾害频发的重要因素之一。本文基于中国港口入境船舶压舱水输入总量估算模型，通过调查国家交通运输部和国家海关总署公开发布的外贸航运及商品进出口信息，在确立中国港口入境船舶压舱水输入总量和中国五大港口群体压舱水输入比值的基础上，分析了 2007 年至 2012 年中国近海入境船舶压舱水的输入特征和环境生态风险。结果表明：我国五大港口群体入境船舶压舱水的输入总量极不平衡，经济最发达的长江三角洲区域输入的境外压舱水总量最多，2012 年输入量为 10 368 万吨，其次是环渤海地区，为 7 371 万吨，珠江三角洲地区排第三位，为 6 729 万吨，东南沿海地区和西南沿海地区输入的压舱水总量较少，仅有 1 659 万吨和 571 万吨。入境船舶压舱水的大量排放对我国尤其是经济发达区域的港口海域生态环境构成了巨大的威胁。

关键词：压舱水；压舱水输入量；海洋环境与生态；风险分析

Community characteristics of macrobenthos community in Changli Gold Coast National Nature Reserve of Hebei in China

KOU Cun-hui[1], ZHANG Qing-tian[1], YU Hang[2], LI De-liang[1], ZHAO Xing-gui[1], ZHANG Peng-ru-yan[1], LIU Xian-bin[1]*

1. *Tianjin Marine Environmental Protection and Restoration Technology Engineering Center, Tianjin Key Laboratory of Marine Resources and Chemistry, Tianjin University of Science & Technology, Tianjin* 300457, *China;*

2. *Tianjin Research Institute for Water Transport Engineering. M.O.T, Tianjin* 300459, *China*

Abstract: Macrobenthic communities in the surrounding waters of Changli were investigated during spring and summer in 2016. Differences in species quantity, abundance and biomass, the dominant species and species diversity index of macrobenthos were analyzed. The results showed that 58 macrobenthos species were identified in spring, and 92 macrobenthos species were identified in summer. The composition of dominant species seasonally varied; however, most of them were species belonging to Polychaeta. The abundance of macrobenthos in summer was slightly higher than that in spring, while the biomass in summer was significantly smaller than that in spring. Bray-Curtis cluster analysis and multi-dimentional scaling (MDS) analysis indicated that macrobenthic communities were divided into three communities in spring, and two in summer. The abundance-biomass comparison (ABC) curve method was used to monitor the disturbance of environmental pollution for macrobenthic community. The results showed that the macrobenthos in this area received serious disturbance from environmental pollution.

Keywords: Changli, macrobenthos, diversity, cluster analysis, ABC curve method

1 Introduction

Marine macrobenthos, mainly composed of Mollusca, Crustacea, Echinodermata, Polychaeta, etc., mostly live in the surface of sediments which are rich in organic matters. They play an important role in energy flow and material circulation of marine ecosystems and are important parts of marine ecosystem. Marine macrobenthos can accelerate the decomposition of underwater debris, regulate the exchange of matters at the

Received on May 23, 2017

Corresponding author: lxb0688@tust.edu.cn

sediment-water interface and promote the self-purification of water bodies. They are also important parts of the food chain of the water ecosystem. The amount of marine macrobenthos affects the amount of fish and shrimp resources and the development of fisheries. At the same time, macrobenthos have weak mobility, stable habitat and sensitivity to marine environmental pollution. Therefore, the effect of pollution towards the marine macrobenthos is indicative, comprehensive and sustainable. It has great academic value and application prospect to study the structure, diversity and dominance of marine macrobenthos, which is relatively significant for evaluating the health of marine ecosystem and protecting the marine environment and biodiversity [1-10].

Changli located in the east of the Bohai Seabelongs to Hebei Province, which is under the jurisdiction of Qinhuangdao. Changli County's coastline is 52.1 km long, which is 10.7% of the total length of Hebei's coastline. The coastal beach area is about 4 million square meters and the shallow sea area under 10 m is 447 km^2. Changli coastal zone has a unique landscape, complex habitats, high biodiversity, and rich marine and coastal resources. The main habitats include sand dunes, sandbanks, lagoons, forest belts, forest depressions, estuaries and oceans. The area belongs to the warm temperate and semi-humid continental monsoon climate, where the sunshine is abundant and the four seasons are distinct. The special natural environment has produced abundant natural resources and provided a good foundation for ecotourism. With the rapid development of tourism, fishery and maritime transport, the area has been polluted to a certain extent. On September 30, 1990, the State Council approved the establishment of a national nature reserve in Changli Gold Coast, which mainly protects the coastal natural landscape and offshore ecosystem [11-17]. The establishment of the Changli Gold Coast Nature Reserve is of great significance to studying the change of sea and land and protecting marine ecological environment and biodiversity.

Changli Gold Coast Nature Reserve is one of the most abundant areas in China. In recent years, there are many studies on the ecology and diversity of macrobenthos in the Bohai Sea, Wangyu et al. (2010) [18] studied the macrobenthos community in the coastal waters of Bohai Bay; Cai Wenqian et al. (2013)[19] studied the long-term changes of dominant species of macrobenthos in Bohai Bay; Hanjie et al. (2003)[20] studied the abundance, abundance and biomass of macrobenthos in the central and southern Bohai Bay. In this work, through the survey in the waters of Changli Gold Coast Nature Reserve in spring (May) and summer (August), the distribution type, density and biomass of macrobenthos and other communities' characteristics in this sea areas were obtained, which could be utilized for analyzing the characteristics and causes of its temporal and spatial changes and providing basic information for the protection and rational

development of ecological environment in this region.

2 Materials and methods

2.1 Sample collection and analysis

Combined with the topography and surrounding conditions of the study area, 16 stations were selected for sampling (Fig. 1). The collection of macrobenthos was carried out using the 0.09 m^2 grab-type sluice for 3 times (the successful sampling) in the spring (May) and summer (August) of 2016. Then a screen with aperture of 0.5 mm was used to remove the mud, and the biological sample was fixed with 75% alcohol, according to the specific operational reference "Marine Monitoring Norms (GB17378.5-2007) Part VII: coastal pollution ecological survey and biological monitoring treatment" [21].

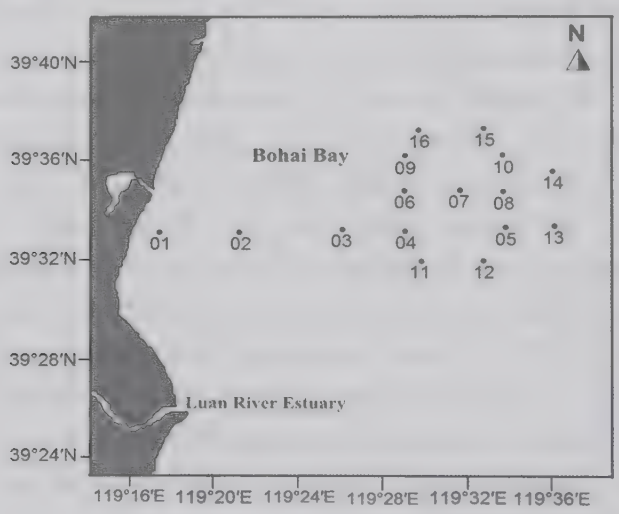

Fig. 1 Investigation sites of macrobenthos in Changli Gold Coast Nature Reserve, 2016

2.2 Statistical analysis

The biodiversity of community was analyzed by Shannon - Winner diversity index (*H'*), Pielou evenness (*J'*) and Abundance index (*d*). The formula is as follows:

$$H' = \sum_{i=1}^{S} p_i \log_2 p_i (p_i = n_i / N)$$

$$J' = H' / \log_2 S$$

$$d = (S-1) / \log_2 N$$

where n_i is the number of individuals of species i; N is the total number of individuals of all species; S is total species.

Dominant species formula is as follows:

$$Y = \frac{n_i}{N} f_i$$

where f_i is the frequency of occurrence of this species, when Y >0.02 and the species are dominant [22].

The community structure of macrobenthos in Changli Gold Coast Nature Reserve was analyzed using the multivariate statistical software Primmer 6.0[23]. In order to avoid the accidental errors caused by excessive or low individual values, the data of habitat density of macrobenthos habitats were converted and standardized by four square roots, then based on the similarity of Bray-Curtis, Cluster analysis and multidimensional scaling ordination analysis (MDS) were used to analyze the similarity of community structure. The stability and perturbation of the community were analyzed by using the abundance-biomass comparison (ABC) curve method.

3 Results

3.1 Species composition and dominant species

A total of 94 species of macrobenthos were identified from the Changli Gold Coast Nature Reserve. There were 55 species of Polychaeta, 20 species of Crustacea, 10 species of Mollusca and 9 species of other genera. 58 species of macrobenthos were identified in May, among which there were 36 species of Polychaeta, 11 species of Crustacea, 5species of Mollusca and 6 species of other genera. The dominant species were *Xenophthalmus pinnotheroides, Notomastus latericeus* and *Branchiostoma belcheri.* In August, there were 92 species of macrobenthos identified, among which there were 53 species of Polychaeta, 20 species of Crustacea, 10 species of Mollusca and 9 species of other genera. The dominant species were *Xenophthalmus pinnotheroides, Ogyrides orientalis* and *Branchiostoma belcheri* (Tab. 1). In spring, all kinds of species were smaller than those in summer. Except for *Amphictene japonica* and *Diopatra neapolitana,* all species in spring were included in summer.

3.2 Macrobenthos biomass and abundance

The average biomass of macrobenthos in Changli Gold Coast Nature Reserve was 10.47 g/m^2. The average biomass in spring was 15.49 g/m^2, and the variation range was

1.68 - 45.68 g/m^2. The biomass of station 9 was the highest, and the biomass of *Xenophthalmus pinnotheroides* was 27.87 g/m^2, accounting for 61.0% of the total biomass of that station. Total biomass ranged from 0.50 to 11.45 g/m^2 (average = 5.46 g/m^2) in summer, and the biomass of station No.9 was still the highest, and the biomass of *Xenophthalmus pinnotheroides* was 27.87 g/m^2, accounting for 88.4% of the total biomass of that station. It can be seen from Fig. 2 that there were obvious differences in the biomass distribution of each station in spring and summer. In addition, the spring biomass, as well as the summer biomass, was gradually increasing from the near shore to the outer sea.

Tab. 1 Composition of macrobenthos in Changli Gold Coast Nature Reserve during spring and summer in 2016

Time	Species			
	Polychaete	Crustacea	Mollusca	Other species
Spring	36	11	5	6
Summer	53	20	10	9
Common	34	11	5	6
Comprehensive	55	20	10	9

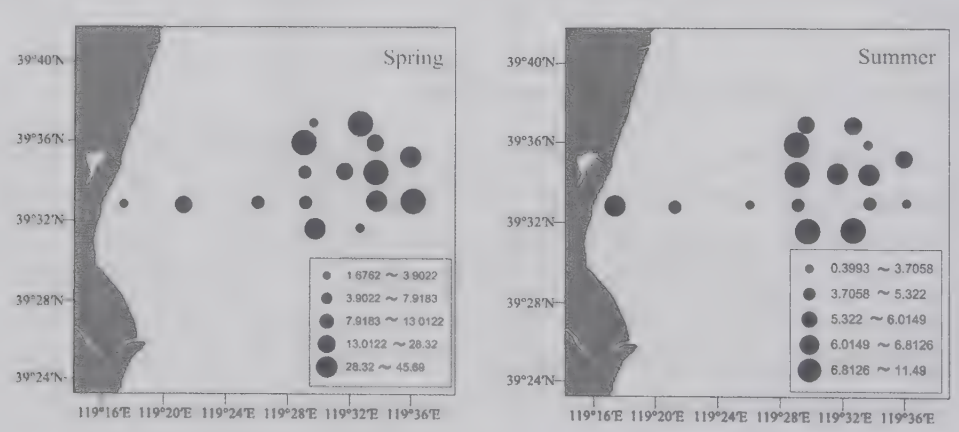

Fig. 2 Horizontal distribution of macrobenthos biomass (g/m^2) in Changli Gold Coast Nature Reserve in spring and summer 2016

The average abundance of macrobenthos in this area was 368.23 ind/m^2, and the average abundance in spring was 155 ind/m^2, with a range of 28 - 433 ind/m^2. Station No. 2 had the lowest abundance, while station No. 8 had the highest abundance. Among the abundance of station No.8, the abundance of *Notomastus latericeus* was 83.33 ind/m^2, which accounted for 17.86% of the total abundance of the station. The average abundance in summer was 208 ind/m^2 and the variation range was 4~641 ind/m^2. It could be found in

Fig. 3 that the abundance distribution of macrobenthos in the monitoring stations of the two seasons was relatively agreed.

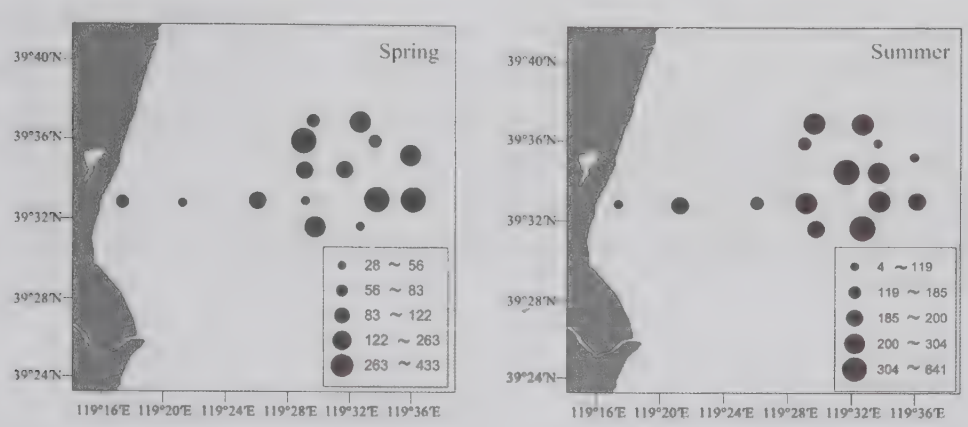

Fig. 3 Horizontal distribution of macrobenthos abundance (ind/m2) in Changli Gold Coast Nature Reserve in spring and summer , 2016

3.3 Diversity

The variation range of the richness index in spring was 0~5.20 and the mean richness index was 2.47. The spatial difference of richness index was obvious, the highest number appeared in station No.8 (d = 5.20). The evenness index in spring except the station No. 3 (J'= 0) was 0.6~1.0. The variation range of the spring diversity index was 0~4.06 and the mean spring diversity index was 2.31. The spatial variation of diversity index was also obvious, and the highest number appears in station No. 8 (H'= 4.06). The variation range of summer richness index was 0~ 3.74 and the mean value was 2.41. The spatial difference of the richness index was obvious, and the highest number appeared in station No.8 (d = 3.74). In summer, the evenness index of other stations was from 0.6 to 1.0, except for station No. 6, No.10 and No.12. The summer biodiversity index was mainly concentrated from 2.0 to 3.6, and was not evenly distributed. Richness and evenness index in spring were greater than that in summer, while the biodiversity index in spring was smaller than that in summer.

3.4 Community composition

Bray-Curtis cluster analysis and multi-dimentional scaling (MDS) analysis were conducted on macrobenthos in spring and summer in Changli Gold Coast Nature Reserve (Fig. 5). The results showed that the similarity coefficients among groups were low (10~70%), and the station distribution of each group was dispersed, without obvious distribution trend. The stress indexes in the two seasons were all less than 0.2 and the

results were consistent with the results of cluster analysis, which further confirmed the results of cluster analysis.

In spring, those at 20% similarity level could be divided into 3 groups; group I included station No.2, No.3, No.4, No.6, No.12, No.15 and No.16, with an average similarity of 38%; group II included station No.1, No.9 and No.11, with an average similarity of 67%; group III included station No.5, No.7, No.8, No.10, No.13 and No.14, with an average similarity of 33%. In summer, it can be divided into two groups; group I contained only station No.10; group II contained the remaining fifteen stations, with the average similarity of 76%.

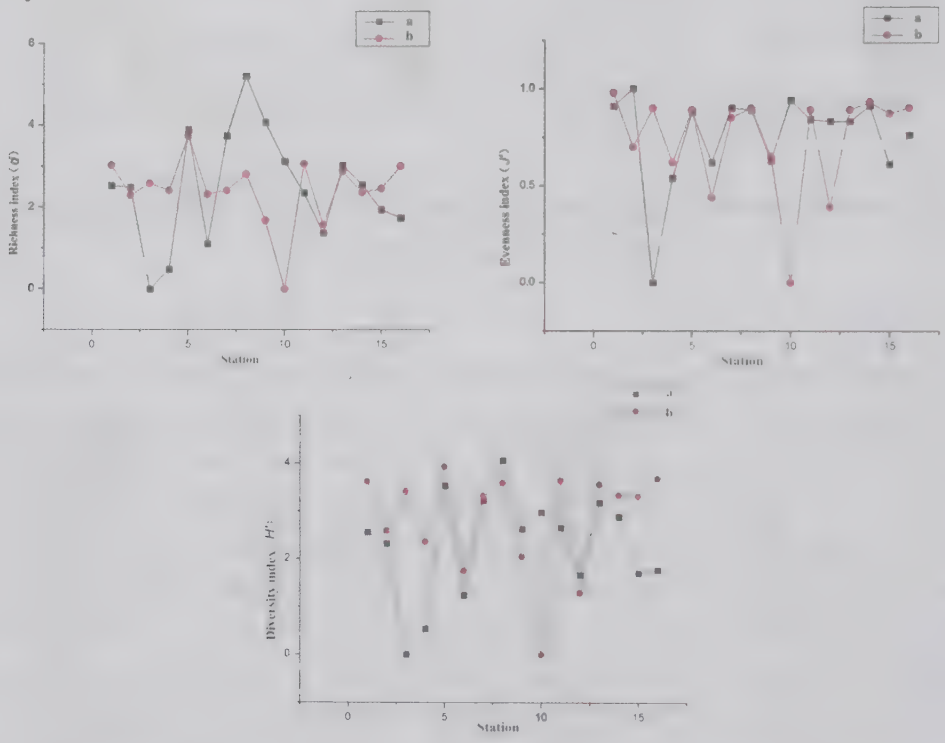

Fig. 4 Richness index (d), evenness index (J '), biodiversity index (H') in spring (a) and summer (b)

3.5 ABC curve analysis

Warwick proposed the use of the abundance/biomass comparison curve (ABC curve) method in 1968 to monitor the disturbance of environmental pollution to macrobenthos[24], and the macrobenthic communities in different areas and different habitats were verified. The results showed that the ABC curves could accurately reflect the changes of macrobenthos caused by any physical, biological and pollution disturbances. In this study, the ABC curves of abundance and biomass of macrobenthos in Changli Gold Coast Nature Reserve were analyzed. The results showed that the abundance curves in spring and

summer were all above the biomass curves (Fig. 6), indicating that the macrobenthos in Changli Gold Coast Nature Reserve Area were seriously disturbed by human activities or environmental pollution[25].

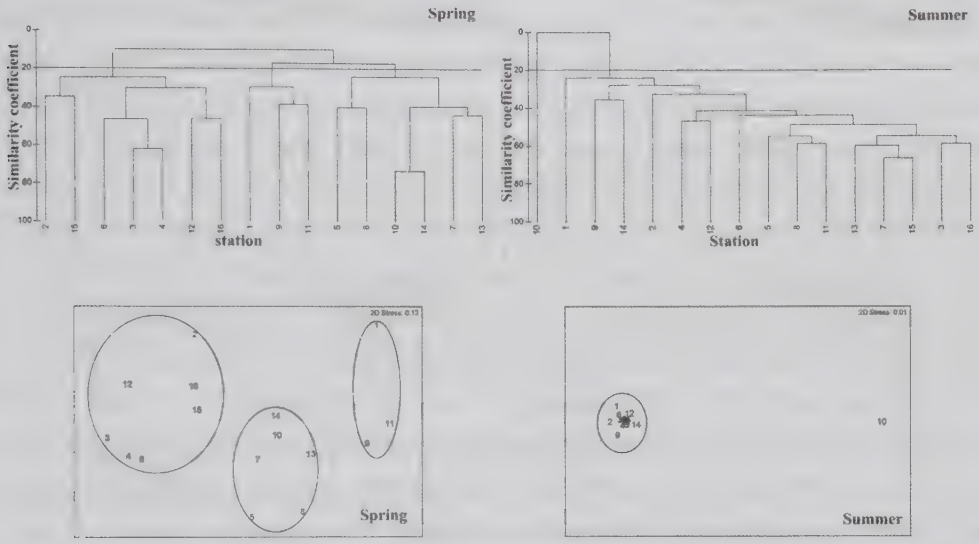

Fig. 5 Cluster analysis and multidimensional scale analysis of macrobenthios in spring and summer, 2016

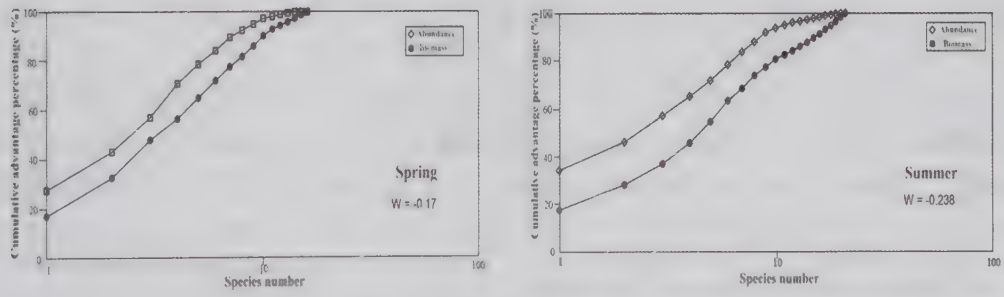

Fig. 6 Benthos community ABC curve in spring and summer, 2016

4 Discussion

4.1 Community structure characteristics

In this survey, 94 species of macrobenthos were identified, among which Polychaeta was the major species, accounting for about 58.5% of the total species, followed by crustacean accounting for 21.3%. There were 56 species in both spring and summer, accounting for 59.6% of the total species. Lili et al. (2011) [26] collected 90 species of

macrobenthos in the spring and summer of 2011. The difference in the number of visible species was normal, and the proportion of the main group was basically stable and had no major changes.

In spring, 58 species of macrobenthos were identified, most of Polychaeta (36 species) accounted for about 62.1%. The number of species varied from 1 to 26, and stations No.3 and No.4 contained only 1or 2 species of macrobenthos, which might due to the fact that the two stations are located adjacent to each other in the middle of the survey area, and these two stations are the most frequent areas of fishing. Compared with the spring of 2011 (55 species), there was no significant change. In summer, 92 species were identified, among which Polychaete (53 species) was the majority, accounting for 57.6%. The number of species varied from 1 to 2, and the number of species in each station was relatively agreed. In addition, there was no significant rule for distribution except station No.10. Compared with 2011 (74 species), the number of species in the summer of 2016 increased by about 24.3%, but, the biomass decreased by about 65.7% (from 15.9 g/m^2 to 5.46 g/m^2), due to the overfishing. Although the number of species gradually increased, the various types of individual sizes gradually decreased [27].

4.2 Abundance and biomass

Changes in abundance and biomass could reflect changes in the community in different periods of certain areas, which could be inferred from the change of environment [28]. Compared with the average abundance and biomass in spring and summer of 2011, the average abundance and biomass in this study were lower. Meanwhile, the abundance of large Echinodermate was reduced, and the number of small Polychaeta or Crustacea was increased, indicating that the sensitive species gradually disappeared and the opportunity species gradually became the dominant group in Changli Gold Coast Nature Reserve [29,30].

The abundance in summer was slightly higher than that in spring, but the average biomass in spring was significantly higher than that in summer. This might due to the lower temperature in spring, which provided more survival time for larger crustaceans, and the more frequent fishing activities in summer, which greatly made the population number of macrobenthos reduced.

4.3 Disturbance of benthic communities

The ABC curve of the spring and summer in Changli Gold Coast Nature Reserve showed that the macrobenthos in this area were subjected to more severe environmental pollution or disturbance. The causes of these pollution or disturbances were complex and might be closely related to overfishing, tourism development, and aquaculture [31]. The

excessive expansion of fish and marine aquaculture area made the sea area of macrobenthos biomass decreased sharply, and the rapid development of tourism made the man-made disturbance increased, which had great influence on the species and quantity of macrobenthos and their habitat[32].

5 Conclusions

(1) In 2016, 58 species and 92 species of macrobenthos were obtained in spring and summer, respectively, and most of them were Polychaeta. Compared with the species of macrobenthos obtained in spring and summer of 2011, the number of macrobenthos was increased by 4 species, which belonged to normal annual fluctuations. Due to the increase of temperature, the number of species of macrobenthos in summer was significantly higher than that in spring.

(2) The average biomass and abundance of each station in spring of 2016 were 15.49 g/m^2 and 155 ind/m^2, and they were 5.46 g/m^2 and 208 ind/m^2 in summer, respectively. These numbers were smaller than the average value of stations in 2011, except for the abundance in spring, 2016.

(3) The results showed that the macrobenthos could be divided into three communities in the spring of 2016, and two communities in summer. Each group similarity coefficient was low, and groups were scattered. There was no obvious distribution trend. The ABC curves indicated that the macrobenthos community in this region had serious environmental pollution or disturbance, which may be related to overfishing, tourism development, and aquaculture.

Acknowledgments

This paper is supported by Ecological Restoration Technique in Typical Bay (No. TKS160226) and Tianjin Municipal Science and Technology Planning Project (15ZCZDSF00620).

References

[1] Ji Y L, Zhao N,Yang C P, et al. Primary study on Secondary production of Macrobenthos in Western water of Liaodong Bay [J]. Periodical of Ocean University of China, 2015, 45: 53 - 58.

[2] Dong P, Zhang H B, Ye X S, et al. Community structure and biodiversity characteristics of macrobenthos in the middle of Xiangshan Bay [J]. Journal of Shanghai Ocean University, 2015, 24:

430 - 440.

[3] Jaleel K U A, Kumar P R A, Khan K N, et al. Polychaete community structure in the South Eastern Arabian Sea continental margin (200 m - 1000m) [J]. Deep Sea Research Part I: Oceanographic Research Papers, 2014, 93: 60 - 71.

[4] Liu K, Lin H S, He X B, et al. Functional feeding groups of macrozoobenthos and their relationships to environmental factors in Xiamen coastal waters [J]. Acta Oceanlogica Sinica, 2016, 38: 95 - 105.

[5] Yuan T P, Li H X, Li L, et al. Community structure of macrobenthos in summer in Daya Bay [J]. Journal of Tropical Oceanography, 2017, 36: 41 - 47.

[6] Gu X Y, Tao L, You Z J, et al. The macrobenthic community of the Xiangshan Bay [J]. Oceanologia et Limnologia Sinica, 2010, 41: 208 - 213.

[7] Wu R S S, SHIN P K S. Sediment characteristics and colonization of soft-bottom benthos: A field manipulation experiment [J]. Marine Biology, 1997, 128: 475 - 487.

[8] Wilson W H. Competition and predation in marine soft-sediment communities [J]. Annual Review of Ecology and Systematics, 1991, 21: 221 - 241.

[9] Stenton-Dozey J M E, Jackson L F, Busby A J. Impact of mussel culture on macrobenthic community structure in Saldanha Bay, South Africa [J]. Marine Pollution Bulletin, 1999: 39: 357 - 366.

[10] Resh V H, Norris R H, Barbour M T. Design and implementation of rapid assessment approaches for water resource monitoring using benthic macroinvertebrates [J]. Australian Journal of Ecology, 1995, 20: 108 - 121.

[11] Zhao Z N, Liang X L, Zhang Y M, et al. Studies on the biodiversity of macrozoobenthos in august in Changli Ecological Monitoring Area of Hebei Province [J]. Advances in Marine Science, 2014, 32: 363 - 373.

[12] Zhang P R Y, Li D L, Liu X B, et al. Phytoplankton community composition in the surrounding waters of Changli, Hebei, China [J]. Marine Science Bulletin, 2016, 18: 79 - 96.

[13] Li D L, Liu X B, Liu Z G, et al.Zooplankton community structure in relation to environmental factors in the coastal water near Luan River Estuary, China [J]. Marine Science Bulletin, 2016, 18: 41 - 55.

[14] Wang Z D, Lian J S, Hu J X, et al. Characteristics of degraded ecosystem in Daya Bay China [J]. Ecologic Science, 2003, 22: 313 - 320.

[15] Resh V H, Norris R H, Barbour M T. Design and implementation of rapid assessment approaches for water resource monitoring using benthic macroinvertebrates [J]. Australian Journal of Ecology, 1995, 20: 108 - 121.

[16] Smith S D A, Simpson R D. Recovery of benthic communities at Macquarie Island (sub-Antarctic) following a small oil spill [J]. Marine Biology, 1998, 131: 567 - 581.

[17] Alke B, Manfred R, Luise B C. Muricauda ruestringensis gen, Nov, sp. Nov.,afacultatively anaerobic, appendaged bacterium from german north sea intertidal sediment [J]. International Journal of Systematic and Evolutionary Microbiology, 2001, 51: 1997 - 2006.

[18] Wang Y, Liu L S, Liu C Q, et al. Community structure characteristics of macrobenthos in the coastal seawaters of Bohai Bay in spring [J]. Research of Environmental Sciences,2010, 23: 430 - 436.

[19] Cai W Q, Meng W, Liu L S, et al. Long-term trends of the dominant macrozoobenthos in Bohai Bay [J]. Acta Scientiae Cicumstantiae, 2013, 33:2 332 - 2 340.

[20] Han J, Zhang Z N, Yu Z S, et al. Macrobenthic species diversity in southern and central Bohai Sea, China [J]. Biodiversity Science, 2003, 11: 20 - 27.

[21] GB 17378. 7 - 2007 The specification for marine monitoring - Part 7: Ecological survey for offshore pollution and biological monitoring [S]. Beijing: Standards Press of China, 2008: 12 -17.

[22] Clarke K R, Warwick R M. Change in marine communities: An approach to statistic analysis and interpretation [M]. Plymouth Marine Laboratory, 1994.

[23] Clarke K R. Non-parametric multivariate analyses of changes in community structure [J]. Australian Journal of Ecology, 1993, 18:117 - 143.

[24] Warwick R M. A new method for detecting pollution effects on marine macrobenthic communities [J]. Mar. Biol., 1968, 92: 557 - 562.

[25] John R C. Coastal Zone Management Handbook [M]. State of Florida: CRC-Press, 1996: 219 - 220.

[26] Li L, Chen W J, Zhang Z. Ecological characteristics of macrobenthic communities in Luanhe River Estuary - Beidaihe [J]. Journal of Anhui Agriculture, 2012, 4: 13 049 - 13 054.

[27] Li Y H, Zhang K X, Duan X Y et al. The study on ecotourism development of the national nature reserve of Golden Coast in Changli County [J]. Chinese Journal of Eco-Agriculture, 2004, 12: 202 - 205.

[28] John P W, Clifford W C. Phylogeography and historical ecology of the north atlantic intertidal [J]. Evolution, 2007, 55: 2 455 - 2 469.

[29] Landis W G, Wiegers J A. Design considerations and a suggested approach for regional and comparative ecological risk assessment [J]. Human and Ecological Risk Assessment, 1997,3: 287 - 297.

[30] Hu G K , Zhang Q T. Investigation of Macrobenthos in the intertidal zone of Tianjin and discuss ion on biorem ediation [J]. Marine Science bulletin. 2004, 6: 66 - 73.

[31] Beukema J J. An evaluation of the ABC-method (a abundance /biomass comparison) as applied to macrozo-obenthic communities living on tidal flats in the Dutch Wadden Sea [J]. Mar. Biol., 1988, 99: 425 - 433.

[32] Meire P M, Dereu J. Use of the abundance / biomass comparison method for detecting environmental stress: some considerations based on intertidal macrozoobenthos and bird Communities [J]. Journal of Applied Ecology, 1990, 27: 210 - 223.

河北昌黎黄金海岸国家级自然保护区海域大型底栖动物群落特征研究

寇存辉[1]，张青田[1]，于 航[2]，李德亮[1]，赵兴贵[1]，
张彭如雁[1]，刘宪斌[1*]

（1. 天津科技大学 天津市海洋环境保护与修复技术工程中心 天津市海洋资源与化学重点实验室，天津 300457；
2. 交通运输部天津水运工程科学研究所，天津 300459）

摘 要：2016 年春季（5 月）和夏季（8 月）对河北昌黎黄金海岸自然保护区海域大型底栖动物群落进行了调查，对比分析了春、夏两季大型底栖动物种类数、丰度、生物量、优势种和生物多样性指数的差异。结果表明：春、夏季共鉴定出大型底栖动物分别为 58 种和 92 种，两季种类组成皆以多毛类为主；夏季大型底栖动物丰度略高于春季，而生物量要明显小于春季。采用 Bray-Curtis 相似性系数聚类分析和多维排列尺度（MDS）分析相结合的方法，分析了春、夏季大型底栖动物群落结构，春季可分为 3 个群落，夏季可分为 2 个群落。采用 ABC 曲线法来监测环境污染对大型底栖动物群落的扰动情况，表明该海域大型底栖动物群落受到了严重的环境污染或扰动。

关键词：昌黎；大型底栖动物；多样性；聚类分析；ABC 曲线法

Inversion and verification of chlorophyll *a* concentration in the Bohai Bay

ZHENG Xiao-shen , ZHANG Xue , JIA Chen

Tianjin Key Laboratory of Marine Resources and Chemistry, Tianjin Marine Environmental Protection and Restoration Technology Engineening Center, Tianjin University of Science & Technology, Tianjin 300457, *China*

Abstract: Chlorophyll *a* concentration is to characterize the amount of phytoplankton. In this paper, the chlorophyll *a* concentration is retrieved using the OC3M and OC2 algorithms based on the MODIS remote sensing data, and using the band ratio, OC3G and YOC algorithms based on the GOCI remote sensing data. Based on the chlorophyll *a* measured data in the Bohai Bay in spring, 2012, the spatial distribution trends of retrieval results are consistent with the measured results. By the inversion precision analysis, the accuracy of retrieval results of band ratio method based on GOCI is similar to that of OC3M method based on the MODIS. The precision retrieval results of YOC method based on GOCI are higher than the other methods.

Keywords: chlorophyll *a* concentration, Bohai Bay; MODIS, GOCI

1 Introduction

Chlorophyll is a good indicator for marine phytoplankton biomass and the main pigment for photosynthesis of ocean phytoplankton. Chlorophyll a concentration has an important economic effect on the coastal marine environment of fisheries resources and marine aquaculture development [1-4]. Chlorophyll a concentration is retrieved based on the color satellite remote sensing data, which has been an important method to monitor the marine chlorophyll a concentration.

Since the launch in 1978 of the first ocean color remote sensing satellite, Coastal Zone Color Scanner (CZCS), many studies have attempted to monitor Chlorophyll *a* concentration on the sea surface using remote sensing techniques. For the Case I water, the inversion algorithms of chlorophyll *a* concentration is already quite mature. But for the Case II water, the inversion methods of chlorophyll *a* concentration should be further studied. However, most of the satellite sensors, including Sea-viewing Wide Field-of-view Sensor (SeaWiFS) and Moderate-resolution Imaging Spectroradiometer (MODIS) had

Received on June. 23, 2016

Corresponding author: zhengxiaoshen@163.com

insufficient temporal resolution to reveal dynamic variations in Chlorophyll *a* concentration. Up to now, domestic and foreign scholars have done a lot of research [5-8]. But the Bohai Bay is a semi-enclosed bay, a number of coastal rivers into the sea, poor water exchange, low self-purification capacity and assimilative capacity, the distribution of phytoplankton have strong regional characteristics, so the inversion algorithm and inversion model of chlorophyll a concentration must be regional.

The Geostationary Ocean Color Imager (GOCI) enables hourly monitoring of variations in ocean properties [9]. GOCI, which was the first ocean color observation satellite t be placed in a geostationary orbit, can monitor near real-time marine environments in northeast Asia, with a spatial resolution of 500 m. GOCI has six visible bands with band center 412 nm, 443 nm, 490 nm, 555 nm, 660 nm and 680 nm, and two near-infrared bands with band center 745 nm and 865 nm.[10-12]. The chlorophyll *a* concentration is retrieved the band ratio, OC2, OC3G and YOC methods based on the GOCI remote sensing data. In this paper, the chlorophyll *a* concentration is retrieved using the OC3 and OC2 algorithms based on the MODIS remote sensing data, and using the band ratio, OC3G and YOC algorithms based on the GOCI remote sensing data.

2 Data and methods

2.1 Situ data

The hydrological, chemical and biological situ observation stations in the Bohai Bay (37.80N-39.20N, 117.80E-119.30E) were shown in Fig. 1. The time of observation was from April 3 to April 8 in 2012. The stations were arranged from the Beitang and Haihe River to sea, and each station was about 7 - 10 miles, following the bathymetry. The stations sites and bathymetry were shown in Fig. 1.

2.2 MODIS data and the retrieval methods of the Chlorophyll a concentration

The standard mapped satellite images from MODIS/Aqua were used to derive the Chlorophyll *a* concentration in the Bohai Bay. Daily remote sensing reflectance (Rrs) values from April 3 to April 8 in 2012 were used. These satellite data were obtained from the Ocean Biology Processing Group (OBPG) of the Goddard Space Flight Center (GSFC) (http://oceandata.sci.gsfc.nasa.gov/MODIS- Aqua/Mapped/Daily/ 4km/Rrs/2012/)[13-14]. The retrieval methods of the Chlorophyll *a* concentration were described and used, such as the OC3M algorithm and OC2 algorithm.

2.2.1 The OC3M algorithm

The OC3M algorithm is an algorithm for retrieving chlorophyll *a* concentration in

coastal waters based on MODIS sensor data. The formula is shown as following:

$$\log[Chl]=a_0+a_1X+a_2X^2+a_3X^3+a_4X^4 \quad (1)$$

$$X=\log[(\max(R_{rs}(443),R_{rs}(489)))/R_{rs}(555)] \quad (2)$$

where, Chl is the concentration of chlorophyll *a*; a0, a1, a2, a3, a4 as a coefficient; Rrs is the remote sensing reflectance; λ is the MODIS band of the central length.

OC3M algorithm specific expression is as follows:

$$C_{Chla}=10^{(0.283-2.753R_3+1.457R_3^2+0.659R_3^3-1.403R_3^4)} \quad (3)$$

where C_{Chla} is the chlorophyll *a* concentration, and R_3 is the band ratio of the OC3M algorithm.

$$R_3=\lg[\max(R_{rs}(443,488))/R_{rs}(551)] \quad (4)$$

where, Rrs (λ) is the λ-band remote sensing reflectivity.

2.2.2 The OC2 algorithm

The formula of OC2（OC2v2）algorithm is shown as follows:

$$Chl_a=e_0+10^{e_1+e_2*R+e_3*R2+e_4*R3} \quad (5)$$

$$\text{where} \quad R=\log_{10}\left(\frac{R_{rs}(490)}{R_{rs}(555)}\right) \quad (6)$$

$$e_0=-0.0929,\ e_1=0.2974,\ e_2=-2.2429,\ e_3=0.8358,\ e_4=-0.0077$$

where, Chl_a is the chlorophyll *a* concentration; e0, e1, e2, e3, e4 for the coefficient; R for the band coefficient; R_{rs} for the selected λ-band remote sensing reflectance.

2.3 GOCI data and the retrieval methods of the Chlorophyll a concentration

GOCI satellite image data with 500 m spatial resolution and 1-hour temporal resolution were used to get the hourly map of $C_{chl\text{-}a}$. Match up data, GOCI level-1b, from April 3 to April 8 in 2012 (full clear-sky scenes) were obtained from the Korea Ocean Satellite Center (http://kosc.kordi.re.kr/). The technical software for GOCI (GDPS) was specialized for the ocean, and land information was masked during data processing. Thus, GOCI level-1b data were converted to calibrated radiance data using the self-compiled ENVI–IDL (Interface description language) software package, in which all calibration parameters were from a hierarchical data of the GOCI image [15, 16]. A geometric correction was also included in the software package. Atmospheric influence was corrected (atmospheric correction) based on the radiative-transfer calculations from the Second

Simulation of the Satellite Signal in the Solar Spectrum (6Smodel). The continental aerosol type and atmospheric profiles (middle latitude summer type) embedded in the 6S model were used. The retrieval methods of the Chlorophyll *a* concentration were described and used, such as the band ratio algorithm, the OC3G algorithm and the YOC algorithm.

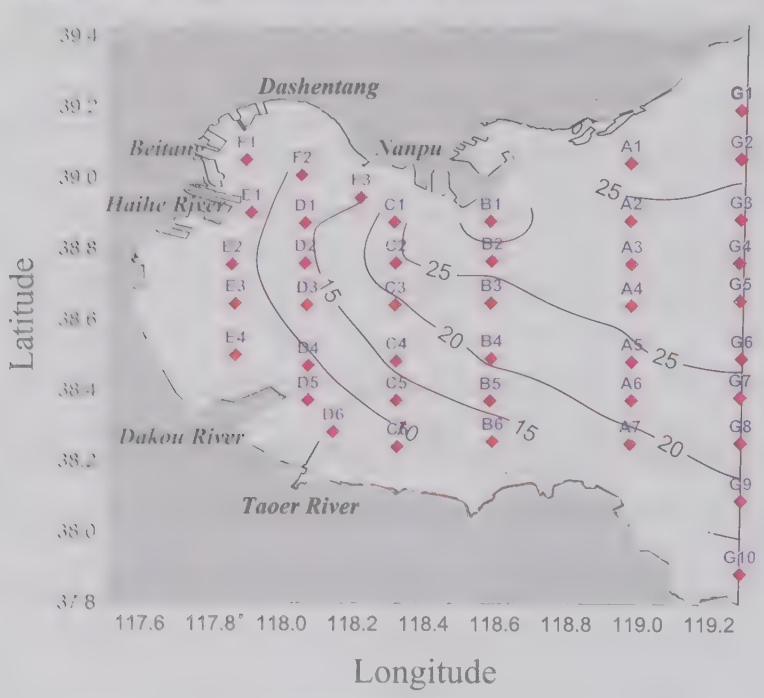

Fig. 1 The station sites and bathymetry in the Bohai Bay

2.3.1 The band ratio algorithm

The classical blue-green band ratio method was used to invert the concentration of chlorophyll a, and the expression was as follows:

$$Chl_{GDPS}=1.8528*R^{-3.263} \quad (7)$$

$$R=[R_{rs}(443)+R_{rs}(490)-R_{rs}(412)]/R_{rs}(555) \quad (8)$$

where Chl_{GDPS} is the chlorophyll *a* concentration retrieved from GDPS; R is the band factor; Rrs (λ) is the remote sensing reflectance of the selected λ band. The four bands of 412 nm, 443 nm, 490 nm and 555 nm can effectively reduce the effect of colored dissolved organic matter (CDOM) on the chlorophyll *a* concentration inversion.

2.3.2 The OC3G algorithm

OC3G (OC4v4) model uses Rrs (510) as the most primitive band channel. Since the GOCI data does not have a band of 510nm, the OC3G model used by the GDPS software uses Rrs (443), Rrs (490) and Rrs (555). These bands are more suitable for chlorophyll

inversion of GOCI data. Specific model formula is as follows:

$$Chl_a=10^{f_0+f_1*R+f_2*R2+f_3*R3+f_4*R4} \quad (9)$$

$$R=\log_{10}\left(\frac{\max(R_{rs}(443),R_{rs}(490))}{R_{rs}(555)}\right) \quad (10)$$

$$f_0=0.366,\ f_1=-3.067,\ f_2=1.93,\ f_3=0.649,\ f_4=-1.532$$

where, Chl_a is the chlorophyll *a* concentration; f_0, f_1, f_2, f_3, f_4 for the coefficient; R is the band coefficient; R_{rs} is the selected λ-band remote sensing reflectance.

2.3.3 The YOC algorithm

The YOC algorithm was designed the function in 1994, while the parameters were made to run in 2011. The parameters of the algorithm are based on situ observation stations radiometric and pigment measurements in the East China Sea, the Yellow Sea and the South Sea of Japan during the past decade. Specific model formula is as follows:

$$Chl_a=10^{[c1+c2\log_{10}(R)+c3\log_{10}2(R)]} \quad (11)$$

$$R=\left(\frac{R_{rs}(490)}{R_{rs}(555)}\right)*[Rrs(443)]^{c4} \quad (12)$$

$$c_1=0.342,\ c_2=2.511,\ c_3=0.277,\ c_4=-1.012$$

where, Chl_a is the chlorophyll *a* concentration; c_0, c_1, c_2, c_3, c_4 for the coefficient; R is the band coefficient.

3 Results and discussions

3.1 The results based on the MODIS data

According to the latitude and longitude of the measured data, the chlorophyll *a* concentration corresponding to the remote sensing inversion results can be found. Tab. 1 shows the chlorophyll *a* concentration inversion results based on the MODIS data using the OC3M algorithm and relative error between the measured and the inversion results.

The results show that the highest relative error is 365.4%; the lowest is 1.6%; the average error is 145.9%; the highest relative error is at station A2; the station is close to the coast and the measured data is small. The minimum relative error is at the D1 station, which is at the exit of the harbor, and it is in the high value areas of chlorophyll *a* concentration. Therefore, according to the relative errors, it has good agreement between the inversion results of chlorophyll *a* concentration and the measured data in the

high-value areas, but it is different between the inversion results and the measured values in the middle and low chlorophyll *a* concentration

Tab. 1 The chlorophyll *a* concentration values and relative error of the OC3M algorithm

Stations	A1	A2	B1	D1	D2	E1	E2	F1	F2	G1	G2	G10	Average relative error%
measured chl-a (mg/m³)	1.794	1.023	2.451	4.503	1.092	5.219	3.297	5.246	1.166	1.519	2.029	2.363	
OC3(mg/m3)	4.693	4.761	4.428	4.576	4.603	6.435	5.789	5.572	5.011	4.946	3.906	3.946	
relative error %	161.6	365.4	80.7	1.6	321.5	23.3	75.6	6.2	329.8	225.6	92.5	67.0	145.9

Tab. 2 The chlorophyll *a* concentration values and relative error of the OC2 algorithm

Stations	A1	A2	B1	D1	D2	E1	E2	F1	F2	G1	G2	G10	Average relative error%
measured chl-a (mg/m³)	1.794	1.023	2.451	4.503	1.092	5.219	3.297	5.246	1.166	1.519	2.029	2.363	
OC2(mg/m3)	5.513	4.137	4.854	3.548	3.900	6.581	5.148	6.179	4.624	3.580	3.479	3.743	
relative error %	207.3	304.4	98.0	21.2	257.1	26.1	56.1	17.8	296.6	135.7	71.5	58.4	129.2

Tab. 2 shows the chlorophyll *a* concentration inversion results based on the MODIS data using the OC2 algorithm and relative error between the measured and the inversion results.

Based on the OC2 algorithm inversion results, the relative error is smaller at the D1, E1 and F1 stations, which is about less than 30%. The average relative errors of the chlorophyll *a* concentration inversion results are about 129.2%. The minimum values of relative error are also in the area near the shore, and the chlorophyll *a* concentration is high and the distribution is obvious. According to the average relative error, the inversion results of OC2 algorithm has the same trend as that of OC3M algorithm, but the precision of chlorophyll *a* concentration inversion of OC2 algorithm is better than that of OC3M algorithm.

From Tab. 1 and Tab. 2, it can be seen that the higher inversion values of the chlorophyll *a* concentration are close to the coastal area near Tianjin Port in the Bohai Bay. The reason may be that the algae and phytoplankton begin to increase gradually in spring. Enough light is conducive to photosynthesis of plants in the water, and the Haihe River and many other rivers into the sea, carrying a lot of nutrients, such as silicate and phosphate,

which will promote the growth of plants in seawater.

3.2 The results based on the GOCI data

Because of GOCI data there are eight remote sensing image maps per day. Choosing suitable GOCI images based on the measured station time, the chlorophyll *a* concentration inversion was performed by the method described above. Tab. 3 shows the inversion results and relative errors based on the GOCI data using the band ratio (BR) algorithm. Tab. 4 shows the results and relative errors of the inversion results based on GOCI data using the OC3G algorithm. Tab.5 shows the results and relative errors of the inversion results based on GOCI data using the YOC algorithm.

Tab. 3 The chlorophyll a concentration values and relative error of the band ratio algorithm

Stations	A1	A2	A3	B1	B2	C3	C4	D1	D2	D3	E1	E2
measured chl-*a* (mg/m^3)	1.794	1.023	0.563	2.451	0.661	0.456	0.426	4.503	1.092	0.479	5.219	3.297
BR(mg/m^3)	2.518	2.454	2.053	2.501	2.376	2.703	2.491	2.194	2.509	2.486	3.094	2.904
relative error %	40.4	139.9	264.7	2.0	259.5	492.8	484.7	51.3	129.8	419.0	40.7	11.9

Stations	F1	F2	G1	G2	G3	G4	G5	G6	G7	G8	G9	G10	Average relative error %
measured chl-*a* (mg/m^3)	5.246	1.166	1.519	2.029	0.672	0.511	0.407	0.326	0.293	0.347	0.346	2.363	
BR(mg/m^3)	3.069	2.768	1.987	1.696	1.432	1.227	1.117	1.088	1.025	1.169	1.198	2.032	
relative error %	41.5	137.4	30.8	16.4	131.1	140.1	174.4	233.7	249.8	236.9	246.2	14.0	166.2

The maximum values of relative error are about 490% between the band ratio algorithm and the measured data, the minimum is 2% and the average relative error is 160%. The larger relative error is at C3 and C4 stations, located in the central water body in the bay, and the values of measured sea surface chlorophyll *a* concentration are very low. The minimum relative error is at B1 site, which is almost the same as the measured data. The values of chlorophyll *a* concentration are at the middle. According to the average relative error, it can be seen that the GOCI band ratio method is in good agreement with the measured data, and the precision of inversion chlorophyll a concentration is high.

Although the trends of spatial distribution of inversion chlorophyll *a* concentrations

based on the OC3G algorithm are close to those of the previous algorithms, and the chlorophyll *a* concentration is much higher than that of the former two algorithms. It can be seen from the relative error that the error of this method is large for the inversion of the case II water body.

Tab. 4 The chlorophyll a concentration values and relative error of the OC3G algorithm

Stations	A1	A2	A3	B1	B2	C3	C4	D1	D2	D3	E1	E2
measured chl-*a* (mg/m^3)	1.794	1.023	0.563	2.451	0.661	0.456	0.426	4.503	1.092	0.479	5.219	3.297
OC3G（mg/m^3）	9.106	6.741	5.292	8.440	6.592	2.744	2.498	5.441	6.207	2.617	12.989	9.172
relative error %	407.6	558.9	840.0	244.3	897.3	501.8	486.4	20.8	468.4	446.3	148.9	178.2

Stations	F1	F2	G1	G2	G3	G4	G5	G6	G7	G8	G9	G10	Average relative error %
measured chl-a (mg/m^3)	5.246	1.166	1.519	2.029	0.672	0.511	0.407	0.326	0.293	0.347	0.346	2.363	
OC3G (mg/m^3)	11.878	7.883	5.507	5.294	3.881	3.638	1.423	1.318	1.277	1.444	1.458	3.743	
relative error %	126.4	576.1	262.5	160.9	477.5	611.9	249.6	304.3	335.8	316.1	320.2	163.4	379.3

Tab. 5 The chlorophyll a concentration values and relative error of the YOC algorithm

Stations	A1	A2	A3	B1	B2	C3	C4	D1	D2	D3	E1	E2
measured chl-*a*(mg/m^3)	1.794	1.023	0.563	2.451	0.661	0.456	0.426	4.503	1.092	0.479	5.219	3.297
YOC(mg/m^3)	1.268	1.274	1.217	1.173	1.248	1.293	1.074	1.417	1.666	1.029	2.047	1.875
relative error %	29.3	24.5	116.1	52.1	88.8	183.5	152.1	68.5	52.6	114.8	60.8	43.1

Stations	F1	F2	G1	G2	G3	G4	G5	G6	G7	G8	G9	G10	Average relative error %
measured chl-a(mg/m^3)	5.246	1.166	1.519	2.029	0.672	0.511	0.407	0.326	0.293	0.347	0.346	2.363	
YOC(mg/m^3)	1.968	1.610	1.391	1.441	0.689	0.683	0.613	0.603	0.583	0.635	0.735	1.634	
relative error %	62.5	38.1	8.4	29.0	2.5	33.7	50.6	85.0	99.0	83.0	112.4	48.8	68.3

The YOC algorithm was optimized and validated by extensive field measurements collected in the East China Sea and the Yellow Sea. For the complex water bodies of the East China Sea and the Yellow Sea, the chlorophyll *a* concentration inversion of the surface has a better effect. The YOC algorithm is in good agreement with the measured data, and the average relative error is 68.3%. The YOC algorithm can eliminate the factors that influence the chlorophyll *a* concentration inversion according to the geographical environment and the water quality of the coastal areas of China. Therefore, the YOC algorithm is in good agreement with the measured data and the inversion accuracy is also good.

4 Conclusions

The chlorophyll *a* concentration is retrieved using the OC3 and OC2 algorithms based on the MODIS remote sensing data, and using the band ratio, OC3G and YOC algorithms based on the GOCI remote sensing data. Based on the chlorophyll *a* measured data in the Bohai Bay in spring, 2012, the spatial distribution trends of retrieval results are consistent with the measured results. By the inversion precision analysis, the accuracy of retrieval results of band ratio algorithm based on GOCI is similar to that of OC3 algorithm based on the MODIS. The precision retrieval results of YOC algorithm based on GOCI are higher than the other algorithms.

Acknowledgments

The study was supported by Tianjin Natural Science Foundation Project (14JCYBJC22500).

References

[1] Honeywill C, Paterson D M, Hegerthey S E. Determination of microphytobenthic biomass using pulse-amplitude modulated minimum fluorescence [J]. Eur. J. Phycol., 2002, 37 (4), 485 - 492.

[2] Xiulin Lou, Chuanmin Hu. Diurnal changes of a harmful algal bloom in the East China Sea: Observations from GOCI [J]. Remote Sensing of Environment, 2014, 140: 562 - 572.

[3] Le C F, Li Y M, Zha Y, et al. Remote estimation of chlorophyll a in optically complex waters based on optical classification [J]. Remote Sens. Environ., 2011, 115 (2), 724 - 737.

[4] Paerl H W, Xu H, McCarthy M J, et al. Controlling harmful cyanobacterial blooms in a hyper-eutrophic lake (Lake Taihu, China): The need for a dual nutrient (N & P) management strategy [J]. Water Research, 2011, 45, 1 973 - 1 983.

[5] Chen Z Q, Hu C M, Muller-Karger F. Monitoring turbidity in Tampa Bay using MODIS/Aqua 250-m imagery [J]. Remote Sensing of Environment, 2007, 109, 207 - 220.

[6] Miller R L, McKee B A. Using MODIS Terra 250 m imagery to map concentrations of total suspended matter in coastal waters [J]. Remote Sensing of Environment, 2004, 93, 259 - 266.

[7] Neukermans G, Ruddick K, Bernard E, et al. Mapping total suspended matter from geostationary satellites: A feasibility study with SEVIRI in the Southern North Sea [J]. Optics. Express, 2009, 17, 14 029 - 14 052.

[8] Volpe V, Silvestri S, Marani M. Remote sensing retrieval of suspended sediment concentration in shallow waters [J]. Remote Sensing of Environment, 2011, 115, 44 - 54.

[9] Choi J Y, Kwon Y K, Chung G S. Late quaternary stratigraphy and depositional environment of tidal sand ridge deposits in Gyeonggi Bay, west coast of Korea (Korea ed.) [J]. Journal of the Korean Earth Science Society, 2012, 33, 1 - 10.

[10] Choi J K, Oh H J, Koo B J, et al. Crustacean habitat potential mapping in a tidal flat using remote sensing and GIS [J]. Ecological Modelling, 2011, 222, 1 522 - 1 533.

[11] Choi J K, Park Y J, Ahn J H, et al. GOCI, the world's first geostationary ocean color observation satellite, for the monitoring of temporal variability in coastal water turbidity [J]. Journal of Geophysical Research, 2012, 117, C09004.

[12] Choi J K, Park Y J, Lee B R,et al. Application of the Geostationary Ocean Color Imager (GOCI) to mapping the temporal dynamics of coastal water turbidity [J]. Remote Sens. Environ., 2014, 146, 24 - 35.

[13] Gordon H R. Normalized water-leaving radiance: Revisiting the influence of surface roughness [J]. Applied Optics, 2005, 44, 241 - 248.

[14] Wang M. Effects of ocean surface reflectance variation with solar elevation on normalized water-leaving radiance [J]. Applied Optics., 2006, 45, 4 122 - 4 128.

[15] Lou X, Hu C. Diurnal changes of a harmful algal bloom in the East China Sea: observations from GOCI. Remote Sens. Environ., 2014, 140 (0): 562 - 572.

[16] Yang H, Choi J K, Park Y J, et al. Application of the Geostationary Ocean Color Imager (GOCI) to estimates of ocean surface cur-rents [J]. J. Geophys. Res.-Oceans, 2014, 119 (6): 3 988 - 4 000.

渤海湾叶绿素浓度的反演与验证

郑小慎，张 雪，贾 晨

（天津科技大学 天津市海洋资源与化学重点实验室 天津市海洋环境保护与修复技术工程中心，天津 300457）

摘 要：叶绿素 a 浓度是浮游植物现存量的表征。本文基于 2012 年春季渤海湾叶绿素实测数据，下载了相应的遥感数据，利用 MODIS 数据的 OC3M 和 OC2 方法进行叶绿素浓度 *a* 反演，利用 GOCI 数据的波段比值、OC3G 以及 YOC 算法对叶绿素 *a* 浓度进行反演，反演结果与实测结果的空间分布趋势一致。由反演精度分析，GOCI 的波段比值法与 MODIS 的 OC3M 算法的反演精度相近，GOCI 数据的 YOC 叶绿素浓度算法在渤海湾反演精度比其他反演算法高。

关键词：叶绿素 *a* 浓度，渤海湾，MODIS，GOCI

Comparison of inversion of Chlorophyll concentration in the Bohai Bay based on GOCI Data

ZHANG Xue, ZHENG Xiao-shen*

Tianjin Key Laboratory of Marine Resources and Chemistry, Tianjin Marine Environmental Protection and Restoration Technology Engineening Center, Tianjin University of Science & Technology, Tianjin 300457, *China*

Abstract: Bohai bay has poor water circulation capacity and low self-purification capacity, and a large number of land-sourced pollutants are accepted every year. The estimation of chlorophyll concentration based on remote sensing plays an important role in the study of marine red tide and the monitoring of water quality in the Bohai Bay. So it is necessary to select the best algorithm by comparing the performance of each algorithm. Choosing the best algorithm is helpful to improve the precision of chlorophyll concentration. Based on the in-situ measurement data of the Bohai Bay and the GOCI remote sensing reflectance data, the retrieval models of chlorophyll concentration were established in this paper by using the methods of fluorescence line height (FLH), OC3, blue-green band ratio and NIR-red band ratio. The above algorithms were evaluated by comparing the simulation results and the verification results. The results showed that there are obvious differences in the accuracy of different retrieval methods. The fitting and retrieval effect of FLH is the best and NIR-red band ratio is the worst, and the OC3 is similar to the blue-green band ratio method.

Key words: chlorophyll concentration, GOCI, fluorescence line height method, Bohai Bay

1 Introduction

The estimation of chlorophyll concentration plays an important role in study of marine red tide, characterization of phytoplankton biomass and water quality monitoring. The advantages of remote sensing monitoring chlorophyll concentration are wide range, low cost and convenient for long-term dynamic monitoring. It's a long-term, low cost and convenient way of long-term dynamic monitoring over large areas for understanding chlorophyll concentrations. GOCI is the first geostationary ocean color satellite with high temporal resolution, which provides data for dynamic monitoring of ocean remote sensing.

Received on June 23, 2016

*Corresponding author: zhengxiaoshen@163.com

The spatial resolution is 500 m, which can capture the spectral characteristics of water. (Xu Shiguo et al.) used MODIS data to retrieve chlorophyll-*a*, and observed the spatial and temporal distribution and characteristics of chlorophyll-*a* (Xu, 2015). Compared with MODIS, GOCI has a higher temporal resolution, and has a greater advantage in the temporal and spatial variation monitoring. (Huang C et al.) used GOCI remote sensing data to retrieve chlorophyll-*a*, and the results were consistent with the measured chlorophyll (Huang, 2015). It is feasible to use GOCI data to retrieve chlorophyll concentration.

The Bohai Bay is located on the west side of the Bohai Sea, covering an area of 15.9 thousand square kilometers, accounting for about 1/5 of the Bohai Sea, with an average depth of 12.5 m. The water exchange capacity and self purification of the Bohai Bay are poor. In recent years, with the development of industry, agriculture, aquaculture and port around the Bohai Sea, a lot of nutrients were discharged into the Bohai Bay. Nutrient enrichment will cause changes in the number and types of phytoplankton (Sun, 2008). Therefore, it is necessary to investigate the distribution of chlorophyll concentration in the Bohai Bay, and satellite remote sensing can meet this requirement.

In this paper, the chlorophyll concentration inversion model was established by the method of fluorescence line height, OC3, blue-green band ratio and NIR-red band ratio. The above algorithms were evaluated by comparing the simulation results and the verification results.

2 Data and methodology

2.1 Data sources and pretreatment

2.1.1 Data sources

The in-situ measurements used in this study are from the national science and technology support project during April 2012 in the Bohai bay. The number of observation stations is 42, and the station distribution is shown in Fig. 1.

The satellite remote sensing data used in this paper is the level 2 data of the GOCI sensor, which is the remote sensing reflectance after the Rayleigh correction, with a spatial resolution of 500 m. Satellite remote sensing data are from the Korean Ocean Satellite Center (KOSC) website http://kosc.kiost.ac.

$$\log_{10}[\mathrm{CHL}] = c_0 + c_1 \log_{10} X + c_2 \log_{10}^2 X + c_3 \log_{10}^3 X + c_4 \log_{10}^4 X \quad (1)$$

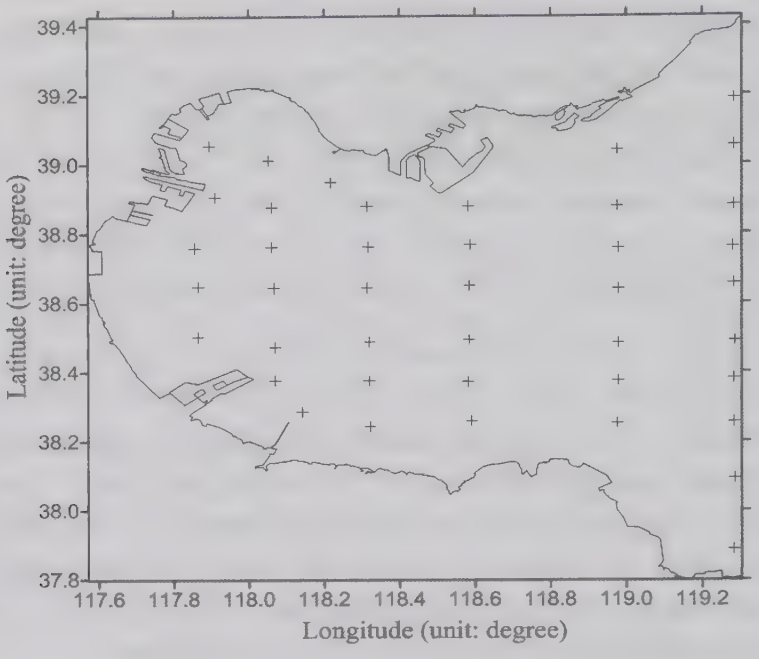

Fig. 1 Distribution of the Bohai Bay voyage in April 2012

2.1.2 Data preprocessing

First of all, the temporally closest GOCI data points were first inspected for availability for time matching. Secondly, the latitude and longitude of the observation site were compared with the remote sensing data for the spatial matching. Finally, according to the time and space location of the site observation, selected the better quality image, and then selected the available data. The optical remote sensing is greatly influenced by the cloud. The cloud in the remote sensing image can block the information. The images including clouds cannot be used for chlorophyll concentration retrieval. This part of the data needs to be removed. In addition, the concentration of suspended matter in the coastal area is very high, which will cover the chlorophyll information. This part of the data also needs to be removed. There are 20 stations that meet the requirements. The 20 stations were divided into two groups, one group was used to retrieve chlorophyll concentration remote sensing model, and the other was used to test the performance of the model.

2.2 Methodology

2.2.1 OC3

OCx is the commonly operational algorithm for each sensor. The functional form of the OCx algorithms are given as

where for OC3, $X = \max(R(443), R(490)) / R(555)$.

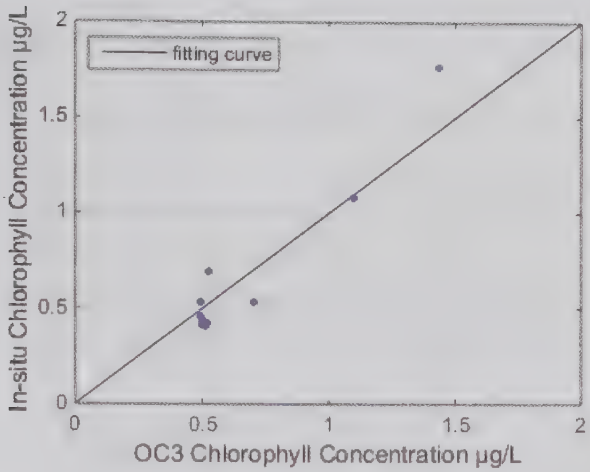

Fig. 2 Scatter plot of chlorophyll concentration values of in-situ and OC3

Regression results were c_0=1.8836, c_1=63.682, c_2=777.342, c_3=4432.0338, c_4=9532.5187. The scatter plot of the estimated chlorophyll concentrations of the OC3 algorithm and in-situ chlorophyll concentration is shown in Fig. 2. The sum of squared error (SSE) is 0.8087, and determination coefficient (R^2) is 0.5996, and root mean square error (RMSE) is 0.212.

2.2.2 blue-green band ratio

With the change of chlorophyll concentration, there are obvious differences in 430 - 700 nm spectra. There is an absorption peak at the wavelength of 440 nm (blue band), and this peak decreases with the increase of chlorophyll concentration. In the 520 nm, the radiation value is not changed with the chlorophyll concentration. The peak value appeared at 550 nm and increased with the increase of chlorophyll concentration (Zhao, 2003). According to this feature, the ratio of the bands on both sides of the 520 nm is selected to enhance the chlorophyll spectral signal, and to improve the accuracy of the inversion of the chlorophyll concentration. The second wavelength of GOCI is 443 nm (blue band), and the wavelength of GOCI is 555nm (green band). These two bands are located on both sides of the 520 nm, so they are selected to calculate the blue-green band ratio.

Linear regression analysis between in-situ chlorophyll concentration and the blue-green band ratio was conducted. Regression equation is $y = 4.715x - 2.175$, where x is the ratio of blue to green. Fig. 3 is the fitting graph, and SSE=0.427 3, R2=0.747 8, RMSE=0.231 1.

2.2.3 NIR-red band ratio

The red band is usually absorbed by phytoplankton, and the near infrared band at

700 - 720 nm is mainly absorbed by water. Jiao Hongbo et al. used the measured hyperspectral data to analyze and calculate the water leaving radiance and remote sensing reflectance of Taihu Lake water, and set up the quantitative estimation model of the chlorophyll *a* concentration in Taihu Lake. The study found that the water remote sensing reflectance ratio spectra in 719 nm and 725 nm has two peaks, of which the peak at 719nm is more obvious and stable and that the linear model established by reflectance ratio R719/R670 is more accurate to estimate chlorophyll a concentration (Jiao, 2006). For GOCI, the 660 nm band is used for the red band, and the 745 nm band, which is the closest to the 700 - 720 nm band, is used for the near infrared band.

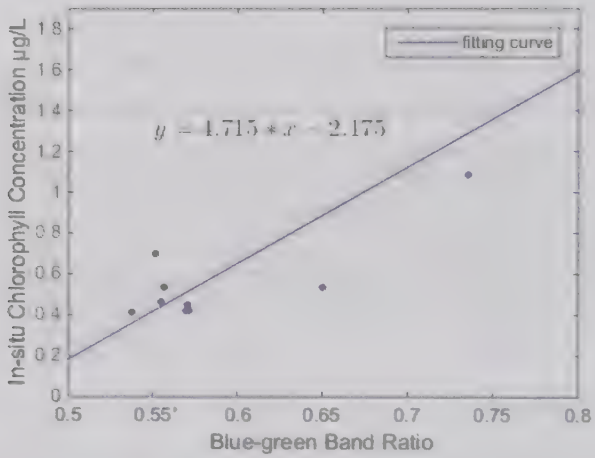

Fig. 3 Fitting graph of in-situ chlorophyll concentration and the blue-green band ratio

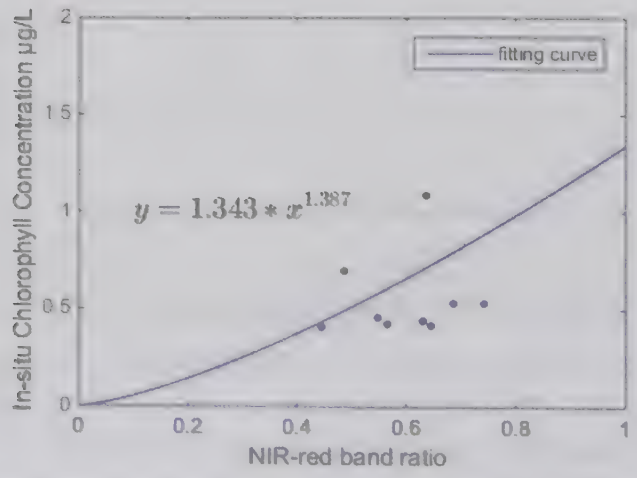

Fig. 4 Fitting graph of in-situ chlorophyll concentration and the NIR-red band ratio

Curvilinear regression analysis was conducted and the result is $y = 1.343x^{1.387}$ .The blue curve in Fig. 4 is the fitting curve, in which SSE=1.508，R2=0.109 6，RMSE=0.434 2.

2.2.4 FLH

FLH method is based on the correlation between the fluorescence line height and chlorophyll concentration. At present, it is common to use this algorithm to retrieve chlorophyll concentration. For instance, (Xu Liang et al.) established the inversion model of chlorophyll-*a* concentration by fluorescence line height method (Xu, 2014); (Gower J et al). compared the relationship between fluorescence signal and in-situ data, and established a simple model (Gower, 2007). Fluorescence line height is calculated by wavelength and reflectance. The center wavelength is the chlorophyll fluorescence peak, other wavelengths were located on both sides of the center wavelength and the connection between their remote sensing reflectance is the baseline. The fluorescence line height is the height of the remote sensing reflectance above the baseline. It is shown in Fig. 5, the abscissa is the wavelength, the ordinate is the remote sensing reflectance, and the DF is the fluorescence line height. DF is calculated by subtracting DE from EF, in which DE is calculated by using the properties of two similar triangles ABC and DEC. The calculation formula of the FLH is as follows:

$$\mathrm{FLH}=\mathrm{R_F}-(\mathrm{R_R}+\frac{\lambda_\mathrm{R}-\lambda_\mathrm{F}}{\lambda_\mathrm{R}-\lambda_\mathrm{L}}\cdot(\mathrm{R_L}-\mathrm{R_R})) \tag{2}$$

In the formula, λ_L , λ_R , λ_F are the fluorescence peak, the left side of the fluorescence peak and the right side of the fluorescence peak respectively, and $\mathrm{R_F}$, $\mathrm{R_L}$, $\mathrm{R_R}$ are the remote sensing reflectance of fluorescence peaks ,the left and right band respectively.

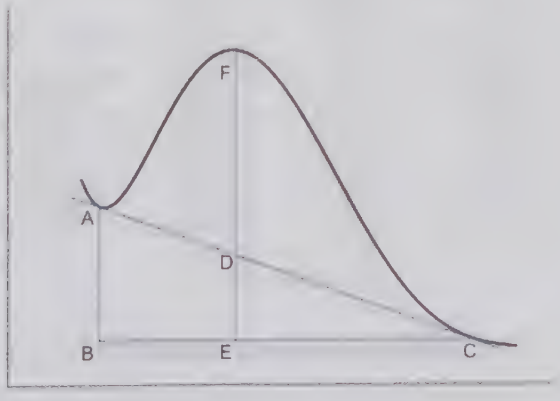

Fig. 5 Schematic diagram of FLH

By measuring the fluorescence line height of the sea surface, Pan Delu et al. selected two groups of bands to measure the sea surface chlorophyll concentration, and it provides the basis for the band selection of chlorophyll concentration sensor. One of the best combination bands is 659.5 - 672.5nm, 673.5 - 688.5nm, 746.2 - 757.8nm, which corresponds to the wavelength of band5 (660 nm), band 6 (680 nm) and band7 (745 nm) of GOCI sensor (Pan, 1989). The fluorescence line height calculated by these 3 bands can be used to retrieve the chlorophyll concentration, and the sixth band is the central wavelength. Using the formula (2) to calculate the height of the fluorescence line, we can find that the relationship between FLH and the in-situ chlorophyll concentration can be seen as the power function.

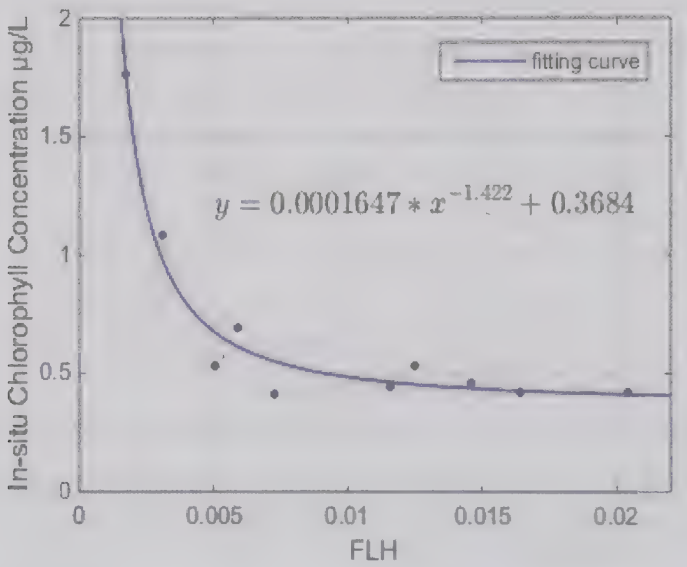

Fig. 6 Fitting graph of in-situ chlorophyll concentration and FLH

Suppose their relationship is $y = ax^b + c$. Curvilinear regression analysis was conducted and the results were a=0.001 647, b=-1.422, c=0.368 4. The blue curve in Fig. 6 is the fitting curve, in which SSE=0.065 57, R2=0.961 3, RMSE=0.096 78.

3 Results and discussion

3.1 Data validation

10 groups of data are used to validate the model and calculate their relative error, as shown in Fig. 7. It can be found that the maximum value appeared in the second groups of NIR-red band ratio method, and the relative error was close to 140%. The relative error of most data of the fluorescence line height method is not more than± 20%. The relative error

of OC3 algorithm is in the range of ±40%, and only the ninth groups is more than 70%. The relative error of the most data of blue green band ratio is also distributed between ± 40%. But the relative error of the NIR-red band ratio method is higher than others.

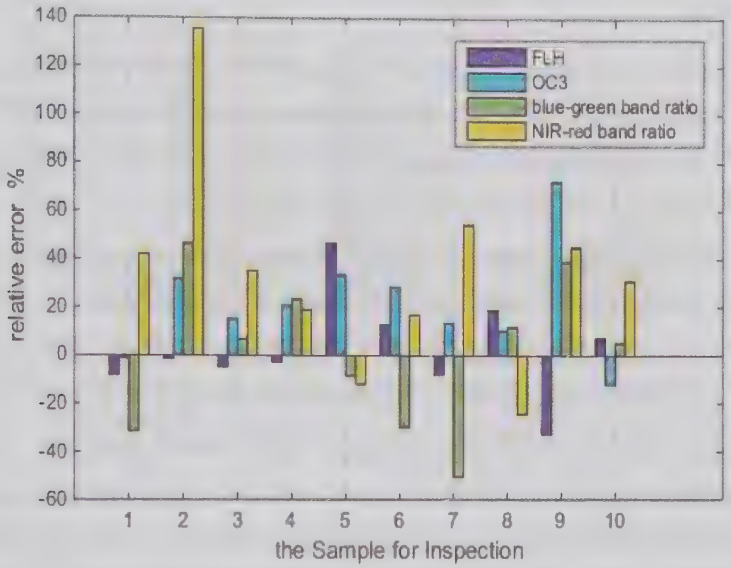

Fig. 7 Relative error of sample data for inspection

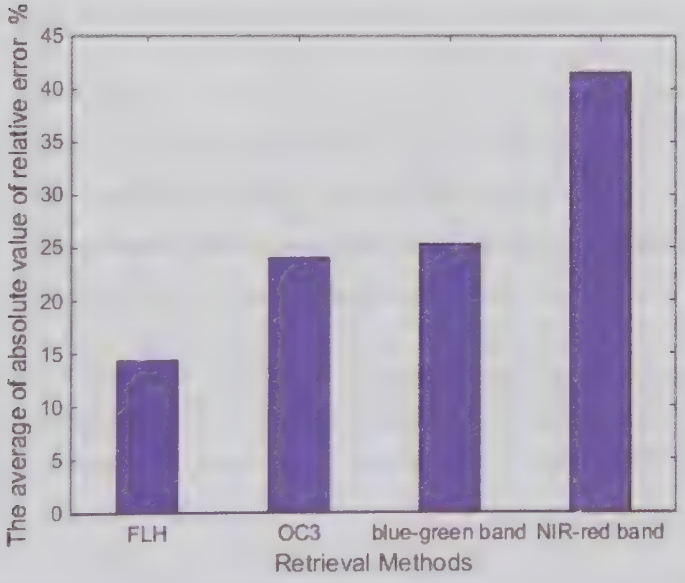

Fig. 8 The average absolute relative error of each algorithm

The relative error of a single sample does not represent the performance of these models, but the average of absolute value of relative error can. It can be seen from Fig. 8, the average absolute relative error of fluorescence line height method is the lowest, close

to 15%, and the average absolute relative error of OC3 algorithm and the blue-green band method is about 25%, and the average absolute relative error of NIR-red band method is more than 40%.

3.2 Result analysis

For the OC3 algorithm, Wonkook Kim et al. used the OC3 algorithm to establish the regression model in Northeast Asia, and the correlation coefficient was 0.69(Kim, 2016). In this study, determinant coefficient R^2 is 0.5996, and its determinant coefficient R is slightly higher than that of the OC3 algorithm in Northeast Asia.

For blue-green band ratio method, Zheng Gaoqiang et al. compared the correlation of the reflectance of each band and the chlorophyll-*a* concentration, confirmed that the correlation between blue-green band ratio was higher than that of blue or green spectral reflectance and chlorophyll-*a* concentration, and the correlation coefficient of the regression model was above 0.7(Zheng, 2015). In this study, the R^2 is 0.747 8.

For the NIR-red band ratio method, through analysing the spectral reflectance and water quality in Meiliang Bay of Taihu, (Ma Ronghua et al.) based on spectral characteristics analysis, found that there was a strong linear relationship between the ratio of the reflectance peak near 706 nm and the reflectance ratio near the 682 nm (R706/ R682) and chlorophyll concentration(Ma, 2005). But in this study, the R^2 is 0.109 6, and the application of this method in the Bohai Bay is not good.

For FLH, (Herman J. Gons) used fluorescence line height method to establish the chlorophyll concentration inversion model, and found that it is a linear relationship between the fluorescence line height and in-situ chlorophyll concentration, and the coefficient of determination R^2>0.89(Gons, 2008). Xing Xiaogang used linear model, binomial model, exponential model and Gower model to regress. It was found that the R^2 of the Gower model is 0.8, and the R^2 of linear , binomial and exponential models are up to 0.89(Xing, 2008). In this study, the R^2 of FLH model reached 0.961 3. It is indicated that the model established by the method of FLH is very suitable for the inversion of chlorophyll concentration in the Bohai Bay.

3.3 Method comparison

The performance of the four methods was evaluated by the regression model fitting results and verification of in-situ data. Fig. 9 shows the statistical results of the fitting parameters of the four algorithms.

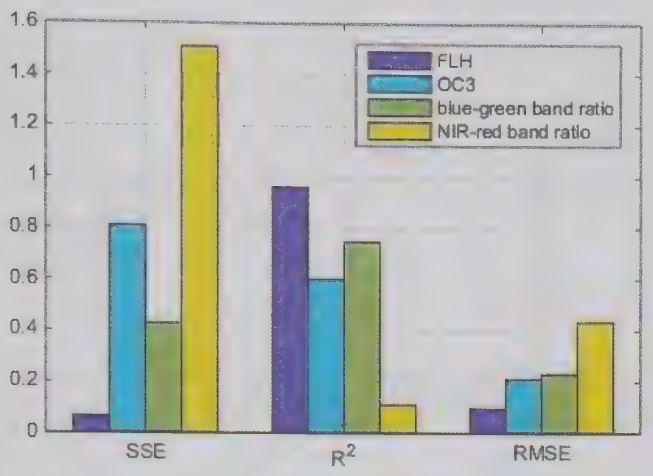

Fig. 9 The evaluation parameters of data fitting

The sum of squares for error (SSE) is the sum of the squared error of the corresponding points between the fitted data and the measured data. SSE is closer to 0, the model selection and fitting effect is better. Fig. 9 shows that the results of SSE of these 4 methods is the FLH < the blue-green band ratio method < OC3 < NIR-red band ratio method. FLH method is the best. The determination coefficient (R^2) determines the degree of correlation, and the FLH > the blue-green band ratio method > OC3 > NIR-red band ratio method. FLH method is the best. The root mean square error (RMSE) is also called the standard error, which indicates the degree of dispersion of the data. The RMSE is larger, the data is more discrete, and the fitting effect is worse. The results of RMSE of these 4 methods is the FLH < OC3< the blue-green band ratio method < NIR-red band ratio method. Through the fitting parameters of the data, we can find that the fitting result of FLH method is the best, followed by the OC3 algorithm and the blue-green band ratio and the NIR-red band ratio method is worst.

In addition, the relative errors of FLH method are not more than ±20%.The most absolute values of relative error of OC3 algorithm are between 10% - 40%. The relative errors of most data of the blue-green band ratio method are less than ± 40%. The absolute values of relative error of NIR-red band ratio method are high, and most of them are distributed in 10% - 60%, and the maximum value is close to 140%. We can find that the most of relative errors of FLH method are lower than that of the OC3 algorithm and the blue-green band ratio method, and much lower than that of NIR-red band ratio method. The average relative error of each algorithm in Fig. 8 also illustrates this idea. Therefore, through the verification of the measured data, the FLH method is the best inversion model, followed by the OC3 algorithm and the blue green band ratio method, and NIR-red band

ratio method is the worst.

Through the comparison of the above two aspects, it was found that FLH method is the best inversion method of chlorophyll concentration in the Bohai Bay based on GOCI data. The OC3 algorithm and the blue-green band ratio method are followed, and their accuracy of inversion is similar. The inversion accuracy of NIR-red band ratio method is the worst. Wonkook Kim's experimental results of Inversion of Chlorophyll Concentration in Northeast Asia based on GOCI data also show that the FLH method is better than NIR-red band ratio method (Kim, 2016).

The reasons for the above results were analyzed. First, the accuracy of OC3 algorithm is consistent with that of the blue green-band ratio method. The X in the formula of OC3 algorithm is also the form of ratio. For most of the data, the remote sensing reflectance at 443 nm is greater than 490nm, in other words, the majority of X here is the blue-green band ratio. So, the results of these two algorithm are coincident approximately. Secondly, the inversion result of the ratio of NIR-red band ratio method is the worst. The best range of the near red band is 700 - 720 nm, but the GOCI data does not correspond to this wavelength band, and the wavelength of 740nm is chosen. The best choice for near red band is between 700 - 720nm, but there is no GOCI data band corresponding to this wavelength range. We can only choose 740nm wavelength instead. Finally, the inversion error of FLH method is the smallest, and there are 3 reasons :(1) The regression model was consistent with the change trend of chlorophyll concentration and FLH. Zhao Dongzhi et al. found that the correlation coefficient obtained by $FLH=a+(Chla)^b$ was better than other models, and the correlation coefficient was greater than 0.93(Zhao, 2005). (2) Gower showed that the increase of suspended matter concentration will lead to a slight decrease of fluorescence signal and the low fluorescence baseline height, indicating that suspended matter has an impact on chlorophyll concentration (Gower, 1999). In addition, Zhang Hongliang found that when the concentration of suspended matter is greater than 8 mg/L, the FLH algorithm is not applicable (Zhang, 2007). In this study, most of the in-situ measurement data are distributed in the inner part of the Bohai b=Bay, and the concentration of suspended matter is low. (3) The range of in-situ chlorophyll concentration is between 0 - 2 mg/L. The chlorophyll concentration is low and the range is not large.

4 Conclusions

Based on the in-situ measurement data of the Bohai Bay and the GOCI remote sensing reflectance data, the retrieval model of chlorophyll concentration was established by using the method of FLH, OC3, blue-green band ratio and NIR-red band ratio. The

above algorithms were evaluated by comparing the simulation results and the verification results. The results are as follows: (1) There are obvious differences in the accuracy of different inversion methods. (2) The accuracy of FLH method is the best, and the inversion accuracy of the NIR–red band ratio method is the worst. (3) The inversion effect of the OC3 algorithm is similar to the inversion effect of the blue-green band ratio method. The conclusion of this study has reference value for the inversion of the chlorophyll concentration in the Bohai Bay.

The number of in-situ measured data samples, which used for the establishment of chlorophyll concentration inversion model and the validation of the model, is small. The in-situ measurement data is only at the time of the beginning of the April. However, the optical properties of phytoplankton may vary in different seasons. It limits the application of the model. Therefore, the universality of the conclusion of this study needs more data to test.

Acknowledgments

The study was supported by Tianjin Natural Science Foundation Project (14JCYBJC22500).

References

[1] Huang C, Shi K, Yang H, et al. Satellite observation of hourly dynamic characteristics of algae with Geostationary Ocean Color Imager (GOCI) data in Lake Taihu [J]. Remote Sensing of Environment, 2015, 159: 278 - 287.

[2] Xu S G, Fu Y Z, Kang P P. Seasonal and interannual variations of Chlorophyll-a in Bohai Sea [J]. Marine Environmental Science, 2015, (06): 898 - 903, 924.

[3] Sun X Q, Dong S G, Tang Z H. Influences of nutrients and illuminance on phytoplankton community structure [J]. South China Fisheries Science,2008,(01):1 - 9.

[4] Zhao Y S. Principles and methods of remote sensing application analysis [M]. Beijing: Science Press, 2003.

[5] Jiao H B, Yao Y, Li Y M, el at. Modelling Chlorophyll-a Concentration in Taihu Lake from Hyperspectral Reflectance Data [J]. Journal of Remote Sensing, 2006,(02): 242 - 248.

[6] Xu L J, Wang H, Huang C C, et al. Fluorescence Inversion of Chlorophyll a in Taihu Lake at Autumn [J]. Remote Sensing Technology and Application, 2014, (03): 433 - 441.

[7] Gower J, King S. Validation of chlorophyll fluorescence derived from MERIS on the west coast of Canada [J]. International Journal of Remote Sensing, 2007, 28(3-4): 625 - 635.

[8] Pan D L, Gower J, Lin S R. A Study of Band Remote Sensing Selection for Fluorescence of Ocean

Chlorophyll-a [J]. Oceanologia Et Limnologia Sinica, 1989, (06): 564 - 570.

[9] Kim W, Moon J, Park Y, et al. Evaluation of Chlorophyll Retrievals from Geostationary Ocean Color Imager (GOCI) for the North-East Asian Region [J]. Remote Sensing of Environment, 2016, 184: 482 - 495.

[10] Zheng G Q, Chen Y Z, Wang X Q, et al. The Chlorophyll-a Concentration Extraction of Xiamen Sea based on the HJ-1 Satellite Image [J]. Remote Sensing Technology and Application, 2015, (02): 235 - 241, 284.

[11] Ma R H, Dai J F. Chlorophyll-a Concentration Estimation with Field Spectra of Water-body near Meiliang Bayou in Taihu Lake [J]. Journal of Remote Sensing, 2005, (01): 78 - 86.

[12] Gons H J, Auer M T, Effler S W. MERIS satellite chlorophyll mapping of oligotrophic and eutrophic waters in the Laurentian Great Lakes[J]. Remote Sensing of Environment, 2008, 112(11): 4 098 - 4 106.

[13] Xing X G. Investigations on Chlorophyll Fluorescence Remote Sensing [D]. Ocean University of China, 2008.

[14] Zhao D Z, Zhang F S, Yang J H, et al. The optimized spectral bands ratio for the relation of sun-induced chlorophyll fluorescence height with high chlorophyll a concentration of algal bloom waters [J]. Acta Oceanologica Sinica, 2005, (06): 148 - 155.

[15] Gower J, Doerffer R, Borstad G A. Interpretation of the 685 nm peak in water-leaving radiance spectra in terms of fluorescence, absorption and scattering, and its observation by MERIS [J]. International journal of Remote Sensing, 1999, 20(9).

[16] Zhang H L. Evaluation Research on Chlorophyll Concentration Retrieval by FLH Algorithm in Bohai Sea [D]. Inner Moncolia University, 2007.

基于 GOCI 数据渤海湾叶绿素浓度反演算法的比较

张 雪，郑小慎

（天津科技大学 天津市海洋资源与化学重点实验室 天津市海洋环境保护与修复技术工程中心，天津 300457）

摘 要：渤海湾水体交换能力差，自净能力低，每年都要接纳大量的陆源污染物，叶绿素浓度的遥感估算对研究渤海湾海洋赤潮，监测海洋水体水质有重要作用，选择最佳算法反演叶绿素浓度有利于提高反演的精度。本文使用渤海湾的现场测量数据及 GOCI 遥感反射率数据，利用荧光线高度法、OC3 算法、蓝绿波段比值法和近红-红波段比值法建立叶绿素浓度反演模型，并利用实测数据进行算法验证，通过比较各算法的拟合效果和验证结果，对各算法模型进行了评价。结果显示，不同的反演方法准确性有明显差别，荧光线高度法的拟合和反演效果为最佳，而近红-红波段比值法的反演效果最差，OC3 算法与蓝绿波段比值法的拟合和反演效果基本相似。

关键词：叶绿素浓度，GOCI，荧光线高度法，渤海湾

Classification system and structure analysis of marine cultural landscapes of China

LI Jia-lin[1, 2], GONG Hong-bo[3]

1. *Department of Geography & Spatial Information Techniques, Ningbo University, Ningbo* 315211, *Zhejiang province, China;*

2. *Research Center for Marine Culture and Economy of Zhejiang Province, Ningbo* 315211, *Zhejiang province, China;*

3. *School of Law, Ningbo University, Ningbo* 315211, *Zhejiang province, China.*

Abstract: Marine cultural landscapes are an important part of cultural landscapes, as a new kind of heritage. With reference to the classification of cultural landscapes, a three-level classification system, composed of the marine cultural landscape type, the marine cultural landscape subtype and the marine cultural landscape model was constructed in this study, based on the spatial and regional characteristics of marine history and culture. By the analysis of the effects of natural and humanity factors on the formation of marine cultural landscapes, the system structure of the marine cultural landscapes was divided into three major parts: the physical foundation, the marked material and the recessive material.

Keywords: marine cultural landscape, landscape type, system composing, classification system

1 Introduction

Ocean is the cradle of the lives on the earth and the source of fundamental material and energy indispensable to human living. The ruins of Homo erectus on the Java Island and other proofs confirmed that the sea was one of the origins of ancient civilizations. The ocean is also the source of human cultural creation. From Homer's Epic, Greek mythologies to the Classic of Mountains and Rivers and the giant legends in the UK, the source of the fantasy artistic creation is the immense and mysterious ocean. The human being has created great cultural wealth while eulogizing the benefits the ocean brings to them, praying the continuous protection of ocean for the happy life of human being and even denouncing the ruthlessness of the ocean [1]. Therefore, marine cultural landscape is not only an important component of cultural landscapes, but also a development trend of

Received on Feb. 20, 2017

Corresponding author: nbnj2001@163.com

the protection of world cultural heritage at present and in the future [2].

2 Marine Cilture and marine cultural landscapes

Briefly, marine culture is the culture related to the ocean. That is to say, culture arises from the ocean. The connotation of life on spiritual, behavioral, social and material civilization is created through the understanding and utilization of human being in the ocean. The essence of the marine culture is the interactive relation between human being and ocean and the products of this relation [3]. A marine culture has the characteristics of extraversion, communication, expansivity and jumping. Marine cultures arise from the ocean and are correlated with the ocean directly. With the immensity and mobility of the ocean, the marine cultures have the characteristics of extraversion and communication. In constant communications, marine cultures are characterized by unsteadiness, and are susceptible to foreign cultures. Thus, marine cultures also present the features of expansivity and jumping.

Marine cultural landscapes are the material and intangible inventions formed during the exploitation of ocean. These inventions include the understanding, concept, thoughts, consciousness and mentality about ocean, as well as the economic structure, legal system, social customs and literature and arts. As one of the components of cultural landscapes, marine cultural landscapes are also the common work of both nature (the ocean) and the human being [4]. Marine cultural landscapes reflect the process of the marine culture and the attitude of human being towards the ocean, as the proofs of existence values of the origin, spreading and development of marine cultures. The marine cultural landscapes formed during the exploitation of the ocean by human being are marked by their era on the structure, form, contents and style of the landscapes.

3 Classfication system of marine cultural landscapes — basis of the Classification of Marine Cultural Landscapes

3.1 Evolution mechanism of marine cultural landscapes

A marine cultural landscape, as a complex material and spiritual wealth system, is formed during a long-term process by multiple mechanisms, involving nature, politics, history, technology, economy and psychology. The connotation of marine cultural landscapes determines their different formation and development patterns in time and space. Therefore, the evolution pattern and the development direction of marine cultural patterns in different periods and regions are different to a certain degree. To classify the

marine cultural landscapes, a deep analysis has to be conducted on the formation and development mechanism of every marine cultural landscape. The classification is realized based on the differences.

3.2 Attributes of marine cultural landscapes

The attributes of marine cultural landscapes refer to the property, characteristics and existence form and status of marine cultural landscapes. The difference of attributes for marine cultural landscape is another important principle in the classification. Due to the difference of the properties and internal structures of marine cultural landscapes, different marine cultural landscapes have different existence forms. Based on the existence forms, the marine cultural landscapes are classified into two types: tangible and intangible. The intangible form is subdivided into human activity forms and historical and cultural forms that have cultural values.

3.3 Functions of marine cultural landscapes

The marine cultural landscapes possess the characteristics of functional diversity, including economic, social, cultural and esthetic functions. The functions for different marine cultural landscapes have different focuses. Thus, the functions are another important criterion of the classification of marine cultural landscapes. The different utilization ways of landscapes are an important factor for the functional diversity of marine cultural landscapes. For example, costal shoal can be transformed into a marine cultural landscape under the influence of human activities [5]. The shoal forms a fishing landscape, if it is used for aquaculture. It forms an agricultural landscape if it is used for agricultural reclamation. The coastal settlements, being the living place of people, have the function of inhabitation. At the same time, they are also the preservation carrier for the architectural culture of coastal settlements, with the function of historical and cultural heritage. Certainly, it should be emphasized that the functions of a marine cultural landscape will change with times, and some of them may disappear or be converted into other new functions [6]. For example, the forts of Weiyuan, Anyuan and Pingyuan in Zhenhaikou have lost their functions of defending foreign invaders in today's peaceful world. This kind of marine cultural landscape has new functions in cultural experience and tourism.

3.4 Classification of marine cultural landscapes

The World Heritage Committee of the UNESCO divides cultural landscapes into three categories: intentionally designed and constructed landscapes, organically evolved landscapes and associative cultural landscape. The organically evolved landscapes are subdivided into two subtypes: relic (or fossil) landscapes and continuous landscapes. The

World Heritage Committee of the UNESCO expresses the cultural landscapes as the works of nature and human being. Their characteristics is the prominent and universal values, precisely defined regional representative of geography and culture and the basic and unique cultural factors representing the region. The US National Park Service divides cultural landscapes into four categories: cultural anthropological landscapes, historical designed landscapes, historical vernacular landscapes and historical sites. It focuses on the cultural connotation of the landscapes as the foundation and criteria in the classification. The cultural contents expressed by the landscapes are the guideline. The classification by the US National Park Service has filled up the shortage in the heritage protection.

Relative to natural landscapes, cultural landscapes have spatiality and regionality. The constitutive factors for natural landscapes include social factors and humanized cultural factors. They can be classified from different perspectives. Marine cultural landscape is a kind of cultural landscapes according to the land-sea geographical position. The unique marine cultural landscapes are formed by the interaction between specific marine or coastal regions and human being. The marine cultural landscapes in different regions present certain distinctiveness. Social factors also have an important influence on the formation and development of marine cultural landscapes. Even so, marine cultural landscape and marine natural landscapes are mutually interconnected and interacted. Therefore, the marine cultural landscape is a kind of heritage that is inseparable from the regional cultural tradition. Different regions have different structural characteristics. The classification is based on the spatial and geographical characteristics of the marine history and culture. According to the principle of relative conformity and distinctiveness, the principle of comprehensiveness and driving factors, the principle of hierarchy and the principle of favorable protection and, based on the study results of landscape and tourism resource classification proposed by researchers, a three-level classification was constructed, including the following categories : the type of marine cultural landscape, the subtype of marine cultural landscape and the model of marine cultural landscape.

The type of marine cultural landscape is the highest structural level of marine cultural landscapes. On this level, marine cultural landscapes are divided into marine material cultural landscapes and marine intangible cultural landscapes. Marine material cultural landscapes are the marine cultural landscapes with material existence. Marine intangible cultural landscapes are the landscapes in oral or other intangible existence.

The subtype of marine cultural landscape is the association of the landscapes with similar attributes and functions. On this level, the marine cultural landscapes are divided into eleven categories, six in material cultural landscapes and five in intangible cultural landscapes. It is worth noting that with the increasing attention of the values of marine

intangible cultural landscapes, it has an important practical significance to increase the number of subtypes of intangible cultural landscape to five categories from the perspective of the excavation and protection of resources of marine intangible cultural landscape. In the classification, besides the commonly known marine folk languages, marine mythologies, folk tales and legends, as well as toponymical culture are classified into this subtype. In addition, in this classification, the marine associative cultural landscapes connected with marine religions, folklores and tourism are added to the range of marine material cultural landscapes. This is in favor of reflecting the cultural connotation of the associative cultural landscapes. Furthermore, with "cultural routes" becoming one of the most important new trends in the protection of world heritages [7], the classification system adds marine cultural routes to marine material cultural landscapes as the important components.

Tab. 1 Classification system of marine cultural landscapes

Landscape type	Landscape subtype	Landscape model
Marine material cultural landscapes	Cultural relic and vestige landscapes	Shell mound cultural landscapes, marine cultural routes, ancient harbors, coast defense relics, submarine relics, sea wall (sea bank)
	Settlement cultural landscapes	Ancient human activity relics, historical cultural cities, coastal fishing villages, ancient towns, marine cultural special streets, marine residence architecture
	Historical site landscapes	Marine historical memorial halls, exposition halls, religious architecture, folk belief sites, temples, memorial temples, worship sites
	Modern marine cultural tourism landscapes	Marine resorts, marine theme parks, marine cultural activity sites, island leisure and entertainment sites, marine gastronomy, marine tourism products
	Marine associative cultural landscapes	Mountain and sea cultural landscape, astronomical phenomena and climate landscapes, coasts, islands, gulves
	Marine facility landscapes	Modern harbors and docks, marine huge constructions, marine traffic facilities, marine production bases
	Human activity record landscapes	Marine historic celebrities, marine historic events
Marine intangible cultural landscapes	Folklore cultural landscapes	Marine folk customs, marine eating habits, marine beliefs, savoir-vivre and customs, fairs and festivals
	Artistic cultural landscapes	Marine literature and arts, marine traditional dances, marine traditional plays, marine traditional workmanships, marine arts and crafts
	Festival activity landscapes	Tourism festival activities, cultural festival activities, commercial festival activities, sport events
	Linguistic cultural landscapes	Marine folk languages, marine folk literature, marine folk stories, marine toponymical landscapes, vocabulary landscapes

The type of marine cultural landscape is the association of the landscapes with similar factors such as formation, development, morphology and characteristics, which are the basic units of classification of marine cultural landscape. On this level, the overall system of marine cultural landscapes is divided into 55 basic models, including 33 material cultural landscapes and 22 intangible cultural landscapes. In the modern marine cultural

landscapes, along with cultural theme parks, leisure resorts, marine gastronomy products and tourism products with the marine themes are added. This conforms to the trends that people favor the marine food and other products as well as marine tourism products with regional characteristics. Thus, these products become main tourism products in the marine cultural tourism.

4 System structure of marine cultural landscapes

The system structure of marine cultural landscapes is extremely complicated. Compared with marine natural landscapes, the former is characterized by a natural geographical basis deeply connected with the sea and profoundly marked by human activities. The natural geographical conditions are the foundation of marine cultural landscapes, while humanity factors are the driving force in the formation of marine cultural landscapes. Since there is a diversity of human material in the constitution of marine cultural landscapes, the material is divided into marked material and recessive material according to the fact whether it has actual appearance existence [8]. Therefore, the system structure of marine cultural landscapes is composed of three major parts: the physical foundation, the marked material and the recessive material.

4.1 Natural geographical basement of marine cultural landscapes

In general, marine cultural landscapes exist on the ocean or in coastal areas, taking a certain geographical space. The natural geographical environment of ocean and coast is the foundation of their formation and continuous development. Without ocean or environment of coastal zone, marine cultural landscapes have no standing point and are like trees without roots.

The significance of the natural geographical basement of ocean and coastal zone to the marine cultural landscapes include the following aspects. First of all, the natural geographical basement of ocean and coastal zone is the spatial support for the formation of marine cultural landscapes. It provides the platform for coastal peoples to make use of and to remake the nature. It also provides a standing condition for the marked material of marine cultural landscapes. Secondly, the unique combination of the natural geographical basement of ocean and coast constitutes a peculiar and beautiful oceanic and coastal natural landscape. This natural landscape is the premise to attract all kinds of cultural activities and to form a marine cultural landscape inlayed on the basement. Thirdly, due to the geographical zonality regularity, the natural geographical basement of ocean and coastal zone itself has an obvious regularity of zonal distribution. Since marine cultural landscapes are constructed on the natural geographical basement of ocean and coastal

zone, some marine cultural landscapes represent a certain zonal characteristics. For example, the architectural form of residences is closely related to the natural geographical conditions, such as topography, rainfall and wind directions of an entire year.

The physical foundation of marine cultural landscapes includes the factors in geology, geomorphology, climate, hydrology, soil and biology and the natural geographical complex formed by their interactions. Different factors have different significance to the formation of marine cultural landscapes. Their effect forms and influential intensities are also different. Geological and geomorphological conditions are generally important factors constituting marine cultural landscapes. Geological and geomorphological conditions influence directly the activity ability and intensity of human beings in this region. Meanwhile, its uniqueness is also a main reason for the formation of marine cultural landscapes in this region. For example, Beilun Harbor, Ningbo, an international modern deepwater harbour in the 1990s, was constructed due to its unique deepwater shorelines, which satisfied the need of rapid development of international trade and the trend of large-scale vessels. In fact, under certain conditions, climate, hydrology, soil and biology are also important factors influencing the formation of marine cultural landscapes.

4.2 Marked material of marine cultural landscapes

Marked material refers to tangible humanity factors with colors and forms that can be perceived by visual sense. That is to say, the marked material is the humanity phenomenon that exists concretely and can be experienced and seen by people [9]. As for the marine cultural landscapes, the marked material includes tangible humanity factors formed on the ocean and in the coastal regions and related to the ocean that can be perceived by the visual sense, such as unique fishing village architecture on the coasts and islands, marine historical celebrities, classic literary works and unique clothes of coastal residents. Due to the difference of the classification criteria, the marked material of marine cultural landscapes can be classified in a variety of ways. For example, it is divided into active material and relatively stable material according to the activity of the marked material. Active material includes marine transportation tools such as fishing boats with local characteristics and ocean going vessels. The relatively stable material refers to marine historical and cultural relics and other constructions and structures with fixed position. The main characteristics of marked material are to constitute the appearance morphology of marine cultural landscapes. That is to say, marked material is the cultural phenomenon that can be perceived directly in the landscapes. The different combinations of marked material for marine cultural landscapes constitute the different appearances of marine cultural landscapes. The constructions are the most visible marked material in marine cultural landscapes, which are predominant over other marked materials of various

cultural landscapes and constitute the core of the whole marine cultural landscape. The structure and appearance of the constructions represent the relations between the different factors in cultural landscapes.

4.3 Marine human activity records

The human activity records of marine cultural landscapes refer to the important historical figures, historical events and historical and cultural classics that are related to the exploitation and utilization of various marine resources and the defense against foreign aggression on the ocean or in the coastal regions since the beginning of history. Marine historic celebrities refer to the marine cultural celebrities or military celebrities who made a great contribution to the marine resource development and marine territory defense. Marine historic events refer to the important events during the marine exploitation and the historic events such as combats defending foreign invasion and protecting marine territory. Marine historical and cultural classics refer to the various literary works formed during the marine exploitation and the defense against foreign aggression.

4.4 Marine spatial morphology

The spatial morphology surpasses the single marked material of marine cultural landscapes. It is a material space confined or defined by natural factors including coasts, mountains, water body, vegetation and human factors including constructions and structures. It has the properties of material, form, texture and color. It emphasizes the cultural relation between the different marked materials in the space range. Therefore, it is an organic fusion of the physical foundation, the marked material and the recessive materials of marine cultural landscapes. The space morphology includes three forms: dots, surfaces and lines.

4.5 Marine construction structure

The construction structure of marine cultural landscapes are constructions, structures and other relics related to the ocean left in history, which reflects the architectural culture, social functions and relative special historic events and figures and is an important support for cultural landscapes. The pattern and order constructed by natural and human factors, such as settlements, streets, building complex, mountains and waters, represent the idea of the spatial layout of a marine cultural landscape. The traces of the fusion of the psychology and behavior with natural environment of a certain geographical and historical conditions are engraved on them. For example, the handrail constructions in the Hemudu sites reflect the adaptation to the tidal flats in the estuarine area.

4.6 Marine Human Settlements

Marine human settlements are the living environments of the settlements or the residence of people. The human settlements of coastal and island refer to the organic combination of natural and human environment, as well as material and spiritual environment, historical and current environment, political and economic environment related to the living forms in the coastal areas, including villages, towns and cities. It is a living environment constructed to maintain human activities, including living, working, healthcare, transportation, communication, ecological environment and cultural entertainment. The human settlements of coastal island are a space closely connected with the living activities of coastal people, which are the base of living for coastal people in the ocean, as well as the support for the development and utilization and protection of the ocean.

4.7 Marine Material Products

The material products of marine cultural landscapes refer to the tangible objects from the ocean or those that are closely connected with coastal people's production and living, and that can be used, consumed by people to meet a certain need of people. The material products include two categories, marine food and crafts and industrial products. Marine food is the material product originated from the ocean and processed in different levels for human consumption. According to the processing level, the marine food is divided into the marine food collected naturally, marine food processed preliminarily and marine food processed further. Crafts and industrial products are various industrial products and handicrafts that are originated from the ocean or closely related to the work and life of coastal people, including handicrafts and crafts of marine materials, industrial products of marine materials for daily use and other products. The crafts and industrial products have both practical and esthetic values. As for the contents, they express the subjective emotions, subjective world, people's characters, spirit and emotions. As for the form, they occupy a certain space.

5 Recessive material of marine cultural landscapes

The recessive material of marine cultural landscapes refer to the intangible humanity factors that cannot be perceived directly, however, have a great effect on the formation and development of the marine cultural landscapes [8]. This kind of material is not represented directly in a marine cultural landscape, but its effects on the formation and connotation for marine cultural landscapes are not to be ignored. The recessive material of marine cultural

landscapes include the unique behavioral patterns, folk arts, technologies, life concept, spiritual culture of coastal people.

5.1 Marine Behavioral Patterns

The Marine behavioral patterns are the routinized, normalized and modeled activities in language, etiquette and actions, which are formed during the work and life of making use of the ocean and defending against the ocean. They are considered to be the direct representation of the marine regional and psychological culture and the representation forms of written culture. They are also the concrete reflection of interpersonal communications. Therefore, they constitute an important connotation in the recessive material of marine cultural landscapes. They are the external representation of the social psychology, way of thinking and social customs formed during a long-term process by the coastal people.

5.2 Marine Folk Arts

The folk arts of marine cultural landscapes are unique cultural connotation and value semiotic system connected with marine regional characteristics formed by coastal people during their social production practices and daily life. The marine folk arts are created by the ancestors of coastal people and inherited and developed by their descendants. With the change in space and time, the existence forms and ways of folk arts vary constantly. The formation, inheritance and mutation of the folk arts formed in the coastal or island regions are closely connected to the ocean. The folk arts of ocean involve the life, marine fishing industry, marine trade and transportation, as well as marine verbal literature and wish folklore. It is the basis of the marine culture. Certainly, ancient folk inheritance is the earliest and most fundamental form of marine culture [8]. The folk arts of marine cultural landscapes are the folk arts and culture including food, architecture, clothes, festivals, entertainment and religion.

5.3 Marine Technologies

The technologies of marine cultural landscapes are the recessive materials that are contained in the marked material such as marine material products and handicrafts. The technologies are the technical flow and the science and technology in which the raw materials originated from the ocean and semi-finished products are processed orderly, successively to transform them into products by industrial enterprises, with the help of tools. According to the time characteristics of formation, technologies are divided into two parts: traditional handicraft and modern technologies. For example, the processing procedures of the famous marine specialties of Ningbo, Salty Chinese Herring and Nonfat Yellow Croaker, include traditional handicrafts such as curing, and modern technologies such as

degreasing and vacuum package.

5.4 Marine Life Concept

Marine life concept refers to the relative consistent ideas, opinions and beliefs in the clothes, food, habitation, transportation, working, entertainment, social interactions and interpersonal communications that coastal and island people have. The life concept is in the historical category. It is closely related to the living habits of coastal people. During a certain historical period, the life concept is a general view of life of coastal people formed during the socialization. With the development and change of social economy, the life concept of coastal people changes accordingly, resulting in the change of their lifestyle. In ancient times, coastal people lived on fishing for generations. Their concepts on clothes, food, habitation and transportation may be related to the fishing industry. However, with the development of modern tourism, tourist industry has been developed with the special natural landscapes and natural resources of the coastal regions in order to create economic benefits different from traditional fishing industry. Thus, the life concept has been greatly changed.

5.5 Marine Spiritual Culture

Marine spiritual culture is the combination of ideology, styles and features and characteristics integrating psychology, ideas, customs, beliefs and standards during the understanding and exploitation of the ocean by coastal people. The unique environmental characteristics forge the spirit of coastal people. Therefore, the marine spiritual culture has become the motive power of the social and economic development and is closely related to the rise and fall of the coastal regions. The power source of marine spirit is the unremitting quest and unyielding mind. It transformed Netherlands from a country facing constant threatening from the ocean to the center of the world and "coachmen on the sea" in the seventeenth century. It forged the UK, an island country surrounded by the ocean, into the hegemony over 200 years. "Ningbo Group" is scattered all over the world. The success derives from the marine spiritual culture with the spirit of tenacious despoliation and risk and innovation of Ningbo people. The mobility of the ocean also makes the marine spiritual culture open and innovative.

In a manner of speaking, the recessive material, different from the specific and substantive objects contained by marked material, is the intangible spirit of the marine cultural landscapes. The goal of request into the marked material of marine cultural landscapes is the appearance of the landscapes. That is to say, the scenery. However, the investigation into the recessive material permits to penetrate the landscapes to seek the spirit and the sentiment inside the scenery. The spirit and the sentiment are interfaced with

the scenery, making the study of cultural landscapes full of the intangible with the concrete and the scenery and the spirit inseparable. Therefore, it is considered that the humanity landscape presented by concrete objects is no more than the shell of marine cultural landscapes. The recessive material is, in fact, the substantive content. Only by the combination of the two can the real connotation of marine cultural landscapes be constructed. In addition, the interactions between the marked materials and recessive materials of marine cultural landscapes also form an atmosphere of marine cultural landscapes that cannot be expressed in general language. This kind of atmosphere can only be experienced by oneself. For example, the Chinese fishing festival of Xiangshan, Ningbo brings the harmonious coexistence of human and the ocean as the theme, putting forward the slogan that 'to be friendly with the ocean is to be friendly with mankind itself". The ocean worshiping activities and the sailing together of thousands of ships during the festival can only be appreciated by people at the site to experience the atmosphere.

6 Conclusions

Cultural landscape, a special type of cultural heritage between natural and cultural heritages, has great importance to the protection of world heritage landscapes [6]. However, due to the cultural differences, 80% of the cultural landscapes which are listed as World Heritage are located in Europe. Few cultural landscapes are distributed outside the Europe. The cultural landscapes of world heritage should be universally representative. China has a long history of philosophical thought of harmony between human and nature. Without the participation of China and the Asia-Pacific region, the cultural landscape system is incomplete [2]. It was investigated through this study that it had an important significance for the discussion of the types of marine cultural landscapes and their system structure, the understanding of the relation between human and nature behind the strengthening of landscape morphology and the spread of the essence of Chinese marine culture. Meanwhile, it contributes the values of China to the diversity of cultural landscapes of world heritage and constructs a more complete international theory and practice system of cultural landscape.

Acknowledgements

This study was supported by the National Natural Science Foundation of China (No. U1609203, 41471004).

References

[1] Ge Y J. The value of Ocean items of World Heritage and its development direction [D]. Master's thesis of Nanjing normal university. 2005.

[2] Han F. World heritage cultural landscapes and new international trends [J]. Chinese Landscape Architecture, 2007, 23(11): 18 - 21.

[3] Qu J L. Outline of ocean culture [M]. Qingdao: Qingdao ocean university press. 1999: 35 - 60.

[4] Wang N X. Classification of marine historical and cultural landscape in China [J]. Exploitation and Management of Marine Resources, 2007,5:83 - 88 .

[5] Jia H Y. Marine resource and its exploitation in China [J]. Journal of Ocean University of China, 2006, 2: 8 - 11 .

[6] Kozlowski J, Vass-Bowen N. Buffering external threats to heritage conservation areas: a planners perspective [J]. Landscape and Urban Planning, 1997, 37(3-4): 245 - 267.

[7] Li W, Yu K. New direction in the conservation of world heritage: cultural routes (cultural itineraries) [J]. Urban Problems, 2005.4: 7 - 12.

[8] Dong X. On the structure of human tourist landscape and the characteristics of the landscape [J]. Human Geography, 1993,8(1): 65 - 69.

[9] Zhou X. Study on Marine Customs and Chinese Marine Customs. In: Study on ocean culture [M]. Beijing: Ocean press. 2000,155 - 166.

中国海洋文化景观系统及其构成

李加林[1,2]，龚虹波[3]

（1. 宁波大学 地理与空间信息技术系，浙江 宁波 315211；2. 浙江省海洋文化与经济研究中心，浙江 宁波 315211；3. 宁波大学 法学院，浙江 宁波 315211）

摘 要：海洋文化景观世界文化景观的重要组成部分。文章基于海洋历史文化的空间和地域特征，进行了海洋文化景观的定义，并将中国海洋文化景观分为海洋遗址遗迹景观、海洋历史场所景观、海洋乡土景观、海洋聚落景观、海洋关联性文化景观和海洋文化线路景观等 6 种类型。并通过自然和人文因素对海洋文化景观形成的作用分析，将海洋文化景观的系统构成划分为自然地理基底、具象质料和非具象质料三大部分。

关键词：海洋文化景观；景观类型；系统构成；分类系统

Ocean ecological compensation mechanism in Liaoning area from the angle of ecological civilization —based on analysis of Dalian' s cooperative governance

CAI Jing[1], WANG Pengda[2], LI Jin[1] ,YU Yue[3]

1. *School of Marxism, Ocean University of Dalian, Dalian* 116023, *Liaoning province, China;*

2. *School of Marine and Civil Engineering ,Ocean University of Dalian, Dalian* 116023, *Liaoning province, China;*

3. *Department of Student Affairs, Ocean University of Dalian, Dalian* 116023, *Liaoning province, China*

Abstracts: How to speed up the establishment of marine ecological compensation and the ecological compensation system is inevitable choice from ocean country to marine power. Therefore, construction of marine ecological compensation mechanism is the effective means which incentives marine ecosystem services supply, improves the quality of marine ecology, and promotes the ocean to the green transformation. Combined with Dalian maritime case study in Liaoning Province, three dimensional interactive marine ecological compensation mechanism, the compensation frame work, path and operation mechanism were built up. Suggestions on accelerating the legislation process; perfecting the management system; establishing proper system for both incentive constraint and reward-punishment; increasing the source of Ocean Ecological Compensation funds; accelerating On the study of the Ocean Ecological Compensation Mechanism in Liaoning Area from the Angl-e of Ecological Civilization Based on Case Analysis of Dalian.

Keywords: marine environment, ecological civilization, compensation mechanism, cooperative governance, ecological compensation

1 Raise questions

21 century is determined by marine. China is an extensive country with maritime space. Marine issues involve in national interest and ocean circulation. It's linked with people's welfare. The Eighteenth National Congress of the Communist Party of China raised important deployment on "The construction of marine power". Chairman Xi

Received on Aug. 5, 2017

Corresponding author: caijing72@163.com

emphasized officially that we should put marine ecological civilization into overall arrangement of marine development in order to accelerate the establishment of Marine ecological compensation and the ecological compensation system on the eighth collective study of the Politburo Standing Committee of the CPC Central Committee. Marine ecological compensation aims to use ecosystem service to protect and regulate the economic benefit among stakeholders, buttresses up power and strengthen responsibility, external tools and economic benefits of institutional arrangement.

1.1 History of the Ocean Ecological Compensation Mechanism

According to the literature existing, the practice started from Qingcheng Mountain, Sichuan province in 1970s. The construction of the Ocean Ecological Compensation Mechanism has been officially christened after holding a seminar on forest ecological compensation in Leshan, Sichuan province, Oct., 1989.

Compared with other countries, the work of ocean ecological compensation in China started late. Work of different regions had their own characteristic each and achieved marked results. 《Plan of cleaning work in Bohai》 was set the project in 2001 to supervise pollution discharge from land in order to gradually reduce the adverse reaction caused by marine engineering project, even protected the legitimate rights of people in charge of fishery production. Ecological Research Center of Chinese Academy of Science had the deeper research on rapport among a variety of ecological system. 《water law》 had been raised and amended during general meeting of Chinese environmental resources law. In 2011, ocean organization unit and environmental administration formulated technical documents including data analysis reports, opinions on common problems and materials of main points according to basic information about preventing and remedying immediate offshore area to conclude main points of remarkable features, principal focus, action framework, feedback system in four territorial waters.

1.2 Statement of research in current situation at home and abroad

Scholars abroad come up with their own ideas aiming at the types and means of ocean ecological compensation while concentrating on ocean ecological values, service for system, value assessment and mechanism. Scientific original articles can be exampled such as <<ecological compensation: international experience and national practice>>, <<theory and application of ecological compensation>>, <<internationally compare: pattern and mechanism>>by China 20th Agenda Management Center, <<Chinese ecological compensation mechanism and policy research>>by group of Chinese ecological compensation mechanism and a series of result by a research team led by Ding Sibao. Zhang Jiwei discussed about ecological compensation on ocean nature reserve referring

to the angle of environmental risks. TangLi had a specialized research on South China Sea via<<exploration and analysis law issues about ecological compensation in South China Sea>>. Li Xiaobing published an article named<<thinking about setting ecological compensation in JinSha River>>. On the whole, general instruments are more than specifications, resource compensation researches of forests and mines are more than ocean research. It concentrates on five aspects. Why? Who? To whom? How? What? Only few research results are about Liaoning water space. Either can be found in chapter 6and8 of <<Study on Regional Ecological Compensation System by Yanwei or can be Embodied in Partial Paper, such as <<Research on Ecological Compensation System in BoHai>> written by QiuJun; <<Research on Setting up Ocean Ecological Protection Compensation Mechanism>> by YuLin. There's no doubt that these researches offer references for the theory and practice in Liaoning. Ecological compensation is a complex system contains multilevel benefit relationship and technical operations vary from industries and fields. Its nature is re-allocated in the benefit of ecological, economy and society. Co-governance makes the allocation come true because cooperation can work miracles and generate great power.

There are some shortages in ocean ecological compensation currently, expressing in four aspects. First, theory system is not shaped. Researches existing tell the necessity, the problems and approaches are separated, lack of systematic integration. Second, researches on existing service type and value assessment have some progress, but for using the technology of ocean ecological system service value assessment are a few. The feature of these is scattered and non-systematic. Third, we are short of research for technology of ecological compensation measures. It covers the measure of ocean ecological resource value and we have no ideas about the method. Fourth, we are lack of typical cases.

2 Construction system of framework

Only few scholars have the research for ecological compensation on oil leak, seldom of them are at filling in the sea project of ecological compensation. The article use Dalian as the case to study, try to discuss the system of construction of framework, path and system and give some policy suggestion.

Case of ocean ecological compensation discussion-taking Dalian as example Dalian has abundant of ocean resource with 1 900 km coast line, area of 23 000 km^2, over twice the water space compared with earth surface water space. Ocean economic aggregate reached to 85 billion RMB in Dalian 2006, rising about19% than 2005, occupied 33% GDP

of the whole city which has developed as a strong economic city in ocean. It has formed the port transport, ocean fishing, coastal tourism, ocean chemical engineering rudiments. As the economic growth, some reasonable developing activities such as filling in the sea have great influence on ocean resource and ecological environment.

2.1 Activities of filling in the sea

In recent years, the area in Dalian positions the first. This has a serious impact on ocean ecological environment, mainly expresses in 6 aspects. First, it aggregates the environmental pollution. Second, it damages the environment of coastal wetland. Third, it causes the water space reduced sharply and the change of the condition of hydrology. Fourth, it damages the resources of islands seriously. Fifth, it causes damage of coastal natural landscape. Sixth It influences other ocean industries. At the same time, human activities bring harmful results such as coastal line resources reduced while man-made increased and this changes the structure of coast, reduces the bay area sharply, weakens the bay nature, makes offshore islands disappeared, important fishing resources recession, damage of coastal nature view. Though Dalian has strengthened the research on marine major function area, program of marine function and filling in the sea in a scientific way, management of marine construction, using argument of area program strictly, supervising and assessment, and also come on the method of compensation. It also exposes some problems. It sacrificed the minority's benefit but it cannot make up for the harm to the public.

2.2 The accident of oil leak in Dalian area and new port

Oil pollution has gradually become the main sector of environmental pollution in Dalian area. Therefore, the most effective way to prevent the pollution is to protect the environment farthest, reduce the accident of shipping pollution, and reduce the loss of pollution. It contains two aspects: precaution and govern. At the same time, we ought to compensate the pollution loss by surveying the accident, sampling the pollution, disposing in an executive way and other work related. We investigated some accidents, did some handling work, analyzed some drawbacks existing in the 300 thousand raw petrol ports, and raised some improvement measures and come up with the system of how to manage the urgent accident. Taking the 300 thousand raw petrol port for example, its position in the urgent system contains:

Taking oil leak in Dalian new port for example, we would like to discuss the economic benefit relationship among countries, regional government, farm plant owners, the public and the investors. As a ocean holder, our nation has the ownership and value proposition right facing marine ecological resource and systematic service. Due to the damage to the

value of marine ecological resource made by oil leak in new port, the country needs to get compensation from the destruction. Marine economy plays an important role in coastal city as the financial root of the government; the accident itself destroyed the resource of the scenery and also had great influence of the local tourist trade. It has an impact on financial income, so that the local government needs to be included as the object in ecological compensation. The accident led the productivity reducing 90%; coastal people who feed on fishing lost a huge amount of product such as fish and shrimps. They also need to be compensated. Sea food may largely be polluted by oil leak and bring harm to the inhabitants. Their food should be concerned and they need to be compensated. Meanwhile the pollution harmed the function of ecological service, and ecological victims should be compensated. There are physical and biological recovery technology for the ecological recovery such as coastal man-made wet land, maple trees, sea weed bed and other typical recovery environment. We can use both the plant and creatures and man-made wet land to recover the damage. Ecological compensation system should pay for all the fees using on the recovery. All the economic expense of technology and management system should be compensated. Research on cultivating the talent, people for management and staffs investment are included.

3 The framework structure, approach and operation system of marine Ecological compensation

There exist many department responsibilities uncertain on oil leak ecological damage compensation in Liaoning

3.1 The framework structure and path to realize

According to the marine compensation theories, it is easy to see the system design containing the following aspects:

3.1.1 Benefit stakeholders

It refers to compensate department relevant, organization or individuals.

3.1.2 Compensation standard

Taking quantification method to set scientific compensation standard after reasonable ecological construction loss and benefit assessment.

3.1.3 Ways to compensate

Process, method and rules are in research elements.

3.1.4 Compensation system

The main point aims at how to solve the "guarantee the compensation" problem.

3.1.5 Assessment on the effect of compensation

The key is to understand the operation effect of ecological compensation system and raise the reference scheme on practice. The scientific lists are below:

3.2 The establishment of operation system by ecological compensation council

The compensation system council is set by the NPC and province government in the ocean bureau. There are four regular offices for the financial compensation, supervising assessment, research and public voice. They divide the work specifically and help even supervise each other. Their duties are as followed:

(a) financial compensation office (main part): It mainly aims at managing financial allocation system. The first system for raising fund financing: it is the principle path to broaden ocean ecological compensation fund; show the effect on ocean ecological environmental taxes: perfection collecting taxes from the companies and individuals taking advantages of ocean resources; set up ocean ecological compensation cash deposit system: it is in direct proportion to using the resource.

(b) the second system for fund budget(government measures): consummating the balanced budget of means of compensation and transfer payment; normalize the fund use on special project transfer payment: considered the government is the subject of public financial payment, it can be the ways of direct investment; government parches and transfer payment to receive the service and products to subsidize the damage; various approaches to compensate: it includes compensation in material object and currency technology training. In market rules, it is correct to give expression to efficiency and fairness in market value to compensate the damage benefit.

(c) the third system is to allocate the fund and choose correctly; compensating by privilege policy; by market: market system occupies the most. Buyers centered by the government may encourage the participation. In order to achieve remarkable result, we ought to use the method of adjusting market ecologic to encourage the public to take part in it.

3.2.1 Supervising assessment office

(a) earlier stage: it mainly expresses on assessment gist. Clear the subjects, objects, modes and means.

(b) middle stage: making sure the standard, through multi-aspect decisions to optimize technology or people related to benefit game to make sure the compensation standard as the basic second step.

(c) to make sure the compensation working, the process should be fair and transparent, focus on the subsequent effect.

3.2.2 Research office: taking charge of managing the research

(a) contact with research organization and office to cultivate the talent on ecological recovery.

(b) raise the project more long-acting and advanced with the times.

(c) protect the intellectual property actively.

3.2.3 Public voice office: to collect the suggestions and opinions from the public and publish the progress

(a) Collect suggestions from media and the public, even some injustice news, sending feedback to three others.

(b) publish the compensation progress in time and the direction of fund.

(c) protect the intellectual property actively.

4 Improve the policy suggestions in area compensation system

(a) Accelerate the process of legislation and make sure it proceeds. Detailing compensation subjects in content standard in different regions and types, and setting up laws & regulations to clear duties, responsibilities and tasks. Make sure the division of labor. Speeding perfects the laws and policy to establish guiding principle in state nation. To create the policy platform by speeding up summarizing experience steps, and increate innovation extent to create a better platform.

(b) Construct government project system overall to intensify the organization. Perfect the management system gradually and establish the organization to coordinate, accelerate the authorized strength to reinforce the cooperation and enhance the benefit. Build criteria of assessment system of rewards and penalties, set up information open system to increase the transparency, accept social supervising.

(c) Perfect financing system, broaden the ways to gain fund source to compensate, build special project fund, publish lottery, BOT financing, and introduce foreign product

environmental devotion, broaden fund source, and perfect safeguard system.

(d) Accelerate property right system pack to boost the marketing progress. First, bound the ownership of resource and infringement act; second, intensify the property right consciousness and build price sharing system;

(e) Put into the research and innovation to advance the protection level of environmental protection on practice basic; provide technology guidance by government enhanced education training.

(f) Mobilize public participation and exert the power of the groups; strengthen the propaganda, and increase the citizen participation consciousness of the eco-environmental protection; gradually establish an evaluation system of ecological compensation; enhance compensation decision-making power; give full play to the force of public supervision; perfect the policies and advices of the public participation system.

Acknowledgements

This paper was supported by the National Social Science Foundation: Research on Fiscal and Tax Policy Innovation and Mechanism of Coordinated Development of Regional Economy (14BJY003); Liaoning Social Science Foundation: Study on Ecological Compensation Mechanism of Liaoning Province (L13djy057); the Second Batch School of Marxism Major Research Direction Foundation Items of Liaoning Province: Study on Liaoning Province Ocean Strengthening Strategic Issues with Five Concepts Leading.

References

[1] The Administrative Center for China's Agenda 21 (ACCA21）. Sustainable Development Strategy Research Group. Ecological Compensation: International experience and China practice [M]. Beijing: Social Sciences Academic Press, 2007.

[2] The Administrative Center for China's Agenda 21 (ACCA21）. Principle and Application of Ecological Compensation [M]. Beijing: Social Sciences Academic Press, 2009.

[3] The Administrative Center for China's Agenda 21 (ACCA21）. International comparison of ecological compensation: models and mechanisms [M]. Beijing: Social Sciences Academic Press, 2012.

[4] China Ecological Compensation Mechanism and Policy Research Group. China Ecological Compensation Mechanism and Policy Research [M]. Beijing: Science Press, 2007.

[5] Tang Li. Analysis of Marine Ecological Compensation Law in the South China Sea [J]. Law Journal, 2010 (1).

[6] Li Xiaobing. Some thoughts on the Establishment of Ecological Compensation Mechanism in Jinsha

river in China [J]. Journal of Yunnan University of Finance and Economics, 2009(2).

[7] Yan Wei. Research on Regional Ecological Compensation System [M]. Beijing: Economic Science Press, 2008.

[8] Qiu Jun. Research on the Ecological Compensation Mechanism in Bohai Sea [J]. China Population Resources and Environment, 2008(2).

[9] Sun Feiya, Yu Lin. Research on the Establishment of Marine Ecological Protection Compensation System in Bohai Sea [J]. Research on Rule of law in Liaoning, 2009(1).

[10] Fox Miller. Postmodern Public Administration - Discourse Direction [M]. Beijing: Renmin University of China press, 2002.

海洋生态文明视野下辽宁海域生态补偿机制研究
—基于大连海域的合作治理分析

蔡 静[1]，王鹏达[2]，李 瑾[1]，于 越[3]

（1. 大连海洋大学 马克思主义学院，大连 116023；2. 大连海洋大学 海洋与土木工程学院 大连 116023；
3. 大连海洋大学 学生工作处，大连 116023）

摘 要：从海洋大国变为海洋强国是必然过程，加快建立海洋生态补偿和生态损害赔偿制度是必然选择。因此，海洋生态补偿机制建设是为了刺激的海洋生态服务的供应，改善海洋生态质量，促进海洋转型必要的方式。结合大连海域个案研究得出对辽宁省的启示，在此基础上尝试构建三维互动的海洋生态补偿机制、补偿框架、路径与运行机制，并提出加速海洋生态补偿立法进程；完善生态补偿管理体制，建立恰当的激励约束与考核奖罚并举的制度体系；增加海洋生态补偿资金来源；加速海洋生态资源产权制度建设；增大相关补偿标准量化方式与相应技术的研究；完善公众参与制度等政策建议。

关键词：海洋环境；生态文明；补偿机制；合作治理；生态补偿

海 洋 通 报（英文版）

HAIYANG TONGBAO

2017 年 10 月 第 19 卷 第 2 期

目 次

中国北黄海微表层海水中细菌多样性……明红霞 等 (19)

中国近海入境船舶压舱水输入特征与风险分析 …… 杜 还 等 (37)

河北昌黎黄金海岸国家级自然保护区海域大型底栖动物群落特征研究

……寇存辉 等 (50)

渤海湾叶绿素浓度的反演与验证 …… 郑小慎 等 (61)

基于 GOCI 数据渤海湾叶绿素浓度反演算法的比较 …… 张 雪 等 (74)

中国海洋文化景观系统及其构成 …… 李加林 等 (87)

海洋生态文明视野下辽宁海域生态补偿机制研究—基于大连海域的合作治理分析

……蔡 静 等 (96)

Marine Science Bulletin

Marine Science Bulletin publishes papers on marine science and technology including physical oceanography, chemical oceanography, marine biology, marine geology, environmental oceanography, estuarine & coastal sciences, marine technology, digital ocean, coastal zone management, ocean engineering, marine economics, etc., and aims to promote international academic exchange.

Editor-in-Chief: SHI Sui-xiang (石绥祥)
Associate Editor-in-Chief: XIANG Wen-xi (相文玺) LI Xue (李雪)
Executive Editor: QIU Wen-jing (邱文静)
Editor: SONG Xue-lian (宋雪莲) DONG Yi (董 艺) LI Xiao-guang (李晓光)
YUAN Ze-yi (袁泽轶)

English proofed by: WANG Qi (王 琦) WAN Fang-fang (万芳芳)

Semi-annually (started in 1999, sum 38)
Publication date: May 15th and Oct. 15th

Marine Science Bulletin **(Vol. 19, No. 2, Oct. 2017)**

Responsible Institution:
State Oceanic Administration of China
Sponsored by:
National Marine Data and Information Service
Edited by:
Office of Marine Science Bulletin (English edition)
Printed by:
Printery of National Marine Date and Information Service

Published by:
Office of Marine Science Bulletin (English edition)
E-mail: msb@nmdis.org.cn
Tel: (022) 24011287
Address: 93 Liuwei Rd., Hedong District, Tianjin 300171, China

---

ISSN1000-9620
CN12-1271/N

Price: $ 30.00 / ￥40.00 Per year

ISSN 1000-9620

9 771000 962001